Available online at www.sciencedirect.com
ScienceDirect
Comput. Methods Appl. Mech. Engrg. 369 (2020) 113185
Computer methods in applied mechanics and engineering
www.elsevier.com/locate/cma

A posteriori error estimates for Biot system using Enriched Galerkin for flow

Vivette Girault[a], Xueying Lu[b], Mary F. Wheeler[b,*]

[a] Sorbonne-Université, CNRS, Université de Paris, Laboratoire Jacques-Louis Lions (LJLL), F-75005 Paris, France
[b] Center for Subsurface Modeling, Oden Institute for Computational Engineering and Sciences, The University of Texas at Austin, TX, USA

Received 25 May 2020; accepted 27 May 2020
Available online 11 June 2020

Abstract

We analyze the Biot system solved with a fixed-stress split, Enriched Galerkin (EG) discretization for the flow equation, and Galerkin for the mechanics equation. Residual-based a posteriori error estimates are established with both lower and upper bounds. These theoretical results are confirmed by numerical experiments performed with the Mandel's problem. The efficiency of these a posteriori error estimators to guide dynamic mesh refinement is demonstrated with a prototype unconventional reservoir model containing a fracture network. We further propose a novel stopping criterion for the fixed-stress iterations using the error indicators to balance the fixed-stress split error with the discretization errors. The new stopping criterion does not require hyperparameter tuning and demonstrates efficiency and accuracy in numerical experiments.

Keywords: A posteriori error estimates; Enriched Galerkin; Biot system; Fixed-stress iterative split

1. Introduction

Applications arising in the geosciences and biosciences such as subsidence events, carbon sequestration, groundwater remediation, hydrocarbon production, and hydraulic fracturing, enhanced geothermal systems, solid waste disposal, and biomedical heart modeling, are driving the development of numerical models coupling flow and poromechanics. In this paper, we focus on deriving a posteriori error indicators for the Biot model that consists of a poromechanics equation coupled to a flow model with the displacement and pressure as unknowns. In contrast to solving the Biot system fully implicitly, we consider fixed stress iterative scheme that allows the decoupling of the flow and mechanics equations. The decoupling scheme offers several attractive features such as the use of existing flow and mechanics codes, use of appropriate preconditioners and solvers for the two models, and ease of implementation. The design of this approach which is currently quite popular is important in the formulation of efficient, convergent, and robust schemes.

In the fixed-stress split algorithm, the flow problem is solved first followed by the mechanics problem, and a constant mean total stress is assumed during the flow solve. Kim et al. [1] demonstrated stability for fixed stress and in [2–4] Mikelić and Wheeler established contractive property of the scheme. Besides, we note here that this approach can be interpreted as a preconditioner technique for solving the fully coupled system. For instance, the

* Corresponding author.
E-mail addresses: girault@ann.jussieu.fr (V. Girault), xueying@oden.utexas.edu (X. Lu), mfw@oden.utexas.edu (M.F. Wheeler).

https://doi.org/10.1016/j.cma.2020.113185
0045-7825/

work of Gai et al. [5] and Gai [6] involved interpreting this scheme as a physics-based preconditioning strategy applied to a Richardson fixed-point iteration. The same preconditioning technique was applied to the fully coupled system in the work of Castelletto et al. [7,8].

Several extensions of the fixed-stress split scheme have been studied. Almani et al. [9] and Kumar et al. [10] extended the fixed-stress split to the multirate case, in which flow takes multiple fine time steps within one coarse mechanics time step. Borregales [11] extended the fixed-stress split to a nonlinear case. Dana et al. [12,13] studied a multiscale extension of the fixed-stress split to a poroelastic–elastic system where the poromechanics equation is solved on a larger domain with a coarse grid and the flow equation is solved on a small domain with finer grid. Moreover, Bause et al. [14] and Borregales et al. [15] explored space–time methods of the fixed-stress split, and the work of Rodrigo et al. [16] considered the stability analysis of the discretization schemes. Storvik et al. [17] studied the optimal choice of the stabilization parameter used in the fixed-stress split. Lu and Wheeler [18] have recently extended the fixed-stress split to a three-way coupling, an adaptive asynchronous coupling scheme that allows over 97.5% reduction in poromechanics computational time due to not requiring the displacement to be computed for every time step.

Here we restrict our attention to the fixed-stress iterative coupling, analyze the enriched Galerkin method (EG) for flow and Galerkin for elasticity. This is an extension of the previous work on Galerkin and/or mixed finite element methods for flow [19] to EG. In the early works of Gai [6] and Wang [20] for two phase Biot system, it was observed that local mass conservation for flow was essential. In Biot studies in fractured porous media, Lee et al. [21] have demonstrated that EG is locally conservative and robust in treating fracture networks including quasi Newtonian flows arising in proppant stimulation. Choo and Lee [22] showed that local mass conservation can also be crucial to accurate simulation of deformation processes in fluid-infiltrated porous materials. Therefore, EG is an attractive method for flow discretization, locally mass conservative, giving rise to inexpensive residual error indicators that are easily incorporated in the code. Mixed methods are also well suited to local mass conservation. Recently, Ahmed et al. derived a posteriori estimates for fully mixed formulations of Biot model for both the monolithic scheme and the fixed-stress split scheme [23,24]. Their approach requires solving local auxiliary problems which are computationally costly. Li and Zikatanov [25] derived residual-based a posteriori error estimates of mixed methods for monolithic three-field Biot's consolidation model that does not require the calculation of local problems, which is promising to be extended for fixed-stress split schemes.

In this paper, we derive error equalities for each iteration of the fixed-stress algorithm at each time step, followed by residual-based a posteriori error estimates. These estimates are based on separate results extended to EG from [19]: contraction mapping, stability estimates and a priori error estimates for the discretized problem that incorporate convergence of the iteration at each time step. Here both lower bound (efficiency) and upper bound estimates (reliability) are obtained, but they are non-optimal in terms of efficiency in the sense that the lower bounds involve weak residual errors that cannot be computed numerically, see Section 6. The upper bound estimates represent an extension of Ern et al. [26] for the monolithic Biot system based on Galerkin approximations. In [26] no lower bounds were derived and as far as the authors are aware none have been derived to date for Galerkin schemes. In our theoretical work, it is clear that obtaining lower bounds for a posteriori errors is difficult, technical, and requires weak error terms that unfortunately do not lead to obtaining the effectivity index easily. This is further aggravated by the imbalance in the constants multiplying the pressure in the flow and displacement equations, see Section 8.1.

While the analysis presented here applies to the poroelastic system, a novel feature of this work involves a generalized poroelastic–elastic system that represents the coupled flow and poromechanics phenomena arising from hydrocarbon production or geological carbon sequestration in deep subsurface reservoirs. The reason for this choice is that in these phenomena the spatial domain in which fluid flow occurs is generally much smaller than the spatial domain over which significant deformation occurs. It also improves standard approaches. Indeed, the typical approaches model the same physics over one domain, either considers only the reservoir with an overburden pressure imposed directly or models the entire reservoir and surrounding rocks with zero permeability in the surrounding rocks. The former approach may misrepresent the mechanics boundary conditions and precludes the study of land subsidence or uplift whereas the latter approach is computationally prohibitive.

This work is organized as follows. In the subsection below we establish notation. In Section 2, a continuous-time model involving the decoupling of the model into elastic and poroelastic domains with interface conditions is formulated in primal variational form. The primal formulation, complete with the fixed-stress splitting algorithm,

is fully discretized with EG for flow and Galerkin for mechanics in Section 3. The a posteriori error equalities are derived in Section 4, and the error indicators are inferred from them. Section 5 is devoted to an upper bound for the total error. Section 6 introduces auxiliary weak residual errors. The lower bounds are discussed in Section 7. Computational results are presented in Section 8. Numerical results on the Mandel problem confirm these upper and lower error bounds. Moreover, the efficiency of using the a posteriori indicators to guide dynamic mesh adaptation and a novel stopping criterion for the fixed-stress iterations are presented. Finally, Section 9 draws some conclusions.

1.1. Notation

To be specific, the notation is expressed in three dimensions in a bounded connected open set $\Omega \subset \mathbb{R}^3$. The scalar product of $L^2(\Omega)$ is denoted by $(\cdot,\cdot)_\Omega$

$$\forall f, g \in L^2(\Omega), \quad (f,g)_\Omega = \int_\Omega f(\boldsymbol{x}) g(\boldsymbol{x}) d\boldsymbol{x},$$

and the index Ω is omitted when the domain of integration is clear from the context. For any non-negative integer m, the classical Sobolev space $H^m(\Omega)$ is defined by (cf. [27] or [28]),

$$H^m(\Omega) = \{v \in L^2(\Omega) \,:\, \partial^k v \in L^2(\Omega) \,\forall\, |k| \le m\},$$

where

$$\partial^k v = \frac{\partial^{|k|} v}{\partial x_1^{k_1} \partial x_2^{k_2} \partial x_3^{k_3}},$$

equipped with the following seminorm and norm for which it is a Hilbert space:

$$|v|_{H^m(\Omega)} = \left[\sum_{|k|=m} \int_\Omega |\partial^k v|^2 \, d\boldsymbol{x} \right]^{\frac{1}{2}}, \quad \|v\|_{H^m(\Omega)} = \left[\sum_{0 \le |k| \le m} |v|^2_{H^k(\Omega)} \right]^{\frac{1}{2}}.$$

This definition is extended to any real number $s = m + s'$ for an integer $m \ge 0$ and $0 < s' < 1$ by defining in dimension d the fractional semi-norm and norm, see [29] and [30],

$$|v|_{H^s(\Omega)} = \left(\sum_{|k|=m} \int_\Omega \int_\Omega \frac{|\partial^k v(\boldsymbol{x}) - \partial^k v(\boldsymbol{y})|^2}{|\boldsymbol{x}-\boldsymbol{y}|^{d+2s'}} \, d\boldsymbol{x}\, d\boldsymbol{y} \right)^{\frac{1}{2}}, \quad \|v\|_{H^s(\Omega)} = \left(\|v\|^2_{H^m(\Omega)} + |v|^2_{H^s(\Omega)} \right)^{\frac{1}{2}}.$$

These fractional order spaces are often used for traces. The following trace property holds in a domain Ω with a Lipschitz continuous boundary $\partial\Omega$: If v belongs to $H^s(\Omega)$ for some $s \in]\frac{1}{2}, 1]$, then its trace on $\partial\Omega$ belongs to $H^{s-\frac{1}{2}}(\partial\Omega)$ and there exists a constant C_s such that

$$\forall v \in H^s(\Omega), \ \|v\|_{H^{s-\frac{1}{2}}(\partial\Omega)} \le C_s \|v\|_{H^s(\Omega)}. \tag{1.1}$$

In particular, $H^{\frac{1}{2}}(\partial\Omega)$ is the trace space of $H^1(\Omega)$, with norm

$$|v|_{H^{\frac{1}{2}}(\Gamma)} = \left(\int_\Gamma \int_\Gamma \frac{|v(\boldsymbol{x}) - v(\boldsymbol{y})|^2}{|\boldsymbol{x}-\boldsymbol{y}|^d} d\boldsymbol{x}\, d\boldsymbol{y} \right)^{\frac{1}{2}},$$

and $H^{-\frac{1}{2}}(\partial\Omega)$ is the dual space of $H^{\frac{1}{2}}(\partial\Omega)$. Finally, if Γ is a subset of $\partial\Omega$ with positive measure, $|\Gamma| > 0$, we say that a function g in $H^{\frac{1}{2}}(\Gamma)$ belongs to $H^{\frac{1}{2}}_{00}(\Gamma)$ if its extension by zero to $\partial\Omega$ belongs to $H^{\frac{1}{2}}(\partial\Omega)$. It is a proper subspace of $H^{\frac{1}{2}}(\Gamma)$, and is normed by

$$\|v\|_{H^{\frac{1}{2}}_{00}(\Gamma)} = \left(|v|^2_{H^{\frac{1}{2}}(\Gamma)} + \int_\Gamma |v(\boldsymbol{x})|^2 \, \frac{d\boldsymbol{x}}{d(\boldsymbol{x},\Gamma)} \right)^{\frac{1}{2}}, \tag{1.2}$$

where $d(\boldsymbol{x},\Gamma)$ denotes the distance to Γ.

We also recall Korn's and Poincaré's inequalities both valid for all functions $\boldsymbol{v}$ in $H^1(\Omega)^3$ that vanish on Γ:

$$|\boldsymbol{v}|_{H^1(\Omega)} \le \mathcal{K} \|\boldsymbol{\varepsilon}(\boldsymbol{v})\|_{L^2(\Omega)}, \tag{1.3}$$

$$\|v\|_{L^2(\Omega)} \leq \mathcal{P}|v|_{H^1(\Omega)}, \tag{1.4}$$

where $\boldsymbol{\varepsilon}(\boldsymbol{v})$ is the strain tensor, and $\mathcal{K}$ and $\mathcal{P}$ are constants depending only on Ω and Γ. These imply

$$\|\boldsymbol{v}\|_{H^1(\Omega)} \leq C_1\|\boldsymbol{\varepsilon}(\boldsymbol{v})\|_{L^2(\Omega)}, \quad C_1 = \mathcal{K}\big(1+\mathcal{P}^2\big)^{\frac{1}{2}}. \tag{1.5}$$

A trace inequality for all functions $\boldsymbol{v}$ in $H^1(\Omega)^3$ that vanish on Γ can be obtained by combining the interpolation inequality

$$\forall v \in H^1(\Omega),\ \|v\|_{L^2(\Gamma)} \leq C(\Omega)\|v\|^{\frac{1}{2}}_{L^2(\Omega)}\|v\|^{\frac{1}{2}}_{H^1(\Omega)},$$

with (1.4) and (1.3),

$$\|\boldsymbol{v}\|_{L^2(\Gamma)} \leq C_2\|\boldsymbol{\varepsilon}(\boldsymbol{v})\|_{L^2(\Omega)}, \quad C_2 = C(\Omega)\big(\mathcal{K}\mathcal{P}C_1\big)^{\frac{1}{2}}. \tag{1.6}$$

As usual, for handling time-dependent problems, it is convenient to consider measurable functions defined on a time interval $]a,b[$ with values in a functional space, say X (cf. [29]). More precisely, let $\|\cdot\|_X$ denote the norm of X; then for any number r, $1 \leq r \leq \infty$, we define

$$L^r(a,b;X) = \{f \text{ measurable in }]a,b[\ : \int_a^b \|f(t)\|_X^r dt < \infty\},$$

equipped with the norm

$$\|f\|_{L^r(a,b;X)} = \left(\int_a^b \|f(t)\|_X^r dt\right)^{\frac{1}{r}},$$

with the usual modification if $r = \infty$. It is a Banach space if X is a Banach space, and for $r = 2$, it is a Hilbert space if X is a Hilbert space. Derivatives with respect to time are denoted by ∂_t and we define for instance

$$H^1(a,b;X) = \{f \in L^2(a,b;X) \ : \ \partial_t f \in L^2(a,b;X)\}.$$

2. Governing equations and formulation

Let Ω be a bounded, connected, Lipschitz domain in $\mathbb{R}^3$. We are interested in the situation where a poro-elastic model holds in a connected subset Ω_1 of Ω (the *pay-zone*), completely embedded into Ω, while an elastic model holds in Ω_2 (the *nonpay-zone*), see Fig. 1, where

$$\Omega_2 = \Omega \setminus \overline{\Omega}_1.$$

Let Γ_{12} denote the boundary of Ω_1, assumed to be Lipschitz, and let $\boldsymbol{n}_{12}$ be the unit normal on Γ_{12} exterior to Ω_1. In the examples we have in mind, Ω_1 is much smaller than Ω. This work extends readily to more general configurations, but for simplicity, we focus on this situation. Let the boundary of Ω, $\partial\Omega$, be partitioned into two disjoint open regions not necessarily connected, but with a finite number of connected components, each with Lipschitz-continuous boundaries,

$$\overline{\partial\Omega} = \overline{\Gamma_D} \cup \overline{\Gamma_N}.$$

We denote by $\boldsymbol{n}_\Omega$ the unit outward normal vector to $\partial\Omega$. To simplify, we assume that the measure of Γ_D is positive: $|\Gamma_D| > 0$.

Let $\boldsymbol{\sigma}$ be the effective linear elastic stress tensor,

$$\boldsymbol{\sigma}(\boldsymbol{u}) = 2G\boldsymbol{\varepsilon}(\boldsymbol{u}) + \lambda(\nabla\cdot\boldsymbol{u})\boldsymbol{I}, \tag{2.1}$$

where $\boldsymbol{\varepsilon}(\boldsymbol{u}) = \frac{1}{2}\big(\nabla\boldsymbol{u} + \nabla^t\boldsymbol{u}\big)$ is the symmetric gradient tensor, $\boldsymbol{I}$ the identity tensor, and $\lambda > 0$ and $G > 0$ are the Lamé coefficients. Let $\boldsymbol{\sigma}^{\text{por}}$ be the linear poro-elastic stress tensor

$$\boldsymbol{\sigma}^{\text{por}}(\boldsymbol{u}, p) = \boldsymbol{\sigma}(\boldsymbol{u}) - \alpha\, p\, \boldsymbol{I}, \tag{2.2}$$

where $\alpha > 0$ is the Biot–Willis coefficient. Let $\boldsymbol{f}$ be the body force in Ω. In the nonpay-zone, i.e., a.e. in $\Omega_2 \times]0,T[$, the governing equations for the displacement $\boldsymbol{u}$ are those of linear elasticity. In the pay-zone Ω_1, the equations are

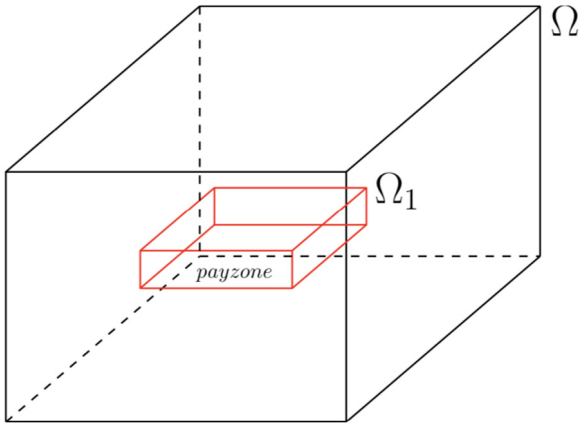

Fig. 1. Pay-zone with surrounding rock.

those of Biot's consolidation model for a linear elastic, homogeneous, isotropic, porous solid saturated with a slightly compressible single-phase fluid. The unknowns are the solid's displacement $\boldsymbol{u}$ and the fluid's pressure p. This model is based on a *quasi-static* assumption, namely it assumes that the material deformation is much slower than the flow rate, and hence the second time derivative of the displacement (i.e., the acceleration) is zero. After linearization and simplifications, it leads to the following system of equations in $\Omega \times]0, T[$,

$$\begin{aligned}
-\nabla \cdot (\lambda(\nabla \cdot \boldsymbol{u})\boldsymbol{I} + 2G\boldsymbol{\varepsilon}(\boldsymbol{u}) - \alpha p \boldsymbol{I}) &= \boldsymbol{f} \quad \text{in } \Omega_1 \times]0, T[,\\
-\nabla \cdot (\lambda(\nabla \cdot \boldsymbol{u})\boldsymbol{I} + 2G\boldsymbol{\varepsilon}(\boldsymbol{u})) &= \boldsymbol{f} \quad \text{in } \Omega_2 \times]0, T[,\\
\partial_t \left(\frac{1}{M} p + \alpha \nabla \cdot \boldsymbol{u} \right) - \frac{1}{\mu_f} \nabla \cdot \left(\boldsymbol{\kappa} (\nabla\, p - \rho_{f,r} g \nabla\, \eta) \right) &= q \quad \text{in } \Omega_1 \times]0, T[,\\
-\frac{1}{\mu_f} \boldsymbol{\kappa} (\nabla p - \rho_{f,r} g \nabla \eta) \cdot \boldsymbol{n}_{12} &= 0 \quad \text{on } \partial\Omega_1 \times]0, T[,\\
[\boldsymbol{u}] &= \boldsymbol{0} \quad \text{on } \partial\Omega_1 \times]0, T[,\\
[\boldsymbol{\sigma}(\boldsymbol{u})]\boldsymbol{n}_{12} &= \alpha\, p\, \boldsymbol{n}_{12} \quad \text{on } \partial\Omega_1 \times]0, T[,\\
\boldsymbol{u} &= \boldsymbol{0} \quad \text{on } \Gamma_D \times]0, T[,\\
\boldsymbol{\sigma}\boldsymbol{n}_\Omega &= \boldsymbol{t}_N \quad \text{on } \Gamma_N \times]0, T[,\\
p(0) &= p_0 \quad \text{in } \Omega_1,
\end{aligned} \tag{2.3}$$

where $M > 0$ is the Biot modulus, μ_f the fluid's viscosity, $\boldsymbol{\kappa}$ the permeability tensor, g the gravity constant, $\rho_{f,r}$ the reference density, η a signed distance in the vertical direction, q a given volumetric fluid source or sink term, and $\boldsymbol{t}_N$ a given normal traction. At initial time, $\boldsymbol{u}(0)$ is defined by the above system with $p(0) = p_0$, except of course, the third and fourth equations. Note that the only boundary conditions on the pressure p are transmission conditions since Ω_1 has no exterior boundary. The tensor $\boldsymbol{\kappa}$ is assumed to be independent of time, symmetric, bounded and uniformly positive definite in space, with largest eigenvalue $\lambda_{\max}$ and smallest eigenvalue $\lambda_{\min} > 0$,

$$\text{a.e. } \boldsymbol{x} \in \Omega_1\,,\ \lambda_{\min} \le \lambda_i(\boldsymbol{x}) \le \lambda_{\max}, \quad i = 1, 2, 3. \tag{2.4}$$

For the sake of simplicity, we assume in addition that the coefficients of $\boldsymbol{\kappa}$ belong locally to some finite-dimensional space, such as a polynomial space. This assumption can be avoided by a suitable approximation of $\boldsymbol{\kappa}$, but it complicates the analysis, see for instance [31].

To simplify the notation, the density indices f and r will be dropped and $\rho_{f,r}$ will be replaced from now on by ρ.

The mean stress $\bar{\sigma}$ that will be used in the algorithm is defined by

$$\bar{\sigma} = K_b \nabla \cdot \boldsymbol{u} - \alpha\, p, \tag{2.5}$$

where K_b is the drained bulk modulus, $K_b = \lambda + \frac{2}{3}G$.

2.1. Primal variational formulation

Define the spaces:

$$H^1_{0D}(\Omega) = \{v \in H^1(\Omega) \,:\, v|_{\Gamma_D} = 0\}, \quad \boldsymbol{W} = H^1_{0D}(\Omega)^d. \tag{2.6}$$

As shown by Girault et al. [32], problem (2.3) has the following equivalent variational formulation, for every solution belonging to the spaces below:

Find $\boldsymbol{u} \in L^\infty(0,T;\boldsymbol{W})$ and $p \in L^\infty(0,T;L^2(\Omega_1)) \cap L^2(0,T;H^1(\Omega_1))$ solving a. e. in $]0,T[$

$$2\mu(\boldsymbol{\epsilon}(\boldsymbol{u}),\boldsymbol{\epsilon}(\boldsymbol{v}))_\Omega + \lambda(\nabla\cdot\boldsymbol{u},\nabla\cdot\boldsymbol{v})_\Omega = (\boldsymbol{f},\boldsymbol{v})_\Omega + \alpha(p,\nabla\cdot\boldsymbol{v})_{\Omega_1} + (\boldsymbol{t}_N,\boldsymbol{v})_{\Gamma_N}, \quad \forall \boldsymbol{v} \in \boldsymbol{W}, \tag{2.7}$$

$$\left(\partial_t\left(\frac{1}{M}p + \alpha\nabla\cdot\boldsymbol{u}\right),\theta\right)_{\Omega_1} + \frac{1}{\mu_f}\big(\boldsymbol{\kappa}(\nabla p - \rho\, g\nabla\eta),\nabla\theta\big)_{\Omega_1} = (q,\theta)_{\Omega_1}, \quad \forall\theta \in H^1(\Omega_1), \tag{2.8}$$

with the initial condition

$$p(0) = p_0 \quad \text{in } \Omega_1. \tag{2.9}$$

This problem has a unique solution for all sufficiently smooth data, say $\boldsymbol{f} \in H^1(0,T;L^2(\Omega)^d)$, $q \in L^2(\Omega\times]0,T[)$, $\boldsymbol{t}_N \in H^1(0,T;H^{-\frac{1}{2}}(\Gamma_N)^d)$, see [33]. The scalar product on Γ_N in (2.7) stands for the duality pairing between $H^{-\frac{1}{2}}(\Gamma_N)^d$ and $H^{\frac{1}{2}}_{00}(\Gamma_N)^d$.

3. Enriched Galerkin approximation

3.1. Mesh and spaces

For $h > 0$, let $\mathcal{T}_h$ be a regular family of conforming simplicial meshes of the domain $\overline{\Omega}$, with h the maximum element diameter. The family of meshes is regular in the sense of Ciarlet [34]: there exists a constant $\sigma > 0$, independent of h, such that

$$\frac{h_E}{\varrho_E} \le \sigma, \quad \forall E \in \mathcal{T}_h, \tag{3.1}$$

where h_E is the diameter of E and ϱ_E the diameter of the ball inscribed in E. We assume that

$$\mathcal{T}_h = \mathcal{T}_h^1 \cup \mathcal{T}_h^2,$$

where $\mathcal{T}_h^1$ is a conforming simplicial mesh of Ω_1 and $\mathcal{T}_h^2$ a conforming simplicial mesh of Ω_2. Let $\mathcal{E}_h$ denote the set of all interior faces of $\mathcal{T}_h$ and $\mathcal{E}_h^\partial$ the set of all its boundary faces. For any e in $\mathcal{E}_h$, ω_e denotes the union of the elements adjacent to e. We suppose that

$$\mathcal{E}_h^\partial = \mathcal{E}_h^{D,\partial} \cup \mathcal{E}_h^{N,\partial},$$

where $\mathcal{E}_h^{D,\partial}$ is the set of all faces lying on Γ_D and $\mathcal{E}_h^{N,\partial}$ those lying on Γ_N. The set of all faces interior to Ω_1 is $\mathcal{E}_h^1$ and that interior to Ω_2 is $\mathcal{E}_h^2$. Finally, the set of faces on Γ_{12} is $\mathcal{E}_h^{12}$. A unit normal vector $\boldsymbol{n}_e$ is attributed to each e in $\mathcal{E}_h$ and $\mathcal{E}_h^\partial$; its direction can be freely chosen. Here, the following rule is applied: if $e \in \mathcal{E}_h^\partial$, then $\boldsymbol{n}_e = \boldsymbol{n}_\Omega$, the exterior normal to Ω; if e is in $\mathcal{E}_h^1$ or $\mathcal{E}_h^2$, then $\boldsymbol{n}_e$ points from E_i to E_j, where E_i and E_j are the two elements of $\mathcal{T}_h$ adjacent to e and the number of E_i is smaller than that of E_j. Finally, if $e \in \mathcal{E}_h^{12}$, then $\boldsymbol{n}_e = \boldsymbol{n}_{12}$, the outward normal to Ω_1. The jumps and averages of any function f on $e \in \mathcal{E}_h$ (smooth enough to have a trace) are defined by

$$[f(\boldsymbol{x})]_e := f(\boldsymbol{x})|_{E_i} - f(\boldsymbol{x})|_{E_j}, \quad \text{when } \boldsymbol{n}_e \text{ points from } E_i \text{ to } E_j,$$

$$\{f(\boldsymbol{x})\}_e := \frac{1}{2}\big(f(\boldsymbol{x})|_{E_i} + f(\boldsymbol{x})|_{E_j}\big).$$

When $e \in \mathcal{E}_h^\partial$, the jump and average coincide with the trace on e.

Let $k \ge 1$ and $m \ge 1$ be two integers. On this mesh, we introduce first the following standard finite element spaces:

$$\boldsymbol{W}_h := \{\boldsymbol{v} \in \boldsymbol{W} \,:\, \boldsymbol{v}|_E \in \mathbb{P}_m(E)^d, \forall E \in \mathcal{T}_h\}, \tag{3.2}$$

$$Q_h = \{q \in H^1(\Omega_1) \,:\, q|_E \in \mathbb{P}_k(E), \forall E \in \mathcal{T}_h^1\}. \tag{3.3}$$

Next, the space Q_h is enriched by piecewise constants in each cell, whence the name enriched,

$$M_h = Q_h + \{q \in L^2(\Omega_1) \,:\, q|_E \in \mathbb{P}_0(E), \forall E \in \mathcal{T}_h^1\}. \tag{3.4}$$

The displacement will be discretized in $\boldsymbol{W}_h$ and the pressure in M_h, and because of the discontinuous constants in M_h, the discrete flow equations will be locally mass conservative. Their structure will be the same as that of a discontinuous Galerkin formulation, but as the jumps involve only constants, their coding will be simpler.

As the exact solution is not necessarily smooth, it is approximated by Scott & Zhang interpolants (see [35]),

$$R_h \in \mathcal{L}(\boldsymbol{W}, \boldsymbol{W}_h), \;\; \Pi_h \in \mathcal{L}(H^1(\Omega_1), Q_h). \tag{3.5}$$

Considering the degree of the polynomial functions in $\boldsymbol{W}_h$ and Q_h, these interpolants have the following quasi-local approximation errors:

$$\forall E \in \mathcal{T}_h, \forall \boldsymbol{v} \in H^s(E)^d \,,\; |\boldsymbol{v} - R_h(\boldsymbol{v})|_{H^j(E)} \le C\, h_E^{s-j} |\boldsymbol{v}|_{H^s(\Delta_E)} \,,\; 1 \le s \le m+1,\; 0 \le j \le s, \tag{3.6}$$

$$\forall E \in \mathcal{T}_h^1, \forall q \in H^s(E) \,,\; |q - \Pi_h(q)|_{H^j(E)} \le C\, h_E^{s-j} |q|_{H^s(\Delta_E)} \,,\; 1 \le s \le k+1,\; 0 \le j \le s, \tag{3.7}$$

with constants C independent of E and h_E, where Δ_E is a small patch of elements including E containing the values used in computing the approximation.

Regarding approximation in time, the interval $[0, T]$ is divided into N equal subintervals with length Δt and endpoints $t_n = n\Delta t$. The choice of equal time steps is a simplification; the material below extends readily to variable time steps. The data is assumed to be continuous in time, and we set a.e. in Ω

$$\boldsymbol{f}^n(\boldsymbol{x}) = \boldsymbol{f}(\boldsymbol{x}, t_n), \;\; q^n(\boldsymbol{x}) = q(\boldsymbol{x}, t_n), \;\; \boldsymbol{t}_N^n(\boldsymbol{x}) = \boldsymbol{t}_N(\boldsymbol{x}, t_n). \tag{3.8}$$

3.2. Fixed-stress iterative coupling

With these spaces, the fully discrete split problem is:

Initialization. Set

$$p_h^0 = \Pi_h(p_0). \tag{3.9}$$

Compute $\boldsymbol{u}_h^0 \in \boldsymbol{W}_h$ and $\bar{\sigma}_h^0$ by solving

$$\forall \boldsymbol{v}_h \in \boldsymbol{W}_h \,,\; 2G\big(\boldsymbol{\varepsilon}(\boldsymbol{u}_h^0), \boldsymbol{\varepsilon}(\boldsymbol{v}_h)\big)_\Omega + \lambda\big(\nabla\cdot\boldsymbol{u}_h^0, \nabla\cdot\boldsymbol{v}_h\big)_\Omega = \alpha\,\big(p_h^0, \nabla\cdot\boldsymbol{v}_h\big)_{\Omega_1} + (\boldsymbol{f}^0, \boldsymbol{v}_h)_\Omega + \big(\boldsymbol{t}_N^0, \boldsymbol{v}_h\big)_{\Gamma_N}, \tag{3.10}$$

and setting

$$\bar{\sigma}_h^0 = K_b \nabla\cdot\boldsymbol{u}_h^0 - \alpha\, p_h^0. \tag{3.11}$$

Time step $n \ge 1$.

1. Set $p_h^{n,0} = p_h^{n-1}$, $\boldsymbol{u}_h^{n,0} = \boldsymbol{u}_h^{n-1}$, and $\bar{\sigma}_h^{n,0} = \bar{\sigma}_h^{n-1}$.
2. For $\ell \ge 1$, compute

   (a) $p_h^{n,\ell} \in M_h$ by solving

$$\begin{aligned}
\forall \theta_h \in M_h, \quad & \Big(\frac{1}{M} + \frac{\alpha^2}{K_b}\Big)\frac{1}{\Delta t}\big(p_h^{n,\ell} - p_h^{n-1}, \theta_h\big)_{\Omega_1} + \frac{1}{\mu_f}\sum_{E\in\mathcal{T}_h^1}\big(\boldsymbol{\kappa}(\nabla\, p_h^{n,\ell} - \rho g \nabla\,\eta), \nabla\,\theta_h\big)_E \\
& - \frac{1}{\mu_f}\sum_{e\in\mathcal{E}_h^1}\Big(\big(\{\boldsymbol{\kappa}(\nabla\, p_h^{n,\ell} - \rho g\nabla\,\eta)\cdot\boldsymbol{n}_e\}_e, [\theta_h]_e\big)_e + \tau_p\big(\{\boldsymbol{\kappa}\nabla\,\theta_h\cdot\boldsymbol{n}_e\}_e, [p_h^{n,\ell}]_e\big)_e\Big) \\
& + \frac{1}{\mu_f}\sum_{e\in\mathcal{E}_h^1}\frac{\gamma_e}{h_e}\big([p_h^{n,\ell}]_e, [\theta_h]_e\big)_e = -\frac{\alpha}{K_b}\frac{1}{\Delta t}\big(\bar{\sigma}_h^{n,l-1} - \bar{\sigma}_h^{n-1}, \theta_h\big)_{\Omega_1} + (q^n, \theta_h)_{\Omega_1};
\end{aligned} \tag{3.12}$$

(b) the predictor of the difference in fluid content δ_ϕ^p by

$$\delta_\phi^p := \Big(\frac{1}{M} + \frac{\alpha^2}{K_b}\Big)(p_h^{n,\ell} - p_h^{n,\ell-1}); \tag{3.13}$$

(c) $\boldsymbol{u}_h^{n,\ell} \in \boldsymbol{W}_h$ by solving for all $\boldsymbol{v}_h \in \boldsymbol{W}_h$,

$$2G\big(\boldsymbol{\varepsilon}(\boldsymbol{u}_h^{n,\ell}), \boldsymbol{\varepsilon}(\boldsymbol{v}_h)\big)_\Omega + \lambda\big(\nabla\cdot\boldsymbol{u}_h^{n,\ell}, \nabla\cdot\boldsymbol{v}_h\big)_\Omega = \alpha\big(p_h^{n,\ell}, \nabla\cdot\boldsymbol{v}_h\big)_{\Omega_1} + \big(\boldsymbol{f}^n, \boldsymbol{v}_h\big)_\Omega + \big(\boldsymbol{t}_N^n, \boldsymbol{v}_h\big)_{\Gamma_N}; \tag{3.14}$$

(d) $\bar\sigma_h^{n,\ell}$ by

$$\bar\sigma_h^{n,\ell} = K_b\nabla\cdot\boldsymbol{u}_h^{n,\ell} - \alpha p_h^{n,\ell}; \tag{3.15}$$

(e) the corrector of the difference in fluid content δ_ϕ^c by

$$\delta_\phi^c := \alpha\nabla\cdot(\boldsymbol{u}_h^{n,\ell} - \boldsymbol{u}_h^{n,\ell-1}) + \frac{1}{M}(p_h^{n,\ell} - p_h^{n,\ell-1}). \tag{3.16}$$

If

$$\big\|\delta_\phi^c - \delta_\phi^p\big\|_{L^\infty(\Omega_1)} > \varepsilon,$$

set $\ell \leftarrow \ell + 1$ and return to (a);
else, set

$$\ell_n := \ell, \quad p_h^n := p_h^{n,\ell_n}, \quad \boldsymbol{u}_h^n := \boldsymbol{u}_h^{n,\ell_n}, \quad \bar\sigma_h^n := \bar\sigma_h^{n,\ell_n}, \tag{3.17}$$

march in time $n \leftarrow n + 1$ and return to 1.

Note that

$$\delta_\phi^c - \delta_\phi^p = \frac{\alpha}{K_b}\big(\bar\sigma_h^{n,\ell} - \bar\sigma_h^{n,\ell-1}\big),$$

and hence the stopping criterion rests on the difference between two iterates of the mean stress. The choice of parameter τ_p leads to different EG schemes. For example, $\tau_p = 1$ leads to the Symmetric Interior Penalty Galerkin (SIPG) scheme, $\tau_p = 0$ leads to the Incomplete Interior Penalty Galerkin (IIPG) scheme, and $\tau_p = -1$ results in the Non-symmetric Interior Penalty Galerkin (NIPG) scheme. For the sake of brevity, we shall mostly focus here on the SIPG scheme. Through the choice of parameters $\gamma_e > 0$, the penalty jump term in (3.12) has the effect of determining the allowable amount of discontinuity across an edge. The parameters can also be modified to take into account the variation of $\boldsymbol{\kappa}$ as in [36], but, as this option complicates the a posteriori analysis, it has not been chosen here. Considering the uniform positive definiteness of the permeability tensor $\boldsymbol{\kappa}$, the parameters γ_e can be tuned so that the system (3.12) has one and only one solution for each right-hand side, see Lemma 2 in Appendix. On the other hand, owing to Korn's inequality, (3.14) is always uniquely solvable for each right-hand side. Thus this algorithm generates a unique sequence. As expected, the approach of [3] can be extended to establish unconditional geometric convergence of the algorithm in the case of NIPG, and conditional geometric convergence, when the parameters γ_e are sufficiently large, in the case of SIPG or IIPG (see Lemma 2 and (A.13) in the Appendix). Under the same conditions, stability estimates and optimal a priori error bounds can be derived, similar to those in [19].

4. A posteriori error equations

In this section, we derive error equalities that bring forth residuals arising during computations. At this stage, the data is assumed to be as smooth as needed.

For a posteriori estimates, it is convenient to interpolate the discrete sequences in time. Thus, for any discrete function in time v^n, let

$$v_\tau^n = v^{n-1} + \frac{t - t_{n-1}}{\Delta t}(v^n - v^{n-1}), \quad t \in [t_{n-1}, t_n]. \tag{4.1}$$

For the sake of conciseness, we shall use the following bilinear forms on the space $H^1(\Omega)+M_h$:

$$\forall p,\theta\in H^1(\Omega)+M_h,\quad J_h(p,\theta):=\sum_{e\in\mathcal{E}_h^1}\frac{\gamma_e}{h_e}\big([p]_e,[\theta]_e\big)_e,$$

$$\forall p,\theta\in H^1(\Omega)+M_h,\quad \big(p,\theta\big)_h:=\sum_{E\in\mathcal{T}_h^1}\big(\boldsymbol{\kappa}\nabla p,\nabla\theta\big)_E,$$

$$\forall p,\theta\in H^1(\Omega)+M_h,\quad (\!(p,\theta)\!)_h:=\big(p,\theta\big)_h+J_h(p,\theta),$$

together with the seminorm

$$\forall\theta\in H^1(\Omega)+M_h,\quad |\theta|_h:=\big(\theta,\theta\big)_h^{\frac12},\tag{4.2}$$

and norm

$$\forall\theta\in H^1(\Omega)+M_h,\quad \|\theta\|_h:=(\!(\theta,\theta)\!)_h^{\frac12}.\tag{4.3}$$

The subscript E (resp. ω_e) is added when these quantities are restricted to E (resp. ω_e).

4.1. Flow error equation

The idea is to derive an error equality tested with an arbitrary function θ in a suitable Sobolev space. The beginning of the following derivation is classical.

With the above notation, the discrete flow equation (3.12) reads in each interval $]t_{n-1},t_n]$

$$\begin{aligned}\forall\theta_h\in M_h,\quad &\Big(\frac1M+\frac{\alpha^2}{K_b}\Big)\big(\partial_t p_{h\tau}^{n,\ell},\theta_h\big)_{\Omega_1}+\frac{1}{\mu_f}\Big((\!(p_h^{n,\ell},\theta_h)\!)_h-\sum_{E\in\mathcal{T}_h^1}\big(\rho g\boldsymbol{\kappa}\nabla\eta,\nabla\theta_h\big)_E\Big)\\&-\frac{1}{\mu_f}\sum_{e\in\mathcal{E}_h^1}\Big(\big(\{\boldsymbol{\kappa}(\nabla p_h^{n,\ell}-\rho g\nabla\eta)\cdot\boldsymbol{n}_e\}_e,[\theta_h]_e\big)_e+\tau_p\big(\{\boldsymbol{\kappa}\nabla\theta_h\cdot\boldsymbol{n}_e\}_e,[p_h^{n,\ell}]_e\big)_e\Big)\\&=-\frac{\alpha}{K_b}\big(\partial_t\bar\sigma_{h\tau}^{n,\ell-1},\theta_h\big)_{\Omega_1}+(q^n,\theta_h)_{\Omega_1}.\end{aligned}\tag{4.4}$$

Hence, assuming that p belongs to $H^{1+\varepsilon}(\Omega_1)$ for some $\varepsilon>0$, and $\partial_t p$ and $\nabla\cdot(\partial_t\boldsymbol{u})$ are sufficiently smooth in each interval $]t_{n-1},t_n]$, the flow's error equation, tested with θ_h, is

$$\begin{aligned}\forall\theta_h\in M_h,\quad &\Big(\frac1M+\frac{\alpha^2}{K_b}\Big)\big(\partial_t(p-p_{h\tau}^{n,\ell}),\theta_h\big)_{\Omega_1}+\frac{1}{\mu_f}(\!(p-p_h^{n,\ell},\theta_h)\!)_h\\&-\frac{1}{\mu_f}\sum_{e\in\mathcal{E}_h^1}\Big(\big(\{\boldsymbol{\kappa}\nabla(p-p_h^{n,\ell})\cdot\boldsymbol{n}_e\}_e,[\theta_h]_e\big)_e+\tau_p\big(\{\boldsymbol{\kappa}\nabla\theta_h\cdot\boldsymbol{n}_e\}_e,[p-p_h^{n,\ell}]_e\big)_e\Big)\\&+\frac{\alpha}{K_b}\big(\partial_t(\bar\sigma-\bar\sigma_{h\tau}^{n,\ell-1}),\theta_h\big)_{\Omega_1}=(q-q^n,\theta_h)_{\Omega_1}.\end{aligned}\tag{4.5}$$

On the other hand, for all $E\in\mathcal{T}_h^1$, let $\theta|_E$ belong to $H^{1+\varepsilon}(E)$, for some $\varepsilon>0$. The exact flow equation (2.8) tested with $\theta-\theta_h$ reads in each interval $]t_{n-1},t_n]$,

$$\begin{aligned}\forall\theta_h\in M_h,\quad &\Big(\frac1M+\frac{\alpha^2}{K_b}\Big)(\partial_t p,\theta-\theta_h)_{\Omega_1}+\frac{1}{\mu_f}\Big((\!(p,\theta-\theta_h)\!)_h-\sum_{E\in\mathcal{T}_h^1}\big(\rho g\boldsymbol{\kappa}\nabla\eta,\nabla(\theta-\theta_h)\big)_E\Big)\\&-\frac{1}{\mu_f}\sum_{e\in\mathcal{E}_h^1}\Big(\big(\{\boldsymbol{\kappa}(\nabla p-\rho g\nabla\eta)\cdot\boldsymbol{n}_e\}_e,[\theta-\theta_h]_e\big)_e+\tau_p\big(\{\boldsymbol{\kappa}\nabla(\theta-\theta_h)\cdot\boldsymbol{n}_e\}_e,[p]_e\big)_e\Big)\\&=-\frac{\alpha}{K_b}\big(\partial_t\bar\sigma,\theta-\theta_h\big)_{\Omega_1}+(q,\theta-\theta_h)_{\Omega_1}.\end{aligned}\tag{4.6}$$

Therefore, by writing $\theta = \theta - \theta_h + \theta_h$ and using (4.4) and (4.6), the flow error tested with any $\theta|_E \in H^{1+\varepsilon}(E)$ for all $E \in \mathcal{T}_h^1$, becomes for all $\theta_h \in M_h$, in each interval $]t_{n-1}, t_n]$,

$$
\begin{aligned}
&\Big(\frac{1}{M} + \frac{\alpha^2}{K_b}\Big)(\partial_t(p - p_{h\tau}^{n,\ell}), \theta)_{\Omega_1} + \frac{1}{\mu_f}(\!(p - p_h^{n,\ell}, \theta)\!)_h \\
&- \frac{1}{\mu_f}\sum_{e\in\mathcal{E}_h^1}\Big(\big(\{\boldsymbol{\kappa}\nabla(p - p_h^{n,\ell})\cdot\boldsymbol{n}_e\}_e, [\theta]_e\big)_e + \tau_p\big(\{\boldsymbol{\kappa}\nabla\theta\cdot\boldsymbol{n}_e\}_e, [p - p_h^{n,\ell}]_e\big)_e\Big) + \frac{\alpha}{K_b}\big(\partial_t(\bar\sigma - \bar\sigma_{h\tau}^{n,\ell-1}), \theta\big)_{\Omega_1} \\
&= (q, \theta - \theta_h)_{\Omega_1} - \Big[\ \Big(\frac{1}{M} + \frac{\alpha^2}{K_b}\Big)(\partial_t p_{h\tau}^{n,\ell}, \theta - \theta_h)_{\Omega_1} + \frac{1}{\mu_f}\Big((\!(p_h^{n,\ell}, \theta - \theta_h)\!)_h - \sum_{E\in\mathcal{T}_h^1}\big(\rho g\boldsymbol{\kappa}\nabla\eta, \nabla(\theta - \theta_h)\big)_E\Big) \\
&\qquad - \frac{1}{\mu_f}\sum_{e\in\mathcal{E}_h^1}\Big(\big(\{\boldsymbol{\kappa}(\nabla p_h^{n,\ell} - \rho g\nabla\eta)\cdot\boldsymbol{n}_e\}_e, [\theta - \theta_h]_e\big)_e + \tau_p\big(\{\boldsymbol{\kappa}\nabla(\theta - \theta_h)\cdot\boldsymbol{n}_e\}_e, [p_h^{n,\ell}]_e\big)_e\Big) \\
&\qquad + \frac{\alpha}{K_b}\big(\partial_t\bar\sigma_{h\tau}^{n,l-1}, \theta - \theta_h\big)_{\Omega_1}\ \Big] + (q - q^n, \theta_h)_{\Omega_1}.
\end{aligned}
\tag{4.7}
$$

This equality is modified first by observing that

$$
(q^n, \theta_h)_{\Omega_1} = (q_h^n, \theta_h)_{\Omega_1} \text{ and } (q, \theta - \theta_h)_{\Omega_1} + (q - q_h^n, \theta_h)_{\Omega_1} = (q - q_h^n, \theta)_{\Omega_1} + (q_h^n, \theta - \theta_h)_{\Omega_1},
$$

where q_h denotes the L^2 projection on $\mathbb{P}_k$ in each cell E; and next by applying Green's formula in each cell E

$$
\begin{aligned}
-\sum_{E\in\mathcal{T}_h^1}\big(\,\boldsymbol{\kappa}(\nabla p_h^{n,\ell} - \rho g\nabla\eta), \nabla(\theta - \theta_h)\,\big)_E &= \sum_{E\in\mathcal{T}_h^1}\big(\nabla\cdot(\boldsymbol{\kappa}(\nabla p_h^{n,\ell} - \rho g\nabla\eta)), \theta - \theta_h\big)_E \\
&- \sum_{e\in\mathcal{E}_h^1}\Big(\big([\boldsymbol{\kappa}(\nabla p_h^{n,\ell} - \rho g\nabla\eta)\cdot\boldsymbol{n}_e]_e, \{\theta - \theta_h\}_e\big)_e + \big(\{\boldsymbol{\kappa}(\nabla p_h^{n,\ell} - \rho g\nabla\eta)\cdot\boldsymbol{n}_e\}_e, [\theta - \theta_h]_e\big)_e\Big) \\
&- \sum_{e\in\mathcal{E}_h^{12}}\big(\boldsymbol{\kappa}(\nabla p_h^{n,\ell} - \rho g\nabla\eta)\cdot\boldsymbol{n}_{12}, \theta - \theta_h\big)_e
\end{aligned}
$$

Then (4.7) becomes for all $\theta|_E \in H^{1+\varepsilon}(E)$ for all $E \in \mathcal{T}_h^1$, all $\theta_h \in M_h$, and in each interval $]t_{n-1}, t_n]$,

$$
\begin{aligned}
&\Big(\frac{1}{M} + \frac{\alpha^2}{K_b}\Big)(\partial_t(p - p_{h\tau}^{n,\ell}), \theta)_{\Omega_1} + \frac{1}{\mu_f}(\!(p - p_h^{n,\ell}, \theta)\!)_h \\
&- \frac{1}{\mu_f}\sum_{e\in\mathcal{E}_h^1}\Big(\big(\{\boldsymbol{\kappa}\nabla(p - p_h^{n,\ell})\cdot\boldsymbol{n}_e\}_e, [\theta]_e\big)_e + \tau_p\big(\{\boldsymbol{\kappa}\nabla\theta\cdot\boldsymbol{n}_e\}_e, [p - p_h^{n,\ell}]_e\big)_e\Big) + \frac{\alpha}{K_b}\big(\partial_t(\bar\sigma - \bar\sigma_{h\tau}^{n,\ell-1}), \theta\big)_{\Omega_1} \\
&= (q - q_h^n, \theta)_{\Omega_1} \\
&+ \sum_{E\in\mathcal{T}_h^1}\big(q_h^n - \big(\frac{1}{M} + \frac{\alpha^2}{K_b}\big)\partial_t p_{h\tau}^{n,\ell} + \frac{1}{\mu_f}\nabla\cdot\big(\boldsymbol{\kappa}(\nabla p_h^{n,\ell} - \rho g\nabla\eta)\big) - \frac{\alpha}{K_b}\partial_t\bar\sigma_{h\tau}^{n,\ell-1}, \theta - \theta_h\big)_E \\
&- \frac{1}{\mu_f}\sum_{e\in\mathcal{E}_h^1}\Big(\big([\boldsymbol{\kappa}(\nabla p_h^{n,\ell} - \rho g\nabla\eta)\cdot\boldsymbol{n}_e]_e, \{\theta - \theta_h\}_e\big)_e - \tau_p\big(\{\boldsymbol{\kappa}\nabla(\theta - \theta_h)\cdot\boldsymbol{n}_e\}_e, [p_h^{n,\ell}]_e\big)_e\Big) \\
&- \frac{1}{\mu_f}\sum_{e\in\mathcal{E}_h^{12}}\big(\boldsymbol{\kappa}(\nabla p_h^{n,\ell} - \rho g\nabla\eta)\cdot\boldsymbol{n}_{12}, \theta - \theta_h\big)_e - \frac{1}{\mu_f}J_h(p_h^{n,\ell}, \theta - \theta_h).
\end{aligned}
\tag{4.8}
$$

Up to this point, the approach presented above is similar to that of [26] for a monolithic scheme. But now, we want to bring forth the effect of the algorithmic error. To this end, we express the time derivative in the left-hand side of (4.8) as it appears in (2.8). By means of formula (2.5) for the mean stress $\bar\sigma$, this gives the following version

of the flow error equality:

$$\begin{aligned}
&\Big(\partial_t\big(\frac{1}{M}(p-p_{h\tau}^{n,\ell})+\alpha\nabla\cdot(\boldsymbol{u}-\boldsymbol{u}_{h\tau}^{n,\ell})\big),\theta\Big)_{\Omega_1}+\frac{1}{\mu_f}(\!(p-p_h^{n,\ell},\theta)\!)_h\\
&=(q-q_h^n,\theta)_{\Omega_1}+\sum_{E\in\mathcal{T}_h^1}\Big(q_h^n-\partial_t(\frac{1}{M}p_{h\tau}^{n,\ell}+\alpha\nabla\cdot\boldsymbol{u}_{h\tau}^{n,\ell})+\frac{1}{\mu_f}\nabla\cdot\big(\boldsymbol{\kappa}(\nabla p_h^{n,\ell}-\rho g\nabla\eta)\big),\theta-\theta_h\Big)_E\\
&+\frac{1}{\mu_f}\sum_{e\in\mathcal{E}_h^1}\Big(\big(\{\boldsymbol{\kappa}\nabla(p-p_h^{n,\ell})\cdot\boldsymbol{n}_e\}_e,[\theta]_e\big)_e+\tau_p\big(\{\boldsymbol{\kappa}\nabla\theta\cdot\boldsymbol{n}_e\}_e,[p-p_h^{n,\ell}]_e\big)_e\Big)\\
&-\frac{1}{\mu_f}\sum_{e\in\mathcal{E}_h^1}\Big(\big([\boldsymbol{\kappa}(\nabla p_h^{n,\ell}-\rho g\nabla\eta)\cdot\boldsymbol{n}_e]_e,\{\theta-\theta_h\}_e\big)_e-\tau_p\big(\{\boldsymbol{\kappa}\nabla(\theta-\theta_h)\cdot\boldsymbol{n}_e\}_e,[p_h^{n,\ell}]_e\big)_e\Big)\\
&-\frac{1}{\mu_f}\sum_{e\in\mathcal{E}_h^{12}}\big(\boldsymbol{\kappa}(\nabla p_h^{n,\ell}-\rho g\nabla\eta)\cdot\boldsymbol{n}_{12},\theta-\theta_h\big)_e-\frac{1}{\mu_f}J_h(p_h^{n,\ell},\theta-\theta_h)-\frac{\alpha}{K_b}\big(\partial_t(\bar\sigma_{h\tau}^{n,\ell}-\bar\sigma_{h\tau}^{n,\ell-1}),\theta_h\big)_{\Omega_1}.
\end{aligned}\tag{4.9}$$

4.2. Elasticity error equation

Again, the idea is to derive an error equality tested with an arbitrary function $\boldsymbol{v}$ in a suitable Sobolev space. We proceed as above, with the exception of the last step. First, we interpolate linearly in time (3.14) in each subinterval and use the L^2 projection $\boldsymbol{f}_h$ of $\boldsymbol{f}$ on $\mathbb{P}_m^3$ in each cell E and the L^2 projection $\boldsymbol{t}_{N,h}$ of $\boldsymbol{t}_N$ on $\mathbb{P}_m^3$ in each face e of $\mathcal{E}_h^{N,\partial}$. Then the discrete elasticity error equation reads in each interval $]t_{n-1},t_n]$

$$\begin{aligned}
\forall\boldsymbol{v}_h\in\boldsymbol{W}_h,\quad &2G\big(\boldsymbol{\varepsilon}(\boldsymbol{u}_{h\tau}^{n,\ell}-\boldsymbol{u}),\boldsymbol{\varepsilon}(\boldsymbol{v}_h)\big)_\Omega+\lambda\big(\nabla\cdot(\boldsymbol{u}_{h\tau}^{n,\ell}-\boldsymbol{u}),\nabla\cdot\boldsymbol{v}_h\big)_\Omega-\alpha\big(p_{h\tau}^{n,\ell}-p,\nabla\cdot\boldsymbol{v}_h\big)_{\Omega_1}\\
&=\big(\boldsymbol{f}_{h\tau}^n-\boldsymbol{f},\boldsymbol{v}_h\big)_\Omega+\big(\boldsymbol{t}_{N,h\tau}^n-\boldsymbol{t}_N,\boldsymbol{v}_h\big)_{\Gamma_N}.
\end{aligned}\tag{4.10}$$

Next, the exact elasticity equation (2.7), tested with $\boldsymbol{v}-\boldsymbol{v}_h$, for all $\boldsymbol{v}$ in $\boldsymbol{W}$ at any time gives

$$\begin{aligned}
\forall\boldsymbol{v}_h\in\boldsymbol{W}_h,\quad &2G(\boldsymbol{\epsilon}(\boldsymbol{u}),\boldsymbol{\epsilon}(\boldsymbol{v}-\boldsymbol{v}_h))_\Omega+\lambda(\nabla\cdot\boldsymbol{u},\nabla\cdot(\boldsymbol{v}-\boldsymbol{v}_h))_\Omega-\alpha(p,\nabla\cdot(\boldsymbol{v}-\boldsymbol{v}_h))_{\Omega_1}\\
&=(\boldsymbol{f},\boldsymbol{v}-\boldsymbol{v}_h)_\Omega+(\boldsymbol{t}_N,\boldsymbol{v}-\boldsymbol{v}_h)_{\Gamma_N}.
\end{aligned}\tag{4.11}$$

Therefore, we infer from (4.10) and (4.11) the following elasticity error equation in each interval $]t_{n-1},t_n]$:

$$\begin{aligned}
\forall\boldsymbol{v}_h\in\boldsymbol{W}_h,\quad &2G(\boldsymbol{\epsilon}(\boldsymbol{u}-\boldsymbol{u}_{h\tau}^{n,\ell}),\boldsymbol{\epsilon}(\boldsymbol{v}))_\Omega+\lambda(\nabla\cdot(\boldsymbol{u}-\boldsymbol{u}_{h\tau}^{n,\ell}),\nabla\cdot\boldsymbol{v})_\Omega-\alpha(p-p_{h\tau}^{n,\ell},\nabla\cdot\boldsymbol{v})_{\Omega_1}\\
&=(\boldsymbol{f}-\boldsymbol{f}_{h\tau}^n,\boldsymbol{v}_h)_\Omega+(\boldsymbol{t}_N-\boldsymbol{t}_{N,h\tau}^n,\boldsymbol{v}_h)_{\Gamma_N}+(\boldsymbol{f},\boldsymbol{v}-\boldsymbol{v}_h)_\Omega+(\boldsymbol{t}_N,\boldsymbol{v}-\boldsymbol{v})_{\Gamma_N}\\
&-\Big[2G(\boldsymbol{\epsilon}(\boldsymbol{u}_{h\tau}^{n,\ell}),\boldsymbol{\epsilon}(\boldsymbol{v}-\boldsymbol{v}_h))_\Omega+\lambda(\nabla\cdot(\boldsymbol{u}_{h\tau}^{n,\ell}),\nabla\cdot(\boldsymbol{v}-\boldsymbol{v}_h))_\Omega-\alpha(p_{h\tau}^{n,\ell},\nabla\cdot(\boldsymbol{v}-\boldsymbol{v}_h))_{\Omega_1}\Big].
\end{aligned}\tag{4.12}$$

Finally, (4.12) is modified by using

$$(\boldsymbol{f},\boldsymbol{v}-\boldsymbol{v}_h)_\Omega+(\boldsymbol{f}-\boldsymbol{f}_{h\tau}^n,\boldsymbol{v}_h)_\Omega=(\boldsymbol{f}-\boldsymbol{f}_{h\tau}^n,\boldsymbol{v})_\Omega+(\boldsymbol{f}_{h\tau}^n,\boldsymbol{v}-\boldsymbol{v}_h)_\Omega,$$

a similar expression for $\boldsymbol{t}_N$, and Green's formula in each cell E. This yields in each interval $]t_{n-1},t_n]$, for all $\boldsymbol{v}$ in $\boldsymbol{W}$

$$\begin{aligned}
\forall\boldsymbol{v}_h\in\boldsymbol{W}_h,\quad &2G(\boldsymbol{\epsilon}(\boldsymbol{u}-\boldsymbol{u}_{h\tau}^{n,\ell}),\boldsymbol{\epsilon}(\boldsymbol{v}))_\Omega+\lambda(\nabla\cdot(\boldsymbol{u}-\boldsymbol{u}_{h\tau}^{n,\ell}),\nabla\cdot\boldsymbol{v})_\Omega-\alpha(p-p_{h\tau}^{n,\ell},\nabla\cdot\boldsymbol{v})_{\Omega_1}\\
&=(\boldsymbol{f}-\boldsymbol{f}_{h\tau}^n,\boldsymbol{v})_\Omega+(\boldsymbol{t}_N-\boldsymbol{t}_{N,h\tau}^n,\boldsymbol{v})_{\Gamma_N}\\
&+\sum_{E\in\mathcal{T}_h^1}(\boldsymbol{f}_{h\tau}^n+\nabla\cdot\boldsymbol{\sigma}(\boldsymbol{u}_{h\tau}^{n,\ell})-\alpha\nabla\,p_{h\tau}^{n,\ell},\boldsymbol{v}-\boldsymbol{v}_h)_E+\sum_{E\in\mathcal{T}_h^2}(\boldsymbol{f}_{h\tau}^n+\nabla\cdot\boldsymbol{\sigma}(\boldsymbol{u}_{h\tau}^{n,\ell}),\boldsymbol{v}-\boldsymbol{v}_h)_E\\
&-\sum_{e\in\mathcal{E}_h}\big([\boldsymbol{\sigma}(\boldsymbol{u}_{h\tau}^{n,\ell})]_e\boldsymbol{n}_e,\boldsymbol{v}-\boldsymbol{v}_h\big)_e+\alpha\sum_{e\in\mathcal{E}_h^1\cup\mathcal{E}_h^{12}}\big([p_{h\tau}^{n,\ell}]_e,(\boldsymbol{v}-\boldsymbol{v}_h)\cdot\boldsymbol{n}_e\big)_e\\
&-\big(\boldsymbol{\sigma}(\boldsymbol{u}_{h\tau}^{n,\ell})\boldsymbol{n}_\Omega-\boldsymbol{t}_{N,h\tau}^n,\boldsymbol{v}-\boldsymbol{v}_h\big)_{\Gamma_N}.
\end{aligned}\tag{4.13}$$

Note that (4.13) is valid at initial time (i.e. when $n = 0$). Note also that when the data and solution are smooth enough, (4.13) can be differentiated with respect to time,

$$\begin{aligned}
&\big(\boldsymbol{\sigma}(\partial_t(\boldsymbol{u}-\boldsymbol{u}_{h\tau}^{n,\ell})),\boldsymbol{\varepsilon}(\boldsymbol{v})\big)_\Omega-\alpha\big(\partial_t(p-p_{h\tau}^{n,\ell}),\nabla\cdot\boldsymbol{v}\big)_{\Omega_1}=\big(\partial_t(\boldsymbol{f}-\boldsymbol{f}_{h\tau}^n),\boldsymbol{v}\big)_\Omega+\big(\partial_t(\boldsymbol{t}_N-\boldsymbol{t}_{N,h\tau}^n),\boldsymbol{v}\big)_{\Gamma_N}\\
&+\sum_{E\in\mathcal{T}_h^1}\big(\partial_t\boldsymbol{f}_{h\tau}^n+\nabla\cdot\boldsymbol{\sigma}(\partial_t\boldsymbol{u}_{h\tau}^{n,\ell})-\alpha\nabla\,\partial_t p_{h\tau}^{n,\ell},\boldsymbol{v}-\boldsymbol{v}_h\big)_E+\sum_{E\in\mathcal{T}_h^2}\big(\partial_t\boldsymbol{f}_{h\tau}^n+\nabla\cdot\boldsymbol{\sigma}(\partial_t\boldsymbol{u}_{h\tau}^{n,\ell}),\boldsymbol{v}-\boldsymbol{v}_h\big)_E\\
&-\sum_{e\in\mathcal{E}_h}\big([\boldsymbol{\sigma}(\partial_t\boldsymbol{u}_{h\tau}^{n,\ell})]_e\boldsymbol{n}_e,\boldsymbol{v}-\boldsymbol{v}_h\big)_e+\alpha\sum_{e\in\mathcal{E}_h^1\cup\mathcal{E}_h^{12}}\big(\partial_t[p_{h\tau}^{n,\ell}]_e,(\boldsymbol{v}-\boldsymbol{v}_h)\cdot\boldsymbol{n}_e\big)_e\\
&-\big(\boldsymbol{\sigma}(\partial_t\boldsymbol{u}_{h\tau}^{n,\ell})\boldsymbol{n}_\Omega-\partial_t\boldsymbol{t}_{N,h\tau}^n,\boldsymbol{v}-\boldsymbol{v}_h\big)_{\Gamma_N}.
\end{aligned}\tag{4.14}$$

4.3. Final error equation

In the spirit of [26,37], an upper bound for the error is obtained by testing, in each interval, (4.9) with $\theta = p - p_{h\tau}^{n,\ell}$, (4.13) with $\boldsymbol{v} = \partial_t(\boldsymbol{u} - \boldsymbol{u}_{h\tau}^{n,\ell})$ and substituting the expression for

$$-\alpha(p - p_{h\tau}^{n,\ell}, \nabla\cdot\partial_t(\boldsymbol{u} - \boldsymbol{u}_{h\tau}^{n,\ell}))_{\Omega_1},$$

into the resulting error flow equation. This gives an equation in each subinterval with left-hand side

$$\begin{aligned}
\text{LHS} :=&\frac{1}{2M}\frac{d}{dt}\|p-p_{h\tau}^{n,\ell}\|_{L^2(\Omega_1)}^2+G\frac{d}{dt}\|\boldsymbol{\varepsilon}(\boldsymbol{u}-\boldsymbol{u}_{h\tau}^{n,\ell})\|_{L^2(\Omega)}^2+\frac{\lambda}{2}\frac{d}{dt}\|\nabla\cdot(\boldsymbol{u}-\boldsymbol{u}_{h\tau}^{n,\ell})\|_{L^2(\Omega)}^2\\
&+\frac{1}{\mu_f}\|p-p_{h\tau}^{n,\ell}\|_h^2,
\end{aligned}\tag{4.15}$$

and right-hand side for all $\theta_h \in H^1(0,T;M_h)$ and all $\boldsymbol{v}_h \in H^1(0,T;\boldsymbol{W}_h)$,

$$\begin{aligned}
\text{RHS} :=&\frac{1}{\mu_f}(\!(p_h^{n,\ell}-p_{h\tau}^{n,\ell},p-p_{h\tau}^{n,\ell})\!)_h-\frac{\alpha}{K_b}\big(\partial_t(\bar\sigma_{h\tau}^{n,\ell}-\bar\sigma_{h\tau}^{n,\ell-1}),\theta_h\big)_{\Omega_1}\\
&+\sum_{E\in\mathcal{T}_h^1}\big(q_h^n-\partial_t(\frac{1}{M}p_{h\tau}^{n,\ell}+\alpha\nabla\cdot\boldsymbol{u}_{h\tau}^{n,\ell})+\frac{1}{\mu_f}\nabla\cdot\big(\boldsymbol{\kappa}(\nabla p_h^{n,\ell}-\rho g\nabla\eta)\big),p-p_{h\tau}^{n,\ell}-\theta_h\big)_E\\
&+\frac{1}{\mu_f}\sum_{e\in\mathcal{E}_h^1}\Big(\big(\{\boldsymbol{\kappa}\nabla(p-p_h^{n,\ell})\cdot\boldsymbol{n}_e\}_e,[p-p_{h\tau}^{n,\ell}]_e\big)_e+\tau_p\big(\{\boldsymbol{\kappa}\nabla(p-p_{h\tau}^{n,\ell})\cdot\boldsymbol{n}_e\}_e,[p-p_h^{n,\ell}]_e\big)_e\Big)\\
&-\frac{1}{\mu_f}\sum_{e\in\mathcal{E}_h^1}\Big(\big([\boldsymbol{\kappa}(\nabla p_h^{n,\ell}-\rho g\nabla\eta)\cdot\boldsymbol{n}_e]_e,\{p-p_{h\tau}^{n,\ell}-\theta_h\}_e\big)_e\\
&-\tau_p\big(\{\boldsymbol{\kappa}\nabla(p-p_{h\tau}^{n,\ell}-\theta_h)\cdot\boldsymbol{n}_e\}_e,[p_h^{n,\ell}]_e\big)_e\Big)\\
&-\frac{1}{\mu_f}\sum_{e\in\mathcal{E}_h^{12}}\big(\boldsymbol{\kappa}(\nabla p_h^{n,\ell}-\rho g\nabla\eta)\cdot\boldsymbol{n}_{12},p-p_{h\tau}^{n,\ell}-\theta_h\big)_e-\frac{1}{\mu_f}J_h(p_h^{n,\ell},p-p_{h\tau}^{n,\ell}-\theta_h)\\
&+\sum_{E\in\mathcal{T}_h^1}\big(\boldsymbol{f}_{h\tau}^n+\nabla\cdot\boldsymbol{\sigma}(\boldsymbol{u}_{h\tau}^{n,\ell})-\alpha\nabla\,p_{h\tau}^{n,\ell},\partial_t(\boldsymbol{u}-\boldsymbol{u}_{h\tau}^{n,\ell}-\boldsymbol{v}_h)\big)_E\\
&+\sum_{E\in\mathcal{T}_h^2}\big(\boldsymbol{f}_{h\tau}^n+\nabla\cdot\boldsymbol{\sigma}(\boldsymbol{u}_{h\tau}^{n,\ell}),\partial_t(\boldsymbol{u}-\boldsymbol{u}_{h\tau}^{n,\ell}-\boldsymbol{v}_h)\big)_E-\sum_{e\in\mathcal{E}_h}\big([\sigma(\boldsymbol{u}_{h\tau}^{n,\ell})]_e\boldsymbol{n}_e,\partial_t(\boldsymbol{u}-\boldsymbol{u}_{h\tau}^{n,\ell}-\boldsymbol{v}_h)\big)_e\\
&+\alpha\sum_{e\in\mathcal{E}_h^1\cup\mathcal{E}_h^{12}}\big([p_{h\tau}^{n,\ell}]_e,\partial_t(\boldsymbol{u}-\boldsymbol{u}_{h\tau}^{n,\ell}-\boldsymbol{v}_h)\cdot\boldsymbol{n}_e\big)_e-\big(\boldsymbol{\sigma}(\boldsymbol{u}_{h\tau}^{n,\ell})\boldsymbol{n}_\Omega-\boldsymbol{t}_{N,h\tau}^n,\partial_t(\boldsymbol{u}-\boldsymbol{u}_{h\tau}^{n,\ell}-\boldsymbol{v}_h)\big)_{\Gamma_N}\\
&+\big(q-q_h^n,p-p_{h\tau}^{n,\ell}\big)_{\Omega_1}+\big(\boldsymbol{f}-\boldsymbol{f}_{h\tau}^n,\partial_t(\boldsymbol{u}-\boldsymbol{u}_{h\tau}^{n,\ell})\big)_\Omega+\big(\boldsymbol{t}_N-\boldsymbol{t}_{N,h\tau}^n,\partial_t(\boldsymbol{u}-\boldsymbol{u}_{h\tau}^{n,\ell})\big)_{\Gamma_N}.
\end{aligned}\tag{4.16}$$

For each n and ℓ, in each interval $]t_{n-1},t_n]$, the usual choice of function $\boldsymbol{v}_h$ is

$$\boldsymbol{v}_h = R_h(\boldsymbol{u}-\boldsymbol{u}_{h\tau}^{n,\ell}),\tag{4.17}$$

whereas the simplest choice for θ_h, considering that M_h contains the constant functions, is the integral mean value in each cell E,

$$\theta_h|_E = m_E(p - p_{h\tau}^{n,\ell}) := \frac{1}{|E|}\int_E (p - p_{h\tau}^{n,\ell}). \tag{4.18}$$

As the surface terms involving $\boldsymbol{\kappa}\nabla p \cdot \boldsymbol{n}$ cannot be controlled by the left-hand side, we apply the argument introduced in [38]. It consists in extracting the problematic surface terms from the consistency error Eq. (4.5) and thus expressing them as functions of quantities that can be estimated. Since these terms depend on the choice of parameter τ_p, to simplify the discussion, we choose from now on $\tau_p = 1$ (i.e., the case SIPG), the other cases are slightly simpler because they involve less terms. With θ_h defined by (4.18), the sum of these surface terms is

$$\frac{1}{\mu_f}\sum_{e\in\mathcal{E}_h^1}\big(\{\boldsymbol{\kappa}\nabla(p - p_h^{n,\ell})\cdot\boldsymbol{n}_e\}_e, [-p_{h\tau}^{n,\ell}]_e\big)_e = -\frac{1}{\mu_f}\sum_{e\in\mathcal{E}_h^1}\big(\{\boldsymbol{\kappa}\nabla(p - p_h^{n,\ell})\cdot\boldsymbol{n}_e\}_e, [p_{h\tau}^{n,\ell} - \theta]_e\big)_e, \tag{4.19}$$

for any function θ in $H^1(0,T;Q_h^1)$, where Q_h^1 denotes the space Q_h defined in (3.3) with degree $k = 1$ (thus having no jump). Then the flow error Eq. (4.5) tested with $p_{h\tau}^{n,\ell} - \theta \in M_h$ yields

$$\begin{aligned}
-\frac{1}{\mu_f}\sum_{e\in\mathcal{E}_h^1}\big(\{\boldsymbol{\kappa}\nabla(p - p_h^{n,\ell})\cdot\boldsymbol{n}_e\}_e, [p_{h\tau}^{n,\ell} - \theta]_e\big)_e &= -\Big(\frac{1}{M} + \frac{\alpha^2}{K_b}\Big)\big(\partial_t(p - p_{h\tau}^{n,\ell}), p_{h\tau}^{n,\ell} - \theta\big)_{\Omega_1}\\
&\quad - \frac{1}{\mu_f}(\!(p - p_h^{n,\ell}, p_{h\tau}^{n,\ell} - \theta)\!)_h + \frac{1}{\mu_f}\sum_{e\in\mathcal{E}_h^1}\big(\{\boldsymbol{\kappa}\nabla(p_{h\tau}^{n,\ell} - \theta)\cdot\boldsymbol{n}_e\}_e, [p - p_h^{n,\ell}]_e\big)_e\\
&\quad - \frac{\alpha}{K_b}\big(\partial_t(\bar\sigma - \bar\sigma_{h\tau}^{n,\ell-1}), p_{h\tau}^{n,\ell} - \theta\big)_{\Omega_1} + (q - q_h^n, p_{h\tau}^{n\ell} - \theta)_{\Omega_1}.
\end{aligned}$$

Bringing forth the algorithmic error, this can be written

$$\begin{aligned}
-\frac{1}{\mu_f}\sum_{e\in\mathcal{E}_h^1}\big(\{\boldsymbol{\kappa}\nabla(p - p_h^{n,\ell})\cdot\boldsymbol{n}_e\}_e, [p_{h\tau}^{n,\ell} - \theta]_e\big)_e &= -\big(\partial_t\big(\frac{1}{M}(p - p_{h\tau}^{n,\ell}) + \alpha\nabla\cdot(\boldsymbol{u} - \boldsymbol{u}_{h\tau}^{n,\ell})\big), p_{h\tau}^{n,\ell} - \theta\big)_{\Omega_1}\\
&\quad - \frac{1}{\mu_f}(\!(p - p_h^{n,\ell}, p_{h\tau}^{n,\ell} - \theta)\!)_h + \frac{1}{\mu_f}\sum_{e\in\mathcal{E}_h^1}\big(\{\boldsymbol{\kappa}\nabla(p_{h\tau}^{n,\ell} - \theta)\cdot\boldsymbol{n}_e\}_e, [p - p_h^{n,\ell}]_e\big)_e\\
&\quad - \frac{\alpha}{K_b}\big(\partial_t(\bar\sigma_{h\tau}^{n,\ell} - \bar\sigma_{h\tau}^{n,\ell-1}), p_{h\tau}^{n,\ell} - \theta\big)_{\Omega_1} + (q - q_h^n, p_{h\tau}^{n\ell} - \theta)_{\Omega_1}.
\end{aligned}$$

Considering that θ does not jump, the double scalar product has the expression

$$-\frac{1}{\mu_f}(\!(p - p_h^{n,\ell}, p_{h\tau}^{n,\ell} - \theta)\!)_h = -\frac{1}{\mu_f}\big(p - p_h^{n,\ell}, p_{h\tau}^{n,\ell} - \theta\big)_h + \frac{1}{\mu_f}J_h(p_h^{n,\ell}, p_{h\tau}^{n,\ell}).$$

Thus

$$\begin{aligned}
-\frac{1}{\mu_f}\sum_{e\in\mathcal{E}_h^1}\big(\{\boldsymbol{\kappa}\nabla(p - p_h^{n,\ell})\cdot\boldsymbol{n}_e\}_e, [p_{h\tau}^{n,\ell} - \theta]_e\big)_e &= -\big(\partial_t\big(\frac{1}{M}(p - p_{h\tau}^{n,\ell}) + \alpha\nabla\cdot(\boldsymbol{u} - \boldsymbol{u}_{h\tau}^{n,\ell})\big), p_{h\tau}^{n,\ell} - \theta\big)_{\Omega_1}\\
&\quad - \frac{1}{\mu_f}\big(p - p_h^{n,\ell}, p_{h\tau}^{n,\ell} - \theta\big)_h + \frac{1}{\mu_f}J_h(p_h^{n,\ell}, p_{h\tau}^{n,\ell}) + \frac{1}{\mu_f}\sum_{e\in\mathcal{E}_h^1}\big(\{\boldsymbol{\kappa}\nabla(p_{h\tau}^{n,\ell} - \theta)\cdot\boldsymbol{n}_e\}_e, [p - p_h^{n,\ell}]_e\big)_e\\
&\quad - \frac{\alpha}{K_b}\big(\partial_t(\bar\sigma_{h\tau}^{n,\ell} - \bar\sigma_{h\tau}^{n,\ell-1}), p_{h\tau}^{n,\ell} - \theta\big)_{\Omega_1} + (q - q_h^n, p_{h\tau}^{n\ell} - \theta)_{\Omega_1}.
\end{aligned}$$

Therefore, by substituting this equality into (4.16) and (4.15), we derive

$$
\begin{aligned}
\text{LHS} =& \frac{1}{\mu_f}(\!(p_h^{n,\ell} - p_{h\tau}^{n,\ell}, p - p_{h\tau}^{n,\ell})\!)_h - \frac{1}{\mu_f}\big(p - p_h^{n,\ell}, p_{h\tau}^{n,\ell} - \theta\big)_h + \frac{1}{\mu_f} J_h(p_h^{n,\ell}, 2p_{h\tau}^{n,\ell} + \theta_h) \\
&- \frac{\alpha}{K_b}\big(\partial_t(\bar{\sigma}_{h\tau}^{n,\ell} - \bar{\sigma}_{h\tau}^{n,\ell-1}), \theta_h\big)_{\Omega_1} - \frac{\alpha}{K_b}\big(\partial_t(\bar{\sigma}_{h\tau}^{n,\ell} - \bar{\sigma}_{h\tau}^{n,\ell-1}), p_{h\tau}^{n,\ell} - \theta\big)_{\Omega_1} \\
&+ \sum_{E\in\mathcal{T}_h^1}\big(q_h^n - \partial_t(\frac{1}{M}p_{h\tau}^{n,\ell} + \alpha\nabla\cdot\boldsymbol{u}_{h\tau}^{n,\ell}) + \frac{1}{\mu_f}\nabla\cdot\big(\boldsymbol{\kappa}(\nabla p_h^{n,\ell} - \rho g\nabla\eta)\big), p - p_{h\tau}^{n,\ell} - \theta_h\big)_E \\
&- \frac{1}{\mu_f}\sum_{e\in\mathcal{E}_h^1\cup\mathcal{E}_h^{12}}\Big(\big([\boldsymbol{\kappa}(\nabla p_h^{n,\ell} - \rho g\nabla\eta)\cdot\boldsymbol{n}_e]_e, \{p - p_{h\tau}^{n,\ell} - \theta_h\}_e\big)_e \\
&+ \frac{1}{\mu_f}\sum_{e\in\mathcal{E}_h^1}\big(\{\boldsymbol{\kappa}\nabla(p_{h\tau}^{n,\ell} - \theta)\cdot\boldsymbol{n}_e\}_e, [p - p_h^{n,\ell}]_e\big)_e \\
&+ \big(q - q_h^n - \partial_t\big(\frac{1}{M}(p - p_{h\tau}^{n,\ell}) + \alpha\nabla\cdot(\boldsymbol{u} - \boldsymbol{u}_{h\tau}^{n,\ell})\big), p_{h\tau}^{n,\ell} - \theta\big)_{\Omega_1} + \big(q - q_h^n, p - p_{h\tau}^{n,\ell}\big)_{\Omega_1} \\
&+ \sum_{E\in\mathcal{T}_h^1}\big(\boldsymbol{f}_{h\tau}^n + \nabla\cdot\boldsymbol{\sigma}(\boldsymbol{u}_{h\tau}^{n,\ell}) - \alpha\nabla\, p_{h\tau}^{n,\ell}, \partial_t(\boldsymbol{u} - \boldsymbol{u}_{h\tau}^{n,\ell} - \boldsymbol{v}_h)\big)_E \\
&+ \sum_{E\in\mathcal{T}_h^2}\big(\boldsymbol{f}_{h\tau}^n + \nabla\cdot\boldsymbol{\sigma}(\boldsymbol{u}_{h\tau}^{n,\ell}), \partial_t(\boldsymbol{u} - \boldsymbol{u}_{h\tau}^{n,\ell} - \boldsymbol{v}_h)\big)_E - \sum_{e\in\mathcal{E}_h}\big([\boldsymbol{\sigma}(\boldsymbol{u}_{h\tau}^{n,\ell})]_e\boldsymbol{n}_e, \partial_t(\boldsymbol{u} - \boldsymbol{u}_{h\tau}^{n,\ell} - \boldsymbol{v}_h)\big)_e \\
&+ \alpha\sum_{e\in\mathcal{E}_h^1\cup\mathcal{E}_h^{12}}\big([p_{h\tau}^{n,\ell}]_e, \partial_t(\boldsymbol{u} - \boldsymbol{u}_{h\tau}^{n,\ell} - \boldsymbol{v}_h)\cdot\boldsymbol{n}_e\big)_e - \big(\boldsymbol{\sigma}(\boldsymbol{u}_{h\tau}^{n,\ell})\boldsymbol{n}_\Omega - \boldsymbol{t}_{N,h\tau}^n, \partial_t(\boldsymbol{u} - \boldsymbol{u}_{h\tau}^{n,\ell} - \boldsymbol{v}_h)\big)_{\Gamma_N} \\
&+ \big(\boldsymbol{f} - \boldsymbol{f}_{h\tau}^n, \partial_t(\boldsymbol{u} - \boldsymbol{u}_{h\tau}^{n,\ell})\big)_\Omega + \big(\boldsymbol{t}_N - \boldsymbol{t}_{N,h\tau}^n, \partial_t(\boldsymbol{u} - \boldsymbol{u}_{h\tau}^{n,\ell})\big)_{\Gamma_N}.
\end{aligned}
\tag{4.20}
$$

Note that this formulation requires that $\partial_t\big(\frac{1}{M}p + \alpha\nabla\cdot\boldsymbol{u}\big)$ be sufficiently smooth to be tested against piecewise polynomial functions.

The functions $\boldsymbol{v}_h$ and θ_h have been chosen by (4.17) and (4.18), respectively. To choose θ, recall that $p_{h\tau} = p_{h\tau}^{\text{ct}} + p_{h\tau}^{\text{disc}}$, where ct denotes its continuous part and disc its discontinuous constant part. Then we take

$$
\theta = p_{h\tau}^{\text{ct}} + S_h(p_{h\tau}^{\text{disc}}), \tag{4.21}
$$

where S_h is an approximation operator of Scott & Zhang type [35] that is globally C^0 and piecewise $\mathbb{P}_1$ in each cell, see [39]. More precisely, for any node $\boldsymbol{a}$ of $\bar{\Omega}_1$, we choose an element $E_{\boldsymbol{a}}$ in $\bar{\Omega}_1$ with vertex $\boldsymbol{a}$, set

$$
S_h(p_{h\tau}^{\text{disc}})(\boldsymbol{a}) = p_{h\tau}^{\text{disc}}|_{E_{\boldsymbol{a}}},
$$

and

$$
\forall\boldsymbol{x}\in\bar{\Omega}_1, \quad S_h(p_{h\tau}^{\text{disc}})(\boldsymbol{x}) = \sum_{\boldsymbol{a}} p_{h\tau}^{\text{disc}}(E_{\boldsymbol{a}})\phi_{\boldsymbol{a}}(\boldsymbol{x}), \tag{4.22}
$$

where $\phi_{\boldsymbol{a}}$ is the standard piecewise $\mathbb{P}_1$ basis function and $\boldsymbol{a}$ runs over all vertices of elements in $\bar{\Omega}_1$.

Now, for each n, we consider (4.20) for the last iterate $\ell = \ell_n$ that achieves convergence of the discrete mean stress so that we can drop everywhere the index ℓ except when it appears as $\ell - 1$, i.e., $p_{h\tau}^n := p_{h\tau}^{n,\ell_n}$, $\boldsymbol{u}_{h\tau}^n := \boldsymbol{u}_{h\tau}^{n,\ell_n}$. In addition, to avoid a multiplicity of notation, we denote by v_h^n the step function in time that takes the value v_h^n in the interval $]t_{n-1}, t_n]$. Then, we integrate both sides of (4.20) from 0 to t, $0 < t \le T$, say $t_{m-1} < t \le t_m$, and again to simplify, this integral of the step function v_h^n is denoted by $\int_0^t v_h$. At this stage, we observe that the time derivative of $\boldsymbol{u} - \boldsymbol{u}_{h\tau}$ and $p - p_{h\tau}$ cannot be absorbed by the left-hand side; and hence will have to be integrated

by parts. Thus, we derive the following error equality:

$$
\begin{aligned}
&\frac{1}{2M}\|(p-p_{h\tau})(t)\|^2_{\Omega_1}+G\|\boldsymbol{\varepsilon}(\boldsymbol{u}-\boldsymbol{u}_{h\tau})(t)\|^2_{\Omega}+\frac{\lambda}{2}\|\nabla\cdot(\boldsymbol{u}-\boldsymbol{u}_{h\tau})(t)\|^2_{\Omega}+\frac{1}{\mu_f}\int_0^t\|p-p_{h\tau}\|_h^2\\
&=\frac{1}{\mu_f}\int_0^t(\!(p_h-p_{h\tau},p-p_{h\tau})\!)_h-\frac{1}{\mu_f}\int_0^t\big(p-p_h,p_{h\tau}-\theta\big)_h+\frac{1}{\mu_f}\int_0^t J_h(p_h,2p_{h\tau}+\theta_h)\\
&-\frac{\alpha}{K_b}\int_0^t\big(\partial_t(\bar\sigma_{h\tau}-\bar\sigma_{h\tau}^{\ell-1}),\theta_h\big)_{\Omega_1}-\frac{\alpha}{K_b}\int_0^t\big(\partial_t(\bar\sigma_{h\tau}-\bar\sigma_{h\tau}^{\ell-1}),p_{h\tau}-\theta\big)_{\Omega_1}\\
&+\int_0^t\sum_{E\in\mathcal{T}_h^1}\Big(q_h-\partial_t(\frac{1}{M}p_{h\tau}+\alpha\nabla\cdot\boldsymbol{u}_{h\tau})+\frac{1}{\mu_f}\nabla\cdot\big(\boldsymbol{\kappa}(\nabla p_h-\rho g\nabla\eta)\big),p-p_{h\tau}-\theta_h\Big)_E\\
&-\frac{1}{\mu_f}\int_0^t\sum_{e\in\mathcal{E}_h^1\cup\mathcal{E}_h^{12}}\Big(\big([\boldsymbol{\kappa}(\nabla p_h-\rho g\nabla\eta)\cdot\boldsymbol{n}_e]_e,\{p-p_{h\tau}-\theta_h\}_e\big)_e+\frac{1}{\mu_f}\int_0^t\sum_{e\in\mathcal{E}_h^1}\big(\{\boldsymbol{\kappa}\nabla(p_{h\tau}-\theta)\cdot\boldsymbol{n}_e\}_e,[p-p_h]_e\big)_e\Big)\\
&+\int_0^t\Big(\big(q-q_h,p_{h\tau}-\theta\big)_{\Omega_1}+\big(q-q_h,p-p_{h\tau}\big)_{\Omega_1}\Big)+\int_0^t\big(\frac{1}{M}(p-p_{h\tau})+\alpha\nabla\cdot(\boldsymbol{u}-\boldsymbol{u}_{h\tau}),\partial_t(p_{h\tau}-\theta)\big)_{\Omega_1}\\
&-\int_0^t\sum_{E\in\mathcal{T}_h^1}\big(\partial_t(\boldsymbol{f}_{h\tau}+\nabla\cdot\boldsymbol{\sigma}(\boldsymbol{u}_{h\tau})-\alpha\nabla p_{h\tau}),\boldsymbol{u}-\boldsymbol{u}_{h\tau}-\boldsymbol{v}_h\big)_E\\
&-\int_0^t\sum_{E\in\mathcal{T}_h^2}\big(\partial_t(\boldsymbol{f}_{h\tau}+\nabla\cdot\boldsymbol{\sigma}(\boldsymbol{u}_{h\tau})),\boldsymbol{u}-\boldsymbol{u}_{h\tau}-\boldsymbol{v}_h\big)_E+\int_0^t\sum_{e\in\mathcal{E}_h}\big([\partial_t\boldsymbol{\sigma}(\boldsymbol{u}_{h\tau})\boldsymbol{n}_e]_e,\boldsymbol{u}-\boldsymbol{u}_{h\tau}-\boldsymbol{v}_h\big)_e\\
&-\int_0^t\alpha\sum_{e\in\mathcal{E}_h^1\cup\mathcal{E}_h^{12}}\big([\partial_t p_{h\tau}]_e,(\boldsymbol{u}-\boldsymbol{u}_{h\tau}-\boldsymbol{v}_h)\cdot\boldsymbol{n}_e\big)_e+\int_0^t\big(\partial_t(\boldsymbol{\sigma}(\boldsymbol{u}_{h\tau})\boldsymbol{n}_\Omega-\boldsymbol{t}_{N,h\tau}),\boldsymbol{u}-\boldsymbol{u}_{h\tau}-\boldsymbol{v}_h\big)_{\Gamma_N}\\
&-\int_0^t\big(\partial_t(\boldsymbol{f}-\boldsymbol{f}_{h\tau}),\boldsymbol{u}-\boldsymbol{u}_{h\tau}\big)_\Omega-\int_0^t\big(\partial_t(\boldsymbol{t}_N-\boldsymbol{t}_{N,h\tau}),\boldsymbol{u}-\boldsymbol{u}_{h\tau}\big)_{\Gamma_N}+\mathrm{Init}+\mathrm{IP}(t)-\mathrm{IP}(0),
\end{aligned}
\tag{4.23}
$$

where

$$
\mathrm{Init}:=\frac{1}{2M}\|p_0-\Pi_h(p_0)\|^2_{\Omega_1}+G\|\boldsymbol{\varepsilon}(\boldsymbol{u}(0)-\boldsymbol{u}_h^0)\|^2_{\Omega}+\frac{\lambda}{2}\|\nabla\cdot(\boldsymbol{u}(0)-\boldsymbol{u}_h^0)\|^2_{\Omega},
\tag{4.24}
$$

$$
\begin{aligned}
\mathrm{IP}(t)=&-\big((\frac{1}{M}(p-p_{h\tau})+\alpha\nabla\cdot(\boldsymbol{u}-\boldsymbol{u}_{h\tau}))(t),(p_{h\tau}-\theta)(t)\big)_{\Omega_1}\\
&+\sum_{E\in\mathcal{T}_h^1}\big((\boldsymbol{f}_{h\tau}+\nabla\cdot\boldsymbol{\sigma}(\boldsymbol{u}_{h\tau})-\alpha\nabla p_{h\tau})(t),(\boldsymbol{u}-\boldsymbol{u}_{h\tau}-\boldsymbol{v}_h)(t)\big)_E\\
&+\sum_{E\in\mathcal{T}_h^2}\big((\boldsymbol{f}_{h\tau}+\nabla\cdot\boldsymbol{\sigma}(\boldsymbol{u}_{h\tau}))(t),(\boldsymbol{u}-\boldsymbol{u}_{h\tau}-\boldsymbol{v}_h)(t)\big)_E-\sum_{e\in\mathcal{E}_h}\big([\boldsymbol{\sigma}(\boldsymbol{u}_{h\tau})(t)\boldsymbol{n}_e]_e,(\boldsymbol{u}-\boldsymbol{u}_{h\tau}-\boldsymbol{v}_h)(t)\big)_e\\
&+\alpha\sum_{e\in\mathcal{E}_h^1\cup\mathcal{E}_h^{12}}\big([p_{h\tau}(t)]_e,(\boldsymbol{u}-\boldsymbol{u}_{h\tau}-\boldsymbol{v}_h)(t)\cdot\boldsymbol{n}_e\big)_e-\big(\boldsymbol{\sigma}(\boldsymbol{u}_{h,\tau}(t))\boldsymbol{n}_\Omega-\boldsymbol{t}_{N,h\tau}(t),(\boldsymbol{u}-\boldsymbol{u}_{h\tau}-\boldsymbol{v}_h)(t)\big)_{\Gamma_N}\\
&+\big((\boldsymbol{f}-\boldsymbol{f}_{h\tau})(t),(\boldsymbol{u}-\boldsymbol{u}_{h\tau})(t)\big)_\Omega+\big((\boldsymbol{t}_N-\boldsymbol{t}_{N,h\tau})(t),(\boldsymbol{u}-\boldsymbol{u}_{h\tau})(t)\big)_{\Gamma_N}.
\end{aligned}
\tag{4.25}
$$

5. Basic upper bounds

Here we bound the expressions on the right-hand side of (4.23), in terms of the errors on its left-hand side, the errors on the data, and what will be recognized as error indicators. Recall that this inequality is written for $t_{m-1}<t\le t_m\le T$, and ℓ is usually omitted because it is understood that at each time t_n, $\ell=\ell_n$, the smallest integer that achieves convergence. Of course the inequality is valid for any $\ell\ge 1$, and for the sake of clarity, the indicators are all defined with the superscript ℓ. Below, $\hat C$ denote various constants that are independent of h, Δt, and ℓ. Recall that $\lambda_{\max}$ and $\lambda_{\min}>0$ are the largest and smallest eigenvalues of $\boldsymbol{\kappa}$ and recall that v_h^n denotes the step

function in time that takes the value v_h^n in the interval $]t_{n-1}, t_n]$ and its integral is denoted by $\int_0^t v_h$. To simplify, it is understood that in $\min \gamma_e$ and $\max \gamma_e$ the minimum and maximum are taken over all faces e of $\mathcal{E}_h^1$. We consider first the expressions not included in Init, or IP.

5.1. Expressions involving θ_h

Recall that θ_h is given in each E by $m_E(p - p_{h\tau})$, see (4.18). There are four expressions, we treat each one in their order of appearance. In the first one, we shall recognize the following indicator that measures the jump of $p_h^{n,\ell}$ on interfaces in each interval $]t_{n-1}, t_n]$,

$$\eta_{\rm pen}^{n,\ell} := (\Delta t)^{\frac{1}{2}} \Big(\frac{\gamma_e}{h_e}\Big)^{\frac{1}{2}} \|[p_h^{n,\ell}]_e\|_{L^2(e)}. \tag{5.1}$$

Note that

$$\sum_{e\in\mathcal{E}_h^1} \big(\eta_{\rm pen}^{n,\ell}\big)^2 = \Delta t\, J_h(p_h^{n,\ell}, p_h^{n,\ell}).$$

Proposition 1. *There exists a constant $\hat{C}$ such that for all constants $\delta_1 > 0$, we have*

$$\begin{aligned} &\frac{1}{\mu_f}\Big| \int_0^t J_h(p_h, 2p_{h\tau} + \theta_h)\Big| \\ &\le \frac{1}{2\mu_f}\Big[\delta_1 \int_0^t \|p_{h\tau} - p\|_h^2 + \frac{1}{\delta_1}\Big(\sum_{n=1}^m \sum_{e\in\mathcal{E}_h^1} \big(\eta_{\rm pen}^n\big)^2 + \hat{C}^2(d+1)\Big) \sum_{n=1}^m \sum_{e\in\mathcal{E}_h^1} \frac{\gamma_e}{\lambda_{\min,e}} \big(\eta_{\rm pen}^n\big)^2\Big], \end{aligned} \tag{5.2}$$

where $\lambda_{\min,e}$ is the smallest eigenvalue of $\boldsymbol{\kappa}$ in the union of the two elements adjacent to e.

Proof. Let $X = J_h(p_h, 2p_{h\tau} + \theta_h) = J_h(p_h, p_{h\tau}) + J_h(p_h, p_{h\tau} + \theta_h)$. First, by Young's inequality, for any $\delta_1 > 0$, and since p does not jump

$$\big|J_h(p_h, p_{h\tau})\big| \le \frac{1}{2}\big(\delta_1 J_h(p_{h\tau} - p, p_{h\tau} - p) + \frac{1}{\delta_1} J_h(p_h, p_h)\big).$$

This will give the first part of (5.2). For the second part, by the definition (4.18) of θ_h, it follows from (A.4) that, for E adjacent to e

$$\|p_{h\tau} - p + \theta_h\|_{L^2(e)} = \|p_{h\tau} - p - m_E(p_{h\tau} - p)\|_{L^2(e)} \le \hat{C} h_E^{\frac{1}{2}} |p_{h\tau} - p|_{H^1(E)} \le \hat{C}\Big(\frac{h_E}{\lambda_{\min,e}}\Big)^{\frac{1}{2}} \|\boldsymbol{\kappa}^{\frac{1}{2}} \nabla(p_{h\tau} - p)\|_{L^2(E)}.$$

Therefore, owing to the regularity of the mesh,

$$\begin{aligned} J_h(p_h, p_{h\tau} + \theta_h) &\le \frac{1}{2}\Big(\delta_1 |p_{h\tau} - p|_h^2 + \frac{\hat{C}^2}{\delta_1}(d+1) \sum_{e\in\mathcal{E}_h^1} \frac{\gamma_e}{h_e} \|[p_h]_e\|_{L^2(e)}^2 \frac{h_E}{h_e} \frac{\gamma_e}{\lambda_{\min,e}}\Big) \\ &\le \frac{1}{2}\Big(\delta_1 |p_{h\tau} - p|_h^2 + \frac{\hat{C}^2}{\delta_1}(d+1) \sum_{e\in\mathcal{E}_h^1} \frac{\gamma_e}{h_e} \|[p_h]_e\|_{L^2(e)}^2 \frac{\gamma_e}{\lambda_{\min,e}}\Big), \end{aligned}$$

After integration in time, this will give the other part of (5.2). □

In the second expression, we recognize the algorithmic error indicator defined in each interval $]t_{n-1}, t_n]$ by

$$\eta_{\rm fs}^{n,\ell} = (\Delta t)^{\frac{1}{2}} \Big\| \frac{1}{\Delta t}\big(\bar{\sigma}_h^{n,\ell} - \bar{\sigma}_h^{n,\ell-1}\big)\Big\|_{L^2(\Omega_1)}. \tag{5.3}$$

Proposition 2. *There exists a constant $\hat{C}$ such that, for any $\delta_2 > 0$,*

$$\frac{\alpha}{K_b}\Big| \int_0^t \big(\partial_t(\bar{\sigma}_{h\tau} - \bar{\sigma}_{h\tau}^{\ell-1}), \theta_h\big)_{\Omega_1}\Big| \le \frac{1}{2}\Big[\frac{\delta_2}{M}\|p_{h\tau} - p\|_{L^\infty(0,t;L^2(\Omega_1))}^2 + \frac{M}{\delta_2}\Big(\frac{\alpha}{K_b}\Big)^2 \Big(\sum_{n=1}^m (\Delta t)^{\frac{1}{2}} \eta_{\rm fs}^{n,\ell}\Big)^2\Big]. \tag{5.4}$$

Proof. Let $X = \frac{\alpha}{K_b}\big(\partial_t(\bar\sigma_{h\tau} - \bar\sigma_{h\tau}^{\ell-1}), \theta_h\big)_{\Omega_1}$. On any interval $]t_{n-1}, t_n]$,

$$X = \frac{\alpha}{K_b}\frac{1}{\Delta t}\big(\bar\sigma_h^{n,\ell} - \bar\sigma_h^{n,\ell-1}, \theta_h\big)_{\Omega_1},$$

and the definition of θ_h implies

$$\big|X\big| \le \frac{1}{\Delta t}\frac{\alpha}{K_b}\|\bar\sigma_h^{n,\ell} - \bar\sigma_h^{n,\ell-1}\|_{L^2(\Omega_1)}\|p_{h\tau} - p\|_{L^2(\Omega_1)}.$$

Hence

$$\int_{t_{n-1}}^{t_n} |X| \le \frac{\alpha}{K_b}\big(\Delta t\big)^{\frac12}\eta_{\rm fs}^{n,\ell}\sup_{t\in]0,t[}\|p_{h\tau} - p\|_{L^2(\Omega_1)},$$

and (5.4) follows by summing this inequality over n and applying Young's inequality. □

The third expression involves the following local interior residual flow error indicator in each interval $]t_{n-1}, t_n]$ and all E of $\mathcal{T}_h^1$:

$$\eta_{E,p}^{n,\ell} := h_E\big(\Delta t\big)^{\frac12}\Big\|q_h^n + \frac{1}{\mu_f}\nabla\cdot\big(\boldsymbol{\kappa}(\nabla p_h^{n,\ell} - \rho g\nabla\eta)\big) - \frac{1}{M}\frac{1}{\Delta t}(p_h^{n,\ell} - p_h^{n-1}) - \alpha\frac{1}{\Delta t}\nabla\cdot(\boldsymbol{u}_h^{n,\ell} - \boldsymbol{u}_h^{n-1})\Big\|_{L^2(E)}. \quad (5.5)$$

Proposition 3. *There exists a constant $\hat C$ such that, for any $\delta_3 > 0$,*

$$\Big|\int_0^t \sum_{E\in\mathcal{T}_h^1}\Big(\, q_h - \partial_t\big(\frac{1}{M}p_{h\tau} + \alpha\nabla\cdot\boldsymbol{u}_{h\tau}\big) + \frac{1}{\mu_f}\nabla\cdot\big(\boldsymbol{\kappa}(\nabla p_h - \rho g\nabla\eta)\big),\, p - p_{h\tau} - \theta_h\,\Big)_E\Big| \le \frac12\Big[\frac{1}{\mu_f}\delta_3\int_0^t |p - p_{h\tau}|_h^2 + \mu_f\frac{1}{\delta_3}\hat C^2\sum_{n=1}^m\sum_{E\in\mathcal{T}_h^1}\frac{1}{\lambda_{\min,E}}\big(\eta_{E,p}^n\big)^2\Big], \quad (5.6)$$

where $\lambda_{\min,E}$ is the smallest eigenvalue of $\boldsymbol{\kappa}$ in E.

Proof. Owing to (A.3), we have

$$\|p - p_{h\tau} - \theta_h\|_{L^2(E)} \le \frac{\hat C}{\lambda_{\min,E}^{\frac12}}h_E\|\boldsymbol{\kappa}^{\frac12}\nabla(p - p_{h\tau})\|_{L^2(E)}.$$

Then, the proof of (5.6) is a straightforward application of this bound and Young's inequality. □

The last expression involves the following local jump flux error indicator, for each e in $\mathcal{E}_h^1\cup\mathcal{E}_h^{12}$ and each interval $]t_{n-1}, t_n]$,

$$\eta_{{\rm flux},e}^{n,\ell} := \big(h_e\Delta t\big)^{\frac12}\big\|[\boldsymbol{\kappa}(\nabla\, p_h^{n,\ell} - \rho g\nabla\eta)\cdot\boldsymbol{n}_e]_e\big\|_{L^2(e)}. \quad (5.7)$$

Proposition 4. *There exists a constant $\hat C$ such that, for any $\delta_3 > 0$,*

$$\frac{1}{\mu_f}\Big|\int_0^t\sum_{e\in\mathcal{E}_h^1\cup\mathcal{E}_h^{12}}\Big(\,[\boldsymbol{\kappa}(\nabla p_h - \rho g\nabla\eta)\cdot\boldsymbol{n}_e]_e, \{p - p_{h\tau} - \theta_h\}_e\,\Big)_e\Big| \le \frac{1}{2\mu_f}\Big[\delta_3\int_0^t|p - p_{h\tau}|_h^2 + \frac{1}{\delta_3}\hat C^2(d+1)\sum_{n=1}^m\sum_{e\in\mathcal{E}_h^1\cup\mathcal{E}_h^{12}}\frac{1}{\lambda_{\min,e}}\big(\eta_{{\rm flux},e}^n\big)^2\Big]. \quad (5.8)$$

Proof. Note that (A.16) implies that θ_h also satisfies for e in $\mathcal{E}_h^1$,

$$\|\{p - p_{h\tau} - \theta_h\}_e\|_{L^2(e)}^2 \le \frac{\hat C^2}{\lambda_{\min,e}}h_e\big(\|\boldsymbol{\kappa}^{\frac12}\nabla(p - p_{h\tau})\|_{L^2(E_1)}^2 + \|\boldsymbol{\kappa}^{\frac12}\nabla(p - p_{h\tau})\|_{L^2(E_2)}^2\big),$$

with only one element E when e is on $\mathcal{E}_h^{12}$. This readily yields (5.8). □

5.2. Expressions involving θ

Recall that θ is defined by (4.21) and (4.22). Here, there are five expressions, examined in their order of appearance. In the first one, we shall recognize two time error indicators in each interval $]t_{n-1}, t_n]$, one for volumes,

$$\eta_{t,p}^{n,\ell} := \big(\frac{\Delta t}{3}\big)^{\frac{1}{2}} \big| p_h^{n,\ell} - p_h^{n-1} \big|_h, \tag{5.9}$$

and one for jumps on each face $e \in \mathcal{E}_h^1$,

$$\eta_{t,J}^{n,\ell} := \Big(\frac{\Delta t}{3}\Big)^{\frac{1}{2}} \Big(\frac{\gamma_e}{h_e}\Big)^{\frac{1}{2}} \| [p_h^{n,\ell} - p_h^{n-1}]_e \|_{L^2(e)}. \tag{5.10}$$

Note that

$$\big(\eta_{t,p}^{n,\ell}\big)^2 + \sum_{e\in\mathcal{E}_h^1} \big(\eta_{t,J}^{n,\ell}\big)^2 = \frac{\Delta t}{3} \| p_h^{n,\ell} - p_h^{n-1} \|_h^2.$$

Proposition 5. *There exists a constant $\hat{C}$ such that, for any $\delta_1 > 0$,*

$$\begin{aligned} \frac{1}{\mu_f} \Big| \int_0^t \big(p - p_h, p_{h\tau} - \theta \big)_h \Big| \le \frac{1}{2\mu_f} \Big[2\delta_1 \int_0^t \| p - p_{h\tau} \|_h^2 \\ + \frac{1}{\delta_1} \hat{C}^2 \big(\frac{d+1}{d}\big)^2 (K-1)^2 \frac{\lambda_{\max}}{\min \gamma_e} \sum_{n=1}^m \Big(\frac{1}{2} \big(\eta_{t,p}^n\big)^2 + \sum_{e\in\mathcal{E}_h^1} \Big(\big(\eta_{t,J}^n\big)^2 + \big(\eta_{\rm pen}^n\big)^2 \Big) \Big) \Big]. \end{aligned} \tag{5.11}$$

Proof. First, we deduce from (A.20) that

$$\begin{aligned} |p_{h\tau} - \theta|_h &\le \hat{C} \frac{d+1}{d} (K-1) \big(\frac{\lambda_{\max}}{\min \gamma_e}\big)^{\frac{1}{2}} J_h(p_{h\tau}, p_{h\tau})^{\frac{1}{2}} \\ &\le \hat{C} \frac{d+1}{d} (K-1) \big(\frac{\lambda_{\max}}{\min \gamma_e}\big)^{\frac{1}{2}} \Big(J_h(p_{h\tau} - p_h, p_{h\tau} - p_h)^{\frac{1}{2}} + J_h(p_h, p_h)^{\frac{1}{2}} \Big). \end{aligned}$$

Next, we split $p - p_h$ into $p - p_{h\tau} + p_{h\tau} - p_h$ and set

$$X_1 = \frac{1}{\mu_f} \int_0^t \big(p - p_{h\tau}, p_{h\tau} - \theta \big)_h, \quad X_2 = \frac{1}{\mu_f} \int_0^t \big(p_{h\tau} - p_h, p_{h\tau} - \theta \big)_h.$$

The above inequality yields

$$|X_1| \le \frac{1}{\mu_f} \hat{C} \frac{d+1}{d} (K-1) \big(\frac{\lambda_{\max}}{\min \gamma_e}\big)^{\frac{1}{2}} \int_0^t |p - p_{h\tau}|_h \Big(J_h(p_{h\tau} - p_h, p_{h\tau} - p_h)^{\frac{1}{2}} + J_h(p_h, p_h)^{\frac{1}{2}} \Big).$$

With Young's inequality, this becomes

$$|X_1| \le \frac{1}{2\mu_f} \Big[2\delta_1 \int_0^t |p - p_{h\tau}|_h^2 + \frac{1}{\delta_1} \hat{C}^2 \big(\frac{d+1}{d}\big)^2 (K-1)^2 \frac{\lambda_{\max}}{\min \gamma_e} \sum_{n=1}^m \sum_{e\in\mathcal{E}_h^1} \Big(\big(\eta_{\rm pen}^n\big)^2 + \big(\eta_{t,J}^n\big)^2 \Big) \Big]. \tag{5.12}$$

Regarding X_2, there is no need to split $J_h(p_{h\tau}, p_{h\tau})$ because the first factor will be bounded by an indicator. Indeed, in view of (5.9), we can write

$$|X_2| \le \frac{1}{2\mu_f} \Big[2\delta_1 \int_0^t J_h(p - p_{h\tau}, p - p_{h\tau}) + \frac{1}{2\delta_1} \hat{C}^2 \big(\frac{d+1}{d}\big)^2 (K-1)^2 \frac{\lambda_{\max}}{\min \gamma_e} \sum_{n=1}^m \big(\eta_{t,p}^n\big)^2 \Big], \tag{5.13}$$

and (5.11) is derived by adding (5.12) and (5.13). □

The second one uses $\eta_{\rm fs}^{n,\ell}$ as follows:

Proposition 6. *There exists a constant $\hat{C}$ such that, for any $\delta_3 > 0$,*

$$\begin{aligned}\frac{\alpha}{K_b}\Big|\int_0^t \big(\,\partial_t(\bar{\sigma}_{h\tau}-\bar{\sigma}_{h\tau}^{\ell-1}),\,p_{h\tau}-\theta\,\big)_{\Omega_1}\Big| \\ \le \frac{1}{2}\Big[\frac{\delta_3}{\mu_f}\int_0^t J_h(p-p_{h\tau},\,p-p_{h\tau})+\frac{\mu_f}{\delta_3}\Big(\frac{\alpha}{K_b}\Big)^2\frac{1}{\min\gamma_e}\hat{C}^2(K-1)^2\sum_{n=1}^m h^2\big(\eta_{\rm fs}^n\big)^2\Big].\end{aligned} \tag{5.14}$$

Proof. The estimate (A.19) implies

$$\|p_{h\tau}-\theta\|_{L^2(\Omega_1)}^2 \le \hat{C}^2(K-1)^2\frac{h^2}{\min\gamma_e}J_h(p_{h\tau},\,p_{h\tau}).$$

From here, we infer (5.14) via Young's inequality. □

The next proposition estimates the third expression.

Proposition 7. *There exists a constant $\hat{C}$ such that, for any $\delta_3 > 0$,*

$$\begin{aligned}&\frac{1}{\mu_f}\Big|\int_0^t\sum_{e\in\mathcal{E}_h^1}\big(\{\boldsymbol{\kappa}\nabla(p_{h\tau}-\theta)\cdot\boldsymbol{n}_e\}_e,\,[p-p_h]_e\big)_e\Big| \\ &\le \frac{1}{2\mu_f}\Big[\delta_3\int_0^t J_h(p-p_{h\tau},\,p-p_{h\tau})+\frac{d+1}{2\delta_3}\Big(\frac{d+1}{d}\Big)^2\hat{C}^2\Big(\frac{\lambda_{\max}}{\min\gamma_e}\Big)^2(K-1)^2\sum_{m=1}^n\sum_{e\in\mathcal{E}_h^1}\big(\eta_{\rm pen}^n\big)^2\Big].\end{aligned} \tag{5.15}$$

Proof. Since θ is a polynomial function, by combining the argument of Proposition 15 with that of (A.20), we obtain for any $\delta > 0$

$$\begin{aligned}&\frac{1}{\mu_f}\Big|\sum_{e\in\mathcal{E}_h^1}\big(\{\boldsymbol{\kappa}\nabla(p_{h\tau}-\theta)\cdot\boldsymbol{n}_e\}_e,\,[p_h]_e\big)_e\Big| \\ &\le \frac{1}{2\mu_f}\Big[\delta J_h(p_h,\,p_h)+\frac{d+1}{2\delta}\Big(\frac{d+1}{d}\Big)^2\hat{C}^2\Big(\frac{\lambda_{\max}}{\min\gamma_e}\Big)^2(K-1)^2J_h(p_{h\tau},\,p_{h\tau})\Big],\end{aligned}$$

Thus, the choice

$$\delta_3=\frac{d+1}{2\delta}\Big(\frac{d+1}{d}\Big)^2\hat{C}^2\Big(\frac{\lambda_{\max}}{\min\gamma_e}\Big)^2(K-1)^2,\quad \text{i.e., } \delta=\frac{d+1}{2\delta_3}\Big(\frac{d+1}{d}\Big)^2\hat{C}^2\Big(\frac{\lambda_{\max}}{\min\gamma_e}\Big)^2(K-1)^2,$$

leads to (5.15). □

The fourth expression is estimated by applying an easy variant of (A.19).

Proposition 8. *There exists a constant $\hat{C}$ such that, for any $\delta_3 > 0$,*

$$\Big|\int_0^t\big(q-q_h,\,p_{h\tau}-\theta\big)_{\Omega_1}\Big| \le \frac{1}{2}\Big[\frac{\delta_3}{\mu_f}\int_0^t J_h(p-p_{h\tau},\,p-p_{h\tau})+\frac{\mu_f}{\delta_3}\hat{C}^2(K-1)^2\frac{h^2}{\min\gamma_e}\int_0^t\|q-q_h\|_{L^2(\Omega_1)}^2\Big]. \tag{5.16}$$

Finally, for the fifth expression, we shall use as indicator the jump of the pressure's time derivative on each face $e\in\mathcal{E}_h^1$ and in each interval $]t_{n-1},\,t_n]$,

$$\eta_{\partial p,J}^{n,\ell} := h_e\Delta t\Big(\frac{\gamma_e}{h_e}\Big)^{\frac{1}{2}}\Big\|\frac{1}{\Delta t}[p_h^{n,\ell}-p_h^{n-1}]_e\Big\|_{L^2(e)}. \tag{5.17}$$

The proof of the next proposition follows easily from (A.19).

Proposition 9. *There exists a constant $\hat{C}$ such that, for any $\delta_2 > 0$ and $\delta_4 > 0$,*

$$\Big| \int_0^t \big(\frac{1}{M}(p - p_{h,\tau}) + \alpha \nabla \cdot (\boldsymbol{u} - \boldsymbol{u}_{h\tau}), \partial_t (p_{h\tau} - \theta)\big)_{\Omega_1} \Big| \le \frac{1}{2} \Big[\frac{\delta_2}{M} \|p - p_{h\tau}\|^2_{L^\infty(0,t;L^2(\Omega_1))} + \lambda \delta_4 \|\nabla \cdot (\boldsymbol{u} - \boldsymbol{u}_{h\tau})\|^2_{L^\infty(0,t;L^2(\Omega_1))} + \big(\frac{1}{M}\frac{1}{\delta_2} + \frac{\alpha^2}{\delta_4 \lambda}\big) \hat{C}^2 \frac{(K-1)^2}{\min \gamma_e} \Big(\sum_{n=1}^m \big(\sum_{e \in \mathcal{E}_h^1} \big(\eta^n_{\partial p, J}\big)^2 \big)^{\frac{1}{2}} \Big)^2 \Big]. \tag{5.18}$$

5.3. Expressions involving $\boldsymbol{v}_h$

Recall that $\boldsymbol{v}_h$ is defined by applying (4.17) with degree one to $\boldsymbol{u} - \boldsymbol{u}_{h\tau}$. Here, they can be combined so that there are five expressions, and each one is estimated straightforwardly by using (3.6) with $s = 1$, either applied directly or following a trace inequality. This leads to the following error indicators in each interval $]t_{n-1}, t_n]$:

the time derivative of the displacement equilibrium in all E of $\mathcal{T}_h^1$,

$$\eta^{n,\ell}_{E,1,\partial \boldsymbol{u}} := h_E \Delta t \| \frac{1}{\Delta t} \big(\boldsymbol{f}_h^n - \boldsymbol{f}_h^{n-1} + \nabla \cdot \boldsymbol{\sigma}(\boldsymbol{u}_h^{n,\ell} - \boldsymbol{u}_h^{n-1}) - \alpha \nabla (p_h^{n,\ell} - p_h^{n-1}) \big) \|_{L^2(E)}, \tag{5.19}$$

the time derivative of the displacement equilibrium in all E of $\mathcal{T}_h^2$,

$$\eta^{n,\ell}_{E,2,\partial \boldsymbol{u}} := h_E \Delta t \| \frac{1}{\Delta t} \big(\boldsymbol{f}_h^n - \boldsymbol{f}_h^{n-1} + \nabla \cdot \boldsymbol{\sigma}(\boldsymbol{u}_h^{n,\ell} - \boldsymbol{u}_h^{n-1}) \big) \|_{L^2(E)}, \tag{5.20}$$

the time derivative of the stress tensor's jump in the pay-zone and interface, i.e., all $e \in \mathcal{E}_h^1 \cup \mathcal{E}_h^{12}$,

$$\eta^{n,\ell}_{e,1,\partial \boldsymbol{\sigma}} := h_e^{\frac{1}{2}} \Delta t \| \frac{1}{\Delta t} [(\boldsymbol{\sigma}(\boldsymbol{u}_h^{n,\ell} - \boldsymbol{u}_h^{n-1}) - \alpha (p_h^{n,\ell} - p_h^{n-1}) \boldsymbol{I}) \boldsymbol{n}_e]_e \|_{L^2(e)}, \tag{5.21}$$

the time derivative of the stress tensor's jump in the interior of the nonpay-zone, i.e., $e \in \mathcal{E}_h^2$,

$$\eta^{n,\ell}_{e,2,\partial \boldsymbol{\sigma}} := h_e^{\frac{1}{2}} \Delta t \| \frac{1}{\Delta t} [\boldsymbol{\sigma}(\boldsymbol{u}_h^{n,\ell} - \boldsymbol{u}_h^{n-1}) \boldsymbol{n}_e]_e \|_{L^2(e)}, \tag{5.22}$$

the time derivative of the stress tensor error on $e \in \Gamma_N$,

$$\eta^{n,\ell}_{e,N,\partial \boldsymbol{\sigma}} := h_e^{\frac{1}{2}} \Delta t \| \frac{1}{\Delta t} \big(\boldsymbol{\sigma}(\boldsymbol{u}_h^{n,\ell} - \boldsymbol{u}_h^{n-1}) \boldsymbol{n}_\Omega - (\boldsymbol{t}_{N,h}^n - \boldsymbol{t}_{N,h}^{n-1}) \big) \|_{L^2(e)}. \tag{5.23}$$

For the sake of conciseness, p is extended by zero in Ω_2. We obtain the following volume estimates for any $\delta > 0$; to simplify, the number of repetitions of an element is not specified and is incorporated in the constant $\hat{C}$,

$$\sum_{i=1}^2 \Big| \int_0^t \sum_{E \in \mathcal{T}_h^i} \big(\partial_t (\boldsymbol{f}_{h\tau} + \nabla \cdot \boldsymbol{\sigma}(\boldsymbol{u}_{h\tau}) - \alpha \nabla\, p_{h\tau}), \boldsymbol{u} - \boldsymbol{u}_{h\tau} - \boldsymbol{v}_h \big)_E \Big| \le \frac{1}{2} \sum_{i=1}^2 \Big[\delta \|\nabla (\boldsymbol{u} - \boldsymbol{u}_{h\tau})\|^2_{L^\infty(0,t;L^2(\Omega_i))} + \frac{1}{\delta} \hat{C}^2 \Big(\sum_{n=1}^m \big(\sum_{E \in \mathcal{T}_h^i} \big(\eta^n_{E,i,\partial \boldsymbol{u}}\big)^2 \big)^{\frac{1}{2}} \Big)^2 \Big].$$

Note that by Korn's inequality (1.3) with $\Gamma = \Gamma_D$

$$\sum_{i=1}^2 \|\nabla (\boldsymbol{u} - \boldsymbol{u}_{h\tau})\|^2_{L^2(\Omega_i)} = \|\nabla (\boldsymbol{u} - \boldsymbol{u}_{h\tau})\|^2_{L^2(\Omega)} \le \mathcal{K}^2 \|\boldsymbol{\varepsilon}(\boldsymbol{u} - \boldsymbol{u}_{h\tau})\|^2_{L^2(\Omega)}.$$

Therefore the two volume estimates can be combined as follows:

$$\sum_{i=1}^2 \Big| \int_0^t \Big(\sum_{E \in \mathcal{T}_h^i} \big(\partial_t (\boldsymbol{f}_{h\tau} + \nabla \cdot \boldsymbol{\sigma}(\boldsymbol{u}_{h\tau}) - \alpha \nabla\, p_{h\tau}), \boldsymbol{u} - \boldsymbol{u}_{h\tau} - \boldsymbol{v}_h \big)_E \Big) \Big| \le \frac{1}{2} \Big[\delta_5 G \|\boldsymbol{\varepsilon}(\boldsymbol{u} - \boldsymbol{u}_{h\tau})\|^2_{L^\infty(0,t;L^2(\Omega))} + \frac{\hat{C}^2 \mathcal{K}^2}{\delta_5 G} \sum_{i=1}^2 \Big(\sum_{n=1}^m \big(\sum_{E \in \mathcal{T}_h^i} \big(\eta^n_{E,i,\partial \boldsymbol{u}}\big)^2 \big)^{\frac{1}{2}} \Big)^2 \Big]. \tag{5.24}$$

A similar argument leads to the interface estimates,

$$\begin{aligned}&\Big|\int_0^t\Big(\sum_{e\in\mathcal{E}_h}\big([\partial_t(\boldsymbol{\sigma}(\boldsymbol{u}_{h\tau})-\alpha p_{h\tau}\boldsymbol{I})\boldsymbol{n}_e]_e,\boldsymbol{u}-\boldsymbol{u}_{h\tau}-\boldsymbol{v}_h\big)_e+\big(\partial_t(\boldsymbol{\sigma}(\boldsymbol{u}_{h\tau})\boldsymbol{n}_\Omega-\boldsymbol{t}_{N,h\tau}),\boldsymbol{u}-\boldsymbol{u}_{h\tau}-\boldsymbol{v}_h\big)_{\Gamma_N}\Big)\Big|\\&\le\frac{1}{2}\Big[\delta_5 G\|\boldsymbol{\varepsilon}(\boldsymbol{u}-\boldsymbol{u}_{h\tau})\|^2_{L^\infty(0,t;L^2(\Omega))}+\frac{\hat{C}^2\mathcal{K}^2}{\delta_5 G}\Big(\Big(\sum_{n=1}^m\Big(\sum_{e\in\mathcal{E}_h}\big(\eta^n_{e,\partial\boldsymbol{\sigma}}\big)^2\Big)^{\frac12}\Big)^2+\Big(\sum_{n=1}^m\Big(\sum_{e\in\mathcal{E}_h^{N,\partial}}\big(\eta^n_{e,N,\partial\boldsymbol{\sigma}}\big)^2\Big)^{\frac12}\Big)^2\Big)\Big],\end{aligned}\tag{5.25}$$

where $\eta_{e,\partial\boldsymbol{\sigma}}$ stands for $\eta_{e,1,\partial\boldsymbol{\sigma}}$ in $\mathcal{E}_h^1\cup\mathcal{E}_h^{12}$ and $\eta_{e,2,\partial\boldsymbol{\sigma}}$ in $\mathcal{E}_h^2$.

5.4. The first expression and the data errors

The first expression has a straightforward bound,

$$\frac{1}{\mu_f}\Big|\int_0^t(\!(p_h-p_{h\tau},p-p_{h\tau})\!)_h\Big|\le\frac{1}{2\mu_f}\Big[\delta_1\int_0^t\|p-p_{h\tau}\|_h^2+\frac{1}{\delta_1}\sum_{n=1}^m\Big(\big(\eta^n_{t,p}\big)^2+\sum_{e\in\mathcal{E}_h^1}\big(\eta^n_{t,J}\big)^2\Big)\Big].\tag{5.26}$$

There remain the three data errors. We start with the error on q,

$$\Big|\int_0^t\big(q-q_h,p-p_{h\tau}\big)_{\Omega_1}\Big|\le\frac{1}{2}\Big[\frac{\delta_2}{M}\|p_{h\tau}-p\|^2_{L^\infty(0,t;L^2(\Omega_1))}+\frac{M}{\delta_2}\|q-q_h\|^2_{L^1(0,t;L^2(\Omega_1))}\Big].\tag{5.27}$$

And we finish with the error on the time derivative of the force and the given traction,

$$\begin{aligned}&\Big|\int_0^t\big(\partial_t(\boldsymbol{f}-\boldsymbol{f}_{h\tau}),\boldsymbol{u}-\boldsymbol{u}_{h\tau}\big)_\Omega\Big|\\&\le\frac{1}{2}\Big[\delta_5 G\|\boldsymbol{\varepsilon}(\boldsymbol{u}-\boldsymbol{u}_{h\tau})\|^2_{L^\infty(0,t;L^2(\Omega))}+\frac{\mathcal{P}^2\mathcal{K}^2}{\delta_5 G}\|\partial_t(\boldsymbol{f}-\boldsymbol{f}_{h\tau})\|^2_{L^1(0,t;L^2(\Omega))}\Big],\\&\Big|\int_0^t\big(\partial_t(\boldsymbol{t}_N-\boldsymbol{t}_{N,h\tau}),\boldsymbol{u}-\boldsymbol{u}_{h\tau}\big)_{\Gamma_N}\Big|\\&\le\frac{1}{2}\Big[\delta_5 G\|\boldsymbol{\varepsilon}(\boldsymbol{u}-\boldsymbol{u}_{h\tau})\|^2_{L^\infty(0,t;L^2(\Omega))}+\frac{C_N^2C_1^2}{\delta_5 G}\|\partial_t(\boldsymbol{t}_N-\boldsymbol{t}_{N,h\tau})\|^2_{L^1(0,t;H^{-1/2}(\Gamma_N))}\Big],\end{aligned}\tag{5.28}$$

where C_1 is the constant of (1.5) and C_N is the constant of a trace inequality on Γ_N, from $H^{\frac12}_{00}(\Gamma_N)^3$ to $\boldsymbol{W}$.

5.5. Bounds for IP(t)

The bounds in this subsection are derived in the interval $]t_{m-1},t_m]$, $1\le m\le N$. They use the following error indicators at time t_n:

the pressure jump

$$\eta^{n,\ell}_{p,J}:=h_e\Big(\frac{\gamma_e}{h_e}\Big)^{\frac12}\|[p_h^{n,\ell}]_e\|_{L^2(e)},\tag{5.29}$$

for $i=1,2$, the displacement equilibrium in all $E\in\mathcal{T}_h^i$, with p_h set to zero in Ω_2

$$\eta^{n,\ell}_{E,i,\boldsymbol{u}}:=h_E\|\boldsymbol{f}_h^n+\nabla\cdot\boldsymbol{\sigma}(\boldsymbol{u}_h^{n,\ell})-\alpha\nabla\,p_h^{n,\ell}\|_{L^2(E)},\tag{5.30}$$

the stress tensor's jump in the pay-zone and interface, i.e., all $e\in\mathcal{E}_h^1\cup\mathcal{E}_h^{12}$,

$$\eta^{n,\ell}_{e,1,\boldsymbol{\sigma}}:=h_e^{\frac12}\|[\big(\boldsymbol{\sigma}(\boldsymbol{u}_h^{n,\ell})-\alpha p_h^{n,\ell}\boldsymbol{I}\big)\boldsymbol{n}_e]_e\|_{L^2(e)},\tag{5.31}$$

the stress tensor's jump in the interior of the nonpay-zone, i.e., $e\in\mathcal{E}_h^2$,

$$\eta^{n,\ell}_{e,2,\boldsymbol{\sigma}}:=h_e^{\frac12}\|[\boldsymbol{\sigma}(\boldsymbol{u}_h^{n,\ell})\boldsymbol{n}_e]_e\|_{L^2(e)}\tag{5.32}$$

the stress tensor's error on $e\in\Gamma_N$,

$$\eta^{n,\ell}_{e,N,\boldsymbol{\sigma}}:=h_e^{\frac12}\|\boldsymbol{\sigma}(\boldsymbol{u}_h^{n,\ell})\boldsymbol{n}_\Omega-\boldsymbol{t}^n_{N,h}\|_{L^2(e)}.\tag{5.33}$$

The first bound follows readily from (A.19): There exists a constant $\hat{C}$ such that, for any $\delta_6 > 0$ and $\delta_7 > 0$,

$$\begin{aligned}\Big| \big((\frac{1}{M}(p - p_{h\tau}) + \alpha\nabla\cdot(\boldsymbol{u} - \boldsymbol{u}_{h\tau}))(t), (p_{h\tau} - \theta)(t) \big)_{\Omega_1} \Big| \\ \le \frac{1}{2}\Big[\frac{\delta_6}{M}\|(p - p_{h\tau})(t)\|^2_{L^2(\Omega_1)} + \lambda\delta_7\|\nabla\cdot(\boldsymbol{u} - \boldsymbol{u}_{h\tau})(t)\|^2_{L^2(\Omega_1)} \\ + \hat{C}^2\big(\frac{1}{\delta_6 M} + \frac{\alpha^2}{\delta_7\lambda}\big)(K-1)^2\frac{1}{\min\gamma_e}\sum_{e\in\mathcal{E}_h^1}\big((1-s)(\eta^{m-1}_{p,J})^2 + s(\eta^m_{p,J})^2\big)\Big],\end{aligned} \tag{5.34}$$

where $0 \le s \le 1$, in fact $s = \frac{t - t_{m-1}}{\Delta t}$ since $t_{m-1} < t \le t_m$. The remaining bounds are straightforward; they hold for the above s and for any $\delta_8 > 0$. We have first the volume estimate,

$$\begin{aligned}&\sum_{i=1}^{2}\Big|\sum_{E\in\mathcal{T}_h^i}\big((\boldsymbol{f}_{h\tau} + \nabla\cdot\boldsymbol{\sigma}(\boldsymbol{u}_{h\tau}) - \alpha\nabla p_{h\tau})(t), (\boldsymbol{u} - \boldsymbol{u}_{h\tau} - \boldsymbol{v}_h)(t)\big)_E\Big| \\ &\le \frac{1}{2}\Big[\delta_8 G\|\boldsymbol{\varepsilon}(\boldsymbol{u} - \boldsymbol{u}_{h\tau})(t)\|^2_{L^2(\Omega)} + \frac{\hat{C}^2\mathcal{K}^2}{\delta_8 G}\sum_{i=1}^{2}\sum_{E\in\mathcal{T}_h^i}\Big((1-s)\big(\eta^{m-1}_{E,i,\boldsymbol{u}}\big)^2 + s\big(\eta^m_{E,i,\boldsymbol{u}}\big)^2\Big)\Big].\end{aligned} \tag{5.35}$$

Next, we have the interface estimate,

$$\begin{aligned}&\Big|\sum_{e\in\mathcal{E}_h}\big([(\boldsymbol{\sigma}(\boldsymbol{u}_{h\tau}) - \alpha p_{h\tau}\boldsymbol{I})(t)\boldsymbol{n}_e]_e, (\boldsymbol{u} - \boldsymbol{u}_{h\tau} - \boldsymbol{v}_h)(t)\big)_e + \big(\boldsymbol{\sigma}(\boldsymbol{u}_{h\tau}(t))\boldsymbol{n}_\Omega - \boldsymbol{t}_{N,h\tau}(t), (\boldsymbol{u} - \boldsymbol{u}_{h\tau} - \boldsymbol{v}_h)(t)\big)_{\Gamma_N}\Big| \\ &\quad\le \frac{1}{2}\Big[\delta_8 G\|\boldsymbol{\varepsilon}(\boldsymbol{u} - \boldsymbol{u}_{h\tau})(t)\|^2_{L^2(\Omega)} \\ &\quad + \frac{\hat{C}^2\mathcal{K}^2}{\delta_8 G}\Big(\sum_{e\in\mathcal{E}_h}\big((1-s)\big(\eta^{m-1}_{e,\boldsymbol{\sigma}}\big)^2 + s\big(\eta^m_{e,\boldsymbol{\sigma}}\big)^2\big) + \sum_{e\in\mathcal{E}_h^{N,\partial}}\big((1-s)\big(\eta^{m-1}_{e,N,\boldsymbol{\sigma}}\big)^2 + s\big(\eta^m_{e,N,\boldsymbol{\sigma}}\big)^2\big)\Big)\Big].\end{aligned} \tag{5.36}$$

Finally, the bound for the data terms is

$$\begin{aligned}&\Big|\big((\boldsymbol{f} - \boldsymbol{f}_{h\tau})(t), (\boldsymbol{u} - \boldsymbol{u}_{h\tau})(t)\big)_\Omega + \big((\boldsymbol{t}_N - \boldsymbol{t}_{N,h\tau})(t), (\boldsymbol{u} - \boldsymbol{u}_{h\tau})(t)\big)_{\Gamma_N}\Big| \le \frac{1}{2}\Big[\delta_8 G\|\boldsymbol{\varepsilon}(\boldsymbol{u} - \boldsymbol{u}_{h\tau})(t)\|^2_{L^2(\Omega)} \\ &+ \frac{\hat{C}^2}{\delta_8 G}\Big(\mathcal{K}^2\|\boldsymbol{f} - \boldsymbol{f}_{h\tau}\|^2_{L^\infty(0,t;L^2(\Omega))} + C_N^2C_1^2\|\boldsymbol{t}_N - \boldsymbol{t}_{N,h\tau}\|^2_{L^\infty(0,t;H^{-1/2}(\Gamma_N))}\Big)\Big].\end{aligned} \tag{5.37}$$

5.6. The initial errors

Let us start with bounds for IP(0). At initial time, these bounds are simpler, mainly because p_h^0 has no jumps, and hence $(p_{h\tau} - \theta)(0) = 0$. Hence a combination of (5.35)–(5.37) gives for all $\delta_8 > 0$

$$\begin{aligned}\big|\mathrm{IP}(0)\big| &\le \frac{1}{2}\Big[3\delta_8 G\|\boldsymbol{\varepsilon}(\boldsymbol{u}(0) - \boldsymbol{u}_h^0)\|^2_{L^2(\Omega)} \\ &+ \frac{\hat{C}^2}{\delta_8 G}\Big(\mathcal{K}^2\Big(\sum_{i=1}^{2}\sum_{E\in\mathcal{T}_h^i}\big(\eta^0_{E,i,\boldsymbol{u}}\big)^2 + \sum_{e\in\mathcal{E}_h^1\cup\mathcal{E}_h^2}\big(\eta^0_{e,2,\boldsymbol{\sigma}}\big)^2 + \sum_{e\in\mathcal{E}_h^{12}}\big(\eta^0_{e,1,\boldsymbol{\sigma}}\big)^2 + \sum_{e\in\mathcal{E}_h^{N,\partial}}\big(\eta^0_{e,N,\boldsymbol{\sigma}}\big)^2 \\ &+ \|\boldsymbol{f} - \boldsymbol{f}_{h\tau}\|^2_{L^\infty(0,t;L^2(\Omega))}\Big) + C_1^2C_N^2\|\boldsymbol{t}_N - \boldsymbol{t}_{N,h\tau}\|^2_{L^\infty(0,t;H^{-1/2}(\Gamma_N))}\Big)\Big].\end{aligned} \tag{5.38}$$

Note that $\eta^0_{e,1,\boldsymbol{\sigma}}$ only appears in the interface because p_h^0 does not jump.

Regarding the initial pressure and displacement errors, by definition the former is simply an interpolation error, see (3.9) and (3.5). But the initial displacement is computed and its error stems from (4.13). By testing (4.13) at $n = 0$ with $\boldsymbol{v} = \boldsymbol{u} - \boldsymbol{u}_h^0$, we readily derive by the above argument that

$$2G\|\boldsymbol{\epsilon}(\boldsymbol{u}(0) - \boldsymbol{u}_h^0)\|^2_{L^2(\Omega)} \le \frac{\alpha^2}{4\lambda}\|p(0) - p_h^0\|^2_{L^2(\Omega_1)} + \big|\mathrm{IP}(0)\big|.$$

Hence the choice $\delta_8 = \frac{2}{3}$ in (5.38) yields

$$
\begin{aligned}
&G\|\boldsymbol{\epsilon}(\boldsymbol{u}(0)-\boldsymbol{u}_h^0)\|^2_{L^2(\Omega)} \le \frac{\alpha^2}{4\lambda}\|p(0)-p_h^0\|^2_{L^2(\Omega_1)}\\
&+\frac{3}{4}\frac{\hat{C}^2}{G}\Big(\mathcal{K}^2\Big(\sum_{i=1}^{2}\sum_{E\in\mathcal{T}_h^i}\big(\eta^0_{E,i,\boldsymbol{u}}\big)^2+\sum_{e\in\mathcal{E}_h^1\cup\mathcal{E}_h^2}\big(\eta^0_{e,2,\boldsymbol{\sigma}}\big)^2+\sum_{e\in\mathcal{E}_h^{12}}\big(\eta^0_{e,1,\boldsymbol{\sigma}}\big)^2+\sum_{e\in\mathcal{E}_h^{N,\partial}}\big(\eta^0_{e,N,\boldsymbol{\sigma}}\big)^2\\
&+\|\boldsymbol{f}-\boldsymbol{f}_{h\tau}\|^2_{L^\infty(0,t;L^2(\Omega))}\Big)+C_1^2C_N^2\|\boldsymbol{t}_N-\boldsymbol{t}_{N,h\tau}\|^2_{L^\infty(0,t;H^{-1/2}(\Gamma_N))}\Big).
\end{aligned}
\tag{5.39}
$$

Similarly, the choice $\delta_8 = \frac{4}{3}$ in (5.38) leads to

$$
\begin{aligned}
&\lambda\|\nabla\cdot(\boldsymbol{u}(0)-\boldsymbol{u}_h^0)\|^2_{L^2(\Omega)} \le \frac{\alpha^2}{\lambda}\|p(0)-p_h^0\|^2_{L^2(\Omega_1)}\\
&+\frac{3}{4}\frac{\hat{C}^2}{G}\Big(\mathcal{K}^2\Big(\sum_{i=1}^{2}\sum_{E\in\mathcal{T}_h^i}\big(\eta^0_{E,i,\boldsymbol{u}}\big)^2+\sum_{e\in\mathcal{E}_h^1\cup\mathcal{E}_h^2}\big(\eta^0_{e,2,\boldsymbol{\sigma}}\big)^2+\sum_{e\in\mathcal{E}_h^{12}}\big(\eta^0_{e,1,\boldsymbol{\sigma}}\big)^2+\sum_{e\in\mathcal{E}_h^{N,\partial}}\big(\eta^0_{e,N,\boldsymbol{\sigma}}\big)^2\\
&+\|\boldsymbol{f}-\boldsymbol{f}_{h\tau}\|^2_{L^\infty(0,t;L^2(\Omega))}\Big)+C_1^2C_N^2\|\boldsymbol{t}_N-\boldsymbol{t}_{N,h\tau}\|^2_{L^\infty(0,t;H^{-1/2}(\Gamma_N))}\Big).
\end{aligned}
\tag{5.40}
$$

5.7. The reliability bound

Let us substitute the above bounds in (4.23). Since there are many indicators, to simplify, they are grouped into categories,

- the algorithmic errors,

$$
\eta^m_{\text{alg}} := \Big(\sum_{n=1}^{m}(\Delta t)^{\frac{1}{2}}\eta^n_{\text{fs}}\Big)^2+\sum_{n=1}^{m}h^2\big(\eta^n_{\text{fs}}\big)^2,
\tag{5.41}
$$

- the time errors,

$$
\eta^m_{\text{time}} := \sum_{n=1}^{m}\Big(\big(\eta^n_{t,p}\big)^2+\sum_{e\in\mathcal{E}_h^1}\big(\eta^n_{t,J}\big)^2\Big),
\tag{5.42}
$$

- the flow errors,

$$
\eta^m_{\text{flow}} := \sum_{n=1}^{m}\sum_{E\in\mathcal{T}_h^1}\big(\eta^n_{E,p}\big)^2+\sum_{n=1}^{m}\sum_{e\in\mathcal{E}_h^1\cup\mathcal{E}_h^{12}}\big(\eta^n_{\text{flux},e}\big)^2,
\tag{5.43}
$$

- the penalty jumps,

$$
\eta^m_{\text{jump}} := \sum_{n=1}^{m}\sum_{e\in\mathcal{E}_h^1}\big(\eta^n_{\text{pen}}\big)^2+\Big(\sum_{n=1}^{m}\Big(\sum_{e\in\mathcal{E}_h^1}\big(\eta^n_{\partial p,J}\big)^2\Big)^{\frac{1}{2}}\Big)^2+\sum_{e\in\mathcal{E}_h^1}\Big(\big(\eta^{m-1}_{p,J}\big)^2+\big(\eta^m_{p,J}\big)^2\Big),
\tag{5.44}
$$

- the errors on the tensor's time derivative,

$$
\eta^m_{\mathcal{E}_{\partial\boldsymbol{\sigma}}} := \Big(\sum_{n=1}^{m}\Big(\sum_{e\in\mathcal{E}_h^1\cup\mathcal{E}_h^{12}}\big(\eta^n_{e,1,\partial\boldsymbol{\sigma}}\big)^2\Big)^{\frac{1}{2}}\Big)^2+\Big(\sum_{n=1}^{m}\Big(\sum_{e\in\mathcal{E}_h^2}\big(\eta^n_{e,2,\partial\boldsymbol{\sigma}}\big)^2\Big)^{\frac{1}{2}}\Big)^2+\Big(\sum_{n=1}^{m}\Big(\sum_{e\in\mathcal{E}_h^{N,\partial}}\big(\eta^n_{e,N,\partial\boldsymbol{\sigma}}\big)^2\Big)^{\frac{1}{2}}\Big)^2,
\tag{5.45}
$$

- the errors on the displacement's time derivative,

$$
\eta^m_{\mathcal{T}_{\partial\boldsymbol{u}}} := \sum_{i=1}^{2}\Big(\sum_{n=1}^{m}\Big(\sum_{E\in\mathcal{T}_h^i}\big(\eta^n_{E,i,\partial\boldsymbol{u}}\big)^2\Big)^{\frac{1}{2}}\Big)^2,
\tag{5.46}
$$

- the errors on the tensor at final time,

$$
\eta^m_{\mathcal{E}_{\boldsymbol{\sigma}}} := \sum_{e\in\mathcal{E}_h^1\cup\mathcal{E}_h^{12}}\Big(\big(\eta^{m-1}_{e,1,\boldsymbol{\sigma}}\big)^2+\big(\eta^m_{e,1,\boldsymbol{\sigma}}\big)^2\Big)+\sum_{e\in\mathcal{E}_h^2}\Big(\big(\eta^{m-1}_{e,2,\boldsymbol{\sigma}}\big)^2+\big(\eta^m_{e,2,\boldsymbol{\sigma}}\big)^2\Big)+\sum_{e\in\mathcal{E}_h^{N,\partial}}\Big(\big(\eta^{m-1}_{e,N,\boldsymbol{\sigma}}\big)^2+\big(\eta^m_{e,N,\boldsymbol{\sigma}}\big)^2\Big),
\tag{5.47}
$$

• the errors on the displacement at final time,

$$\eta^m_{\mathcal{T}_{\boldsymbol{u}}} := \sum_{i=1}^{2} \sum_{E\in\mathcal{T}_h^i} \Big(\big(\eta^{m-1}_{E,i,\boldsymbol{u}}\big)^2 + \big(\eta^{m}_{E,i,\boldsymbol{u}}\big)^2 \Big), \tag{5.48}$$

• the initial errors,

$$\eta^0 := \sum_{i=1}^{2} \sum_{E\in\mathcal{T}_h^i} \big(\eta^0_{E,i,\boldsymbol{u}}\big)^2 + \sum_{e\in\mathcal{E}_h^{12}} \big(\eta^0_{e,1,\boldsymbol{\sigma}}\big)^2 + \sum_{e\in\mathcal{E}_h^1\cup\mathcal{E}_h^2} \big(\eta^0_{e,2,\boldsymbol{\sigma}}\big)^2 + \sum_{e\in\mathcal{E}_h^{N,\partial}} \big(\eta^0_{e,N,\boldsymbol{\sigma}}\big)^2. \tag{5.49}$$

Then, we have the following theorem.

Theorem 1. *The following reliability bound holds for all time t, $t_{m-1} < t \le t_m$, $1 \le m \le N$, with a constant $\hat{C}$ independent of h, Δt, and t,*

$$\begin{aligned}
&\frac{1}{4M}\|p - p_{h\tau}\|^2_{L^\infty(0,t;L^2(\Omega_1))} + \frac{G}{2}\|\boldsymbol{\varepsilon}(\boldsymbol{u}-\boldsymbol{u}_{h\tau})\|^2_{L^\infty(0,t;L^2(\Omega))} + \frac{\lambda}{4}\|\nabla\cdot(\boldsymbol{u}-\boldsymbol{u}_{h\tau})\|^2_{L^\infty(0,t;L^2(\Omega))} \\
&+ \frac{1}{2\mu_f}\int_0^t \|p - p_{h\tau}\|_h^2 \le \hat{C}\Big[\, \eta^0 + \|p(0) - \Pi_h(p(0))\|^2_{L^2(\Omega_1)} + \|q - q_h\|^2_{L^1(0,t;L^2(\Omega_1))} \\
&\qquad + h^2\|q - q_h\|^2_{L^2(\Omega_1)\times]0,t[} \\
&\qquad + \eta^m_{\rm alg} + \eta^m_{\rm time} + \eta^m_{\rm jump} + \eta^m_{\rm flow} + \eta^m_{\mathcal{E}_{\partial\boldsymbol{\sigma}}} + \eta^m_{\mathcal{T}_{\partial\boldsymbol{u}}} + \eta^m_{\mathcal{E}_{\boldsymbol{\sigma}}} + \eta^m_{\mathcal{T}_{\boldsymbol{u}}} \\
&\qquad + \|\partial_t(\boldsymbol{f} - \boldsymbol{f}_{h\tau})\|^2_{L^1(0,t;L^2(\Omega))} + \|\partial_t(\boldsymbol{t}_N - \boldsymbol{t}_{N,h\tau})\|^2_{L^1(0,t;H^{-1/2}(\Gamma_N))} \\
&\qquad + \|\boldsymbol{f} - \boldsymbol{f}_{h\tau}\|^2_{L^\infty(0,t;L^2(\Omega))} + \|\boldsymbol{t}_N - \boldsymbol{t}_{N,h\tau}\|^2_{L^\infty(0,t;H^{-1/2}(\Gamma_N))} \,\Big].
\end{aligned} \tag{5.50}$$

6. Weak residual error terms

We observe that several indicators involve time derivatives, whereas the left-hand side of the reliability bound (5.50) does not. As a consequence, some indicators cannot be bounded by the error terms on this left-hand side. Thus, when developing these bounds we are led to introduce several *weak residual error* terms, relative to derivation in time, that arise in the subsequent section, namely,

$$\begin{aligned}
\big(\mathcal{E}_f^{n,\ell_n}\big)^2 = \int_{t_{n-1}}^{t_n} \sup_{\theta_h\in M_h/\mathbb{R}} \frac{1}{\|\theta_h\|_h^2} \\
\times \Big| \big(q_h^n - q + \partial_t\big(\frac{1}{M}(p - p_{h\tau}^{n,\ell_n}) + \alpha\nabla\cdot(\boldsymbol{u} - \boldsymbol{u}_{h\tau}^{n,\ell_n})\big) + \frac{\alpha}{K_b}\partial_t(\bar{\sigma}_{h\tau}^{n,\ell_n} - \bar{\sigma}_{h\tau}^{n,\ell_n-1}), \theta_h\big)_{\Omega_1} \Big|^2,
\end{aligned} \tag{6.1}$$

$$\mathcal{E}_E^{n,\ell_n} = \big\| q_h^n - q + \partial_t\big(\frac{1}{M}(p - p_{h\tau}^{n,\ell_n}) + \alpha\nabla\cdot(\boldsymbol{u} - \boldsymbol{u}_{h\tau}^{n,\ell_n})\big)\big\|_{L^2(t_{n-1},t_n;H^{-1}(E))}, \tag{6.2}$$

where E is any element of $\overline{\Omega}_1$,

$$\mathcal{E}_{E,i,\partial\boldsymbol{\sigma}}^{n,\ell_n} = \int_{t_{n-1}}^{t_n} \sup_{\boldsymbol{v}\in H_0^1(E)^3} \frac{1}{|\boldsymbol{v}|_{H^1(E)}} \Big| \big(\partial_t\boldsymbol{\sigma}(\boldsymbol{u} - \boldsymbol{u}_{h\tau}^{n,\ell_n}), \boldsymbol{\varepsilon}(\boldsymbol{v})\big)_E - \alpha\big(\partial_t(p - p_{h\tau}^{n,\ell_n}), \nabla\cdot\boldsymbol{v}\big)_E - \big(\partial_t(\boldsymbol{f} - \boldsymbol{f}_{h\tau}^n), \boldsymbol{v}\big)_E \Big|, \tag{6.3}$$

where $E \subset \overline{\Omega}_i$, $i = 1, 2$, and p is set to zero in Ω_2,

$$\mathcal{E}_{\omega_e,\partial\boldsymbol{\sigma}}^{n,\ell_n} = \int_{t_{n-1}}^{t_n} \sup_{\boldsymbol{v}\in H_0^1(\omega_e)^3} \frac{1}{|\boldsymbol{v}|_{H^1(\omega_e)}} \Big| \big(\partial_t\boldsymbol{\sigma}(\boldsymbol{u} - \boldsymbol{u}_{h\tau}^{n,\ell_n}), \boldsymbol{\varepsilon}(\boldsymbol{v})\big)_{\omega_e} - \alpha\big(\partial_t(p - p_{h\tau}^{n,\ell_n}), \nabla\cdot\boldsymbol{v}\big)_{\omega_e} - \big(\partial_t(\boldsymbol{f} - \boldsymbol{f}_{h\tau}^n), \boldsymbol{v}\big)_{\omega_e} \Big|, \tag{6.4}$$

where e is an interior face of Ω, and again p is set zero in Ω_2,

$$\mathcal{E}_{e,N,\partial\boldsymbol{\sigma}}^{n,\ell_n} = \int_{t_{n-1}}^{t_n} \sup_{\boldsymbol{v}\in H_e^1(E)^3} \frac{1}{|\boldsymbol{v}|_{H^1(E)}} \Big| \big(\partial_t\boldsymbol{\sigma}(\boldsymbol{u} - \boldsymbol{u}_{h\tau}^{n,\ell_n}), \boldsymbol{\varepsilon}(\boldsymbol{v})\big)_E - \big(\partial_t(\boldsymbol{t}_N - \boldsymbol{t}_{N,h\tau}^n), \boldsymbol{v}\big)_e - \big(\partial_t(\boldsymbol{f} - \boldsymbol{f}_{h\tau}^n), \boldsymbol{v}\big)_E \Big|, \tag{6.5}$$

where e is a face on Γ_N, E is the element adjacent to e, and exceptionally,

$$H^1_e(E) = \{z \in H^1(E);\ z = 0 \text{ on } \partial E \setminus e\}.$$

Before estimating these terms, we introduce the notation for any function q in $L^1(0,T)$,

$$m(q) = \frac{1}{\Delta t}\int_{t_{n-1}}^{t_n} q(s)ds.$$

We shall also use an auxiliary regularizing operator P_h of Hermite type that will only serve for theoretical purposes, $P_h : H^1(\Omega) \to Z_h$, where

$$Z_h = \{z_h \in \mathcal{C}^1(\overline{\Omega});\ z_h|_E \in \mathbb{P}_r(E), \forall E \in \mathcal{T}_h^1\},$$

with $r \geq k$ sufficiently large to guarantee that the functions of Z_h are globally in $\mathcal{C}^1(\overline{\Omega})$ and satisfy the approximation property (3.7), see for example [34,40,41]. With this operator, we associate the following interpolation error:

$$\mathcal{A}_1(p) = |P_h(p) - p|_h + h\Big(\sum_{E\in\mathcal{T}_h^1} \|\nabla\cdot(\boldsymbol{\kappa}\nabla(P_h(p)-p))\|^2_{L^2(E)}\Big)^{\frac{1}{2}} + h^{\frac{1}{2}}\|\boldsymbol{\kappa}\nabla(P_h(p)-p)\cdot\boldsymbol{n}_{12}\|_{L^2(\Gamma_{12})}. \tag{6.6}$$

To alleviate notation, when there is no ambiguity, the superscript ℓ_n will be omitted.

Proposition 10. *If the data $\boldsymbol{\kappa}$ and the unknown p are sufficiently smooth, we have*

$$\big(\mathcal{E}_f^{n,\ell_n}\big)^2 \leq \frac{\hat{C}}{\mu_f^2}\Big[\big(\eta_{t,p}^{n,\ell_n}\big)^2 + \int_{t_{n-1}}^{t_n}\|p_{h\tau}^{n,\ell_n} - p\|_h^2 + \int_{t_{n-1}}^{t_n}\mathcal{A}_1(p)^2\Big]. \tag{6.7}$$

Proof. Set

$$X = q_h^n - q + \partial_t\big(\frac{1}{M}(p - p_{h\tau}^n) + \alpha\nabla\cdot(\boldsymbol{u} - \boldsymbol{u}_{h\tau}^n)\big) + \frac{\alpha}{K_b}\partial_t(\bar{\sigma}_{h\tau}^n - \bar{\sigma}_{h\tau}^{n,\ell_n-1}). \tag{6.8}$$

The a priori error equation for the pressure (4.5) reads for any θ_h in M_h,

$$\big(X,\theta_h\big)_{\Omega_1} = \frac{1}{\mu_f}\Big[(\!(p_h^n - p,\theta_h)\!)_h - \sum_{e\in\mathcal{E}_h^1}\big(\{\boldsymbol{\kappa}\nabla(p_h^n - p)\cdot\boldsymbol{n}_e\}_e, [\theta_h]_e\big)_e - \sum_{e\in\mathcal{E}_h^1}\big(\{\boldsymbol{\kappa}\nabla\,\theta_h\cdot\boldsymbol{n}_e\}_e, [p_h^n - p]_e\big)_e\Big].$$

Note that this equality is unchanged when any global constant is added to θ_h on its right-hand side, thus justifying the definition of $\mathcal{E}_f^{n,\ell_n}$. By inserting $p_{h\tau}^n$ and $P_h(p)$ on this right-hand side, we obtain

$$\begin{aligned}\big(X,\theta_h\big)_{\Omega_1} = \frac{1}{\mu_f}\Big[\ &(\!(p_h^n - p_{h\tau}^n,\theta_h)\!)_h + (\!(p_{h\tau}^n - p,\theta_h)\!)_h - \sum_{e\in\mathcal{E}_h^1}\big(\{\boldsymbol{\kappa}\nabla(p_h^n - P_h(p))\cdot\boldsymbol{n}_e\}_e, [\theta_h]_e\big)_e\\ &- \sum_{e\in\mathcal{E}_h^1}\big(\{\boldsymbol{\kappa}\nabla(P_h(p)-p)\cdot\boldsymbol{n}_e\}_e, [\theta_h]_e\big)_e - \sum_{e\in\mathcal{E}_h^1}\big(\{\boldsymbol{\kappa}\nabla\,\theta_h\cdot\boldsymbol{n}_e\}_e, [p_h^n - p]_e\big)_e\Big].\end{aligned} \tag{6.9}$$

We infer from Green's formula and the regularity of $\boldsymbol{\kappa}$ and $P_h(p)$ that for all $\theta \in H^1(\Omega_1)$,

$$\begin{aligned}-\sum_{e\in\mathcal{E}_h^1}\big(\{\boldsymbol{\kappa}\nabla(P_h(p)-p)\cdot\boldsymbol{n}_e\}_e, [\theta_h]_e\big)_e &= -\sum_{E\in\mathcal{T}_h^1}\big(\nabla\cdot(\boldsymbol{\kappa}\nabla(P_h(p)-p)), \theta_h - \theta\big)_E\\ &\quad - \big(P_h(p) - p, \theta_h - \theta\big)_h + \int_{\Gamma_{12}}\boldsymbol{\kappa}\nabla(P_h(p)-p)\cdot\boldsymbol{n}_{12}(\theta_h - \theta).\end{aligned}$$

Thus (6.9) reads for all θ_h in M_h and $\theta \in H^1(\Omega_1)$,

$$\begin{aligned}\big(X,\theta_h\big)_{\Omega_1} = \frac{1}{\mu_f}\Big[&(\!(p_h^n - p_{h\tau}^n, \theta_h)\!)_h + (\!(p_{h\tau}^n - p, \theta_h)\!)_h - \big(P_h(p) - p, \theta_h - \theta\big)_h \\ &- \sum_{E\in\mathcal{T}_h^1}\big(\nabla\cdot(\boldsymbol{\kappa}\nabla(P_h(p)-p)), \theta_h-\theta\big)_E + \int_{\Gamma_{12}} \boldsymbol{\kappa}\nabla(P_h(p)-p)\cdot\boldsymbol{n}_{12}(\theta_h-\theta) \\ &- \sum_{e\in\mathcal{E}_h^1}\big(\{\boldsymbol{\kappa}\nabla(p_h^n - P_h(p))\cdot\boldsymbol{n}_e\}_e, [\theta_h]_e\big)_e - \sum_{e\in\mathcal{E}_h^1}\big(\{\boldsymbol{\kappa}\nabla\,\theta_h\cdot\boldsymbol{n}_e\}_e, [p_h^n - p]_e\big)_e\Big].\end{aligned} \tag{6.10}$$

By applying to the last two terms the argument used in proving Proposition 15, we derive

$$\begin{aligned}\Big|\sum_{e\in\mathcal{E}_h^1}\big(\{\boldsymbol{\kappa}\nabla(p_h^n - P_h(p))\cdot\boldsymbol{n}_e\}_e, [\theta_h]_e\big)_e\Big| &\le \hat{C}\sum_{e\in\mathcal{E}_h^1}\Big(\frac{\gamma_e}{h_e}\Big)^{\frac12}\|[\theta_h]_e\|_e\Big(\frac{\lambda_{\max}}{\gamma_e}\Big)^{\frac12}\|\boldsymbol{\kappa}^{\frac12}\nabla(p_h^n - P_h(p))\|_E \\ &\le \hat{C}\Big(\frac{\lambda_{\max}}{\min\gamma_e}\Big)^{\frac12} J_h(\theta_h,\theta_h)^{\frac12}|p_h^n - P_h(p)|_h.\end{aligned}$$

Likewise,

$$\Big|\sum_{e\in\mathcal{E}_h^1}\big(\{\boldsymbol{\kappa}\nabla\,\theta_h\cdot\boldsymbol{n}_e\}_e, [p_h^n - P_h(p)]_e\big)_e\Big| \le \hat{C}\Big(\frac{\lambda_{\max}}{\min\gamma_e}\Big)^{\frac12} J_h(p_h^n - P_h(p), p_h^n - P_h(p))^{\frac12}|\theta_h|_h.$$

Hence, by substituting these two bounds into (6.10) and employing the estimates of Proposition 16, we obtain the following bound for X:

$$\begin{aligned}|\big(X,\theta_h\big)_{\Omega_1}| \le \frac{1}{\mu_f}\Big[&\Big(\|p_h^n - p_{h\tau}^n\|_h + \|p_{h\tau}^n - p\|_h + \hat{C}\Big(\frac{\lambda_{\max}}{\min\gamma_e}\Big)^{\frac12}\|p_h^n - P_h(p)\|_h\Big)\|\theta_h\|_h \\ &+ \hat{C}\,\mathcal{A}_1(p)J_h(\theta_h,\theta_h)^{\frac12}\Big].\end{aligned}$$

Thus

$$\sup_{\theta_h\in M_h/\mathbb{R}}\frac{\big(X,\theta_h\big)_{\Omega_1}^2}{\|\theta_h\|_h^2} \le \frac{\hat{C}}{\mu_f^2}\Big[\|p_h^n - p_{h\tau}^n\|_h^2 + \|p_{h\tau}^n - p\|_h^2 + \mathcal{A}_1(p)^2\Big],$$

which implies (6.7). Note that the second term is an error bounded by Theorem 1. □

The bound (6.7) supposes that $\nabla\cdot\boldsymbol{\kappa}\nabla\, p \in L^2(E\times]t_{n-1},t_n[)$. This only guarantees $H^{-\frac12}$ regularity of the normal trace of $\boldsymbol{\kappa}\nabla\, p$ on the interface Γ_{12}, see [42]; but its L^2 regularity follows from the no flow condition.

Proposition 11. *Let $\eta_{t,p,E}$ denote the restriction of $\eta_{t,p}$ defined in (5.9) to an element E. We have*

$$\big(\mathcal{E}_E^{n,\ell_n}\big)^2 \le 3\Big[C^2(\eta_{E,p}^{n,\ell_n})^2 + \frac{\lambda_{\max}}{\mu_f^2}\Big(\int_{t_{n-1}}^{t_n}|p - p_{h\tau}^{n,\ell_n}|_{h,E}^2 + (\eta_{t,p,E}^{n,\ell_n})^2\Big)\Big]. \tag{6.11}$$

with the constant C of (A.1).

Proof. For any element E in $\overline{\Omega}_1$, take $\theta \in H_0^1(E)$ arbitrary, non zero, and $\theta_h = 0$ in the flow error Eq. (4.9). As θ vanishes on the boundary of E, (4.9) reduces to

$$\begin{aligned}\Big(\, q_h^n - q + \partial_t\big(\,\frac{1}{M}(p - p_{h\tau}^n) + \alpha\nabla\cdot(\boldsymbol{u} - \boldsymbol{u}_{h\tau}^n)\,\big), \theta\,\Big)_E = &-\frac{1}{\mu_f}\Big((p - p_{h\tau}^n, \theta)_{h,E} + (p_{h\tau}^n - p_h^n, \theta)_{h,E}\Big) \\ &+ \Big(q_h^n - \partial_t\Big(\frac{1}{M}p_{h\tau}^n + \alpha\nabla\cdot\boldsymbol{u}_{h\tau}^n\Big) + \frac{1}{\mu_f}\nabla\cdot(\boldsymbol{\kappa}(\nabla\, p_h^n - \rho g\nabla\,\eta)), \theta\Big)_E.\end{aligned}$$

Owing to the local Poincaré inequality (A.1), we have

$$\Big|\big(q_h^n - \partial_t\big(\frac{1}{M}p_{h\tau}^n + \alpha\nabla\cdot\boldsymbol{u}_{h\tau}^n\big) + \frac{1}{\mu_f}\nabla\cdot(\boldsymbol{\kappa}(\nabla\, p_h^n - \rho g\nabla\,\eta)), \theta\big)_E\Big|$$
$$\leq \hat{C}h_E\big\|q^n - \partial_t\big(\frac{1}{M}p_{h\tau}^n + \alpha\nabla\cdot\boldsymbol{u}_{h\tau}^n\big) + \frac{1}{\mu_f}\nabla\cdot(\boldsymbol{\kappa}(\nabla\, p_h^n - \rho g\nabla\,\eta))\big\|_{L^2(E)}|\theta|_{H^1(E)}.$$

Then by dividing by $|\theta|_{H^1(E)}$, squaring, taking the supremum with respect to θ in $H_0^1(E)$, and integrating over $]t_{n-1}, t_n[$, we recover (6.11). □

Take $i = 1$; for $\mathcal{E}_{E,1,\partial\boldsymbol{\sigma}}^{n,\ell_n}$, we test (4.14) with $\boldsymbol{v}_h = \boldsymbol{0}$ and $\boldsymbol{v} \in H_0^1(E)^3$; this gives

$$\big(\boldsymbol{\sigma}(\partial_t(\boldsymbol{u} - \boldsymbol{u}_{h\tau}^n)), \boldsymbol{\varepsilon}(\boldsymbol{v})\big)_E - \alpha\big(\partial_t(p - p_{h\tau}^n), \nabla\cdot\boldsymbol{v}\big)_E - \big(\partial_t(\boldsymbol{f} - \boldsymbol{f}_{h\tau}^n), \boldsymbol{v}\big)_E$$
$$= \big(\partial_t\boldsymbol{f}_{h\tau}^n + \nabla\cdot\boldsymbol{\sigma}(\partial_t\boldsymbol{u}_{h\tau}^n) - \alpha\nabla\,\partial_t p_{h\tau}^n, \boldsymbol{v}\big)_E$$

Therefore, by (A.1), we obtain

$$\Big|\big(\boldsymbol{\sigma}(\partial_t(\boldsymbol{u} - \boldsymbol{u}_{h\tau}^n)), \boldsymbol{\varepsilon}(\boldsymbol{v})\big)_E - \alpha\big(\partial_t(p - p_{h\tau}^n), \nabla\cdot\boldsymbol{v}\big)_E - \big(\partial_t(\boldsymbol{f} - \boldsymbol{f}_{h\tau}^n), \boldsymbol{v}\big)_E\Big|$$
$$\leq C\, h_E\|\partial_t\boldsymbol{f}_{h\tau}^n + \nabla\cdot\boldsymbol{\sigma}(\partial_t\boldsymbol{u}_{h\tau}^n) - \alpha\nabla\,\partial_t p_{h\tau}^n\|_{L^2(E)}|\boldsymbol{v}|_{H^1(E)},$$

and by integrating in time, we derive a bound for $\mathcal{E}_{E,1,\partial\boldsymbol{\sigma}}^{n,\ell_n}$. A bound for $\mathcal{E}_{E,2,\partial\boldsymbol{\sigma}}^{n,\ell_n}$ follows by the same argument, with an analogous formula and we have with the constant C of (A.1),

$$\mathcal{E}_{E,i,\partial\boldsymbol{\sigma}}^{n,\ell_n} \leq C\eta_{E,i,\partial\boldsymbol{u}}^{n,\ell_n}, \quad i = 1, 2. \tag{6.12}$$

Regarding $\mathcal{E}_{\omega_e,\partial\boldsymbol{\sigma}}^{n,\ell_n}$, assume for the moment that e is interior to Ω_1, test (4.14) with $\boldsymbol{v}_h = \boldsymbol{0}$ and $\boldsymbol{v} \in H_0^1(\omega_e)^3$. This choice yields

$$\big(\boldsymbol{\sigma}(\partial_t(\boldsymbol{u} - \boldsymbol{u}_{h\tau}^n)), \boldsymbol{\varepsilon}(\boldsymbol{v})\big)_{\omega_e} - \alpha\big(\partial_t(p - p_{h\tau}^n), \nabla\cdot\boldsymbol{v}\big)_{\omega_e} - \big(\partial_t(\boldsymbol{f} - \boldsymbol{f}_{h\tau}^n), \boldsymbol{v}\big)_{\omega_e}$$
$$= \sum_{E\subset\omega_e}\big(\partial_t\boldsymbol{f}_{h\tau}^n + \nabla\cdot\boldsymbol{\sigma}(\partial_t\boldsymbol{u}_{h\tau}^n) - \alpha\nabla\,\partial_t p_{h\tau}^n, \boldsymbol{v}\big)_E - \big([(\boldsymbol{\sigma}(\partial_t\boldsymbol{u}_{h\tau}^n) - \alpha\partial_t p_{h\tau}^n\boldsymbol{I})\boldsymbol{n}_e]_e, \boldsymbol{v}\big)_e$$
$$\leq \sum_{E\subset\omega_e}\|\partial_t\boldsymbol{f}_{h\tau}^n + \nabla\cdot\boldsymbol{\sigma}(\partial_t\boldsymbol{u}_{h\tau}^n) - \alpha\nabla\,\partial_t p_{h\tau}^n\|_{L^2(E)}\|\boldsymbol{v}\|_{L^2(E)} + \|[(\boldsymbol{\sigma}(\partial_t\boldsymbol{u}_{h\tau}^n) - \alpha\partial_t p_{h\tau}^n\boldsymbol{I})\boldsymbol{n}_e]_e\|_{L^2(e)}\|\boldsymbol{v}\|_{L^2(e)}.$$

By applying (A.2) and (A.5), and dividing both sides by $|\boldsymbol{v}|_{H^1(\omega_e)}$, we deduce

$$\frac{1}{|\boldsymbol{v}|_{H^1(\omega_e)}}\Big|\big(\boldsymbol{\sigma}(\partial_t(\boldsymbol{u} - \boldsymbol{u}_{h\tau}^n)), \boldsymbol{\varepsilon}(\boldsymbol{v})\big)_{\omega_e} - \alpha\big(\partial_t(p - p_{h\tau}^n), \nabla\cdot\boldsymbol{v}\big)_{\omega_e} - \big(\partial_t(\boldsymbol{f} - \boldsymbol{f}_{h\tau}^n), \boldsymbol{v}\big)_{\omega_e}\Big|$$
$$\leq \hat{C}\Big(h_{\omega_e}\Big(\sum_{E\subset\omega_e}\|\partial_t\boldsymbol{f}_{h\tau}^n + \nabla\cdot\boldsymbol{\sigma}(\partial_t\boldsymbol{u}_{h\tau}^n) - \alpha\nabla\,\partial_t p_{h\tau}^n\|_{L^2(E)}^2\Big)^{\frac{1}{2}} + h_e^{\frac{1}{2}}\|[(\boldsymbol{\sigma}(\partial_t\boldsymbol{u}_{h\tau}^n) - \alpha\partial_t p_{h\tau}^n\boldsymbol{I})\boldsymbol{n}_e]_e\|_{L^2(e)}\Big).$$

After an integration in time and maximizing over $\boldsymbol{v} \in H_0^1(\omega_e)^3$, this implies

$$\big|\mathcal{E}_{\omega_e,\partial\boldsymbol{\sigma}}^{n,\ell_n}\big| \leq \hat{C}\Big[\Big(\sum_{E\subset\omega_e}\big(\eta_{E,1,\partial\boldsymbol{u}}^{n,\ell_n}\big)^2\Big)^{\frac{1}{2}} + \eta_{e,1,\partial\boldsymbol{\sigma}}^{n,\ell_n}\Big]. \tag{6.13}$$

When e lies on Γ_{12}, the same argument leads to

$$\big|\mathcal{E}_{\omega_e,\partial\boldsymbol{\sigma}}^{n,\ell_n}\big| \leq \hat{C}\Big[\Big(\big(\eta_{E_1,1,\partial\boldsymbol{u}}^{n,\ell_n}\big)^2 + \big(\eta_{E_2,2,\partial\boldsymbol{u}}^{n,\ell_n}\big)^2\Big)^{\frac{1}{2}} + \eta_{e,1,\partial\boldsymbol{\sigma}}^{n,\ell_n}\Big], \tag{6.14}$$

where $E_1 \subset \Omega_1$ and $E_2 \subset \Omega_2$ are the two elements adjacent to e. When e is an interior face of Ω_2, the relevant bound is

$$\big|\mathcal{E}_{\omega_e,\partial\boldsymbol{\sigma}}^{n,\ell_n}\big| \leq \hat{C}\Big[\Big(\sum_{E\subset\omega_e}\big(\eta_{E,2,\partial\boldsymbol{u}}^{n,\ell_n}\big)^2\Big)^{\frac{1}{2}} + \eta_{e,2,\partial\boldsymbol{\sigma}}^{n,\ell_n}\Big]. \tag{6.15}$$

For $\mathcal{E}^{n,\ell_n}_{e,N,\partial\boldsymbol{\sigma}}$, we proceed as above, but ω_e is reduced to the element E adjacent to e and $\boldsymbol{v}$ vanishes on $\partial E \setminus e$. Then we easily derive

$$\left|\mathcal{E}^{n,\ell_n}_{e,N,\partial\boldsymbol{\sigma}}\right| \le \hat{C}\Big(\eta^{n,\ell_n}_{E,2,\partial\boldsymbol{u}} + \eta^{n,\ell_n}_{e,N,\partial\boldsymbol{\sigma}}\Big). \tag{6.16}$$

Remark 1. The weak residual error terms studied above will affect the effectivity index since they will be used to estimate some of the indicators. Hence, evaluating the effectivity index requires their numerical computation or approximation. Unfortunately, their computation is not straightforward.

7. Lower bounds

Here we bound below the error, i.e., we derive upper bounds for each indicator in terms of the errors on the discrete solution and the data. Some of these bounds will be derived under the assumption that $\boldsymbol{\kappa}$ and the solution are sufficiently smooth. As before, $\hat{C}$ denotes various constants independent of h, n, and Δt.

7.1. The algorithmic error indicator

Let us start with an arbitrary value of ℓ. First, the contraction property (A.14) yields

$$\eta^{n,\ell}_{\rm fs} \le (\Delta t)^{\frac{1}{2}} \frac{1}{(\beta K_b)^{\ell-1}} \Big\| \frac{1}{\Delta t}(\bar{\sigma}^{n,1}_h - \bar{\sigma}^{n-1}_h)\Big\|_{L^2(\Omega_1)}, \tag{7.1}$$

where

$$\bar{\sigma}^{n,1}_h - \bar{\sigma}^{n-1}_h = K_b \nabla\cdot(\boldsymbol{u}^{n,1}_h - \boldsymbol{u}^{n-1}_h) - \alpha(p^{n,1}_h - p^{n-1}_h).$$

Next, a bound for the first term on this right-hand side reduces to a bound for the second term, as shown in the next proposition.

Proposition 12. *We have*

$$\|\nabla\cdot(\boldsymbol{u}^{n,1}_h - \boldsymbol{u}^{n-1}_h)\|^2_{L^2(\Omega_1)} \le \frac{\alpha^2}{\lambda^2}\|p^{n,1}_h - p^{n-1}_h\|^2_{L^2(\Omega_1)} + \frac{1}{2G\lambda}\Big(\mathcal{P}^2\mathcal{K}^2\|\boldsymbol{f}^n - \boldsymbol{f}^{n-1}\|^2_{L^2(\Omega)} + C_1^2 C_N^2 \|\boldsymbol{t}^n_N - \boldsymbol{t}^{n-1}_N\|^2_{H^{-\frac{1}{2}}(\Gamma_N)}\Big). \tag{7.2}$$

Proof. By taking the difference between (3.14) at step n, $\ell = 1$ and at step $n-1$, and testing with $\boldsymbol{v}_h = \boldsymbol{u}^{n,1}_h - \boldsymbol{u}^{n-1}_h$, we obtain, after applying Korn's inequality, a trace inequality, and Young's inequality

$$\begin{aligned}
&2G\|\boldsymbol{\varepsilon}(\boldsymbol{u}^{n,1}_h - \boldsymbol{u}^{n-1}_h)\|^2_{L^2(\Omega)} + \lambda\|\nabla\cdot(\boldsymbol{u}^{n,1}_h - \boldsymbol{u}^{n-1}_h)\|^2_{L^2(\Omega)}\\
&\le \frac{1}{2}\Big(\lambda\|\nabla\cdot(\boldsymbol{u}^{n,1}_h - \boldsymbol{u}^{n-1}_h)\|^2_{L^2(\Omega_1)} + \frac{\alpha^2}{\lambda}\|p^{n,1}_h - p^{n-1}_h\|^2_{L^2(\Omega_1)}\Big) + 2G\|\boldsymbol{\varepsilon}(\boldsymbol{u}^{n,1}_h - \boldsymbol{u}^{n-1}_h)\|^2_{L^2(\Omega)}\\
&+ \frac{1}{4G}\Big(\mathcal{P}^2\mathcal{K}^2\|\boldsymbol{f}^n - \boldsymbol{f}^{n-1}\|^2_{L^2(\Omega)} + C_1^2 C_N^2\|\boldsymbol{t}^n_N - \boldsymbol{t}^{n-1}_N\|^2_{H^{-\frac{1}{2}}(\Gamma_N)}\Big),
\end{aligned}$$

which reduces to (7.2). □

Thus

$$\begin{aligned}
&\|\bar{\sigma}^{n,1}_h - \bar{\sigma}^{n-1}_h\|^2_{L^2(\Omega_1)}\\
&\le 2\alpha^2\Big(1 + \frac{K_b^2}{\lambda^2}\Big)\|p^{n,1}_h - p^{n-1}_h\|^2_{L^2(\Omega_1)} + \frac{K_b^2}{\lambda G}\Big(\mathcal{P}^2\mathcal{K}^2\|\boldsymbol{f}^n - \boldsymbol{f}^{n-1}\|^2_{L^2(\Omega)} + C_1^2 C_N^2\|\boldsymbol{t}^n_N - \boldsymbol{t}^{n-1}_N\|^2_{H^{-\frac{1}{2}}(\Gamma_N)}\Big),
\end{aligned} \tag{7.3}$$

and we must find an estimate for $p^{n,1}_h - p^{n-1}_h$. This is the objective of the next lemma.

Lemma 1. *Suppose that the penalty parameters γ_e satisfy (A.12). Assuming that the solution and $\boldsymbol{\kappa}$ are sufficiently smooth as in Proposition 10, we have for all n, $1 \le n \le N$,*

$$\begin{aligned}
&\frac{1}{2\Delta t}\Big(\frac{1}{M}+\frac{\alpha^2}{K_b}\Big)\|p_h^{n,1}-p_h^{n-1}\|^2_{L^2(\Omega_1)} \le \hat{C}\,\Big[\,|p_h^{n-1}-m(P_h(p))|_h^2 + J_h(p_h^{n-1}-m(p),\,p_h^{n-1}-m(p))\\
&+\ \Delta t\sum_{E\in\mathcal{T}_h^1}\|\nabla\cdot(\boldsymbol{\kappa}\,\nabla m(P_h(p)-p))\|^2_{L^2(E)} + \big(h+\Delta t+h^{\frac12}+(\Delta t)^{\frac12}\big)\|\boldsymbol{\kappa}\,\nabla m(P_h(p)-p)\cdot\boldsymbol{n}_{12}\|^2_{L^2(\Gamma_{12})} \qquad (7.4)\\
&+\ \|q^n-m(q)\|^2_{L^2(\Omega_1\times]t_{n-1},t_n[)} + \|\partial_t\Big(\frac{1}{M}p+\alpha\nabla\cdot\boldsymbol{u}\Big)\|^2_{L^2(\Omega_1\times]t_{n-1},t_n[)}\,\Big].
\end{aligned}$$

Proof. By inserting p_h^{n-1} and $m(P_h(p))$ in (3.12) at step $\ell=1$ with $\tau_p=1$, and recalling that $P_h(p)$ does not jump at interfaces, we derive for all $\theta_h\in M_h$,

$$\begin{aligned}
&\Big(\frac{1}{M}+\frac{\alpha^2}{K_b}\Big)\frac{1}{\Delta t}\big(p_h^{n,1}-p_h^{n-1},\theta_h\big)_{\Omega_1} + \frac{1}{\mu_f}(\!(p_h^{n,1}-p_h^{n-1},\theta_h)\!)_h + \frac{1}{\mu_f}(\!(p_h^{n-1}-m(P_h(p)),\theta_h)\!)_h\\
&+\ \frac{1}{\mu_f}\sum_{E\in\mathcal{T}_h^1}\big(\boldsymbol{\kappa}(\nabla m(P_h(p))-\rho g\nabla\eta),\nabla\theta_h\big)_E - \frac{1}{\mu_f}\sum_{e\in\mathcal{E}_h^1}\big(\{\boldsymbol{\kappa}\nabla(p_h^{n,1}-p_h^{n-1})\cdot\boldsymbol{n}_e\}_e,[\theta_h]_e\big)_e\\
&-\ \frac{1}{\mu_f}\sum_{e\in\mathcal{E}_h^1}\big(\{\boldsymbol{\kappa}\nabla(p_h^{n-1}-m(P_h(p)))\cdot\boldsymbol{n}_e\}_e,[\theta_h]_e\big)_e - \frac{1}{\mu_f}\sum_{e\in\mathcal{E}_h^1}\big(\{\boldsymbol{\kappa}(\nabla m(P_h(p))-\rho g\nabla\eta)\cdot\boldsymbol{n}_e\}_e,[\theta_h]_e\big)_e\\
&-\ \frac{1}{\mu_f}\sum_{e\in\mathcal{E}_h^1}\big(\{\boldsymbol{\kappa}\nabla\theta_h\cdot\boldsymbol{n}_e\}_e,[p_h^{n,1}-p_h^{n-1}]_e\big)_e - \frac{1}{\mu_f}\sum_{e\in\mathcal{E}_h^1}\big(\{\boldsymbol{\kappa}\nabla\theta_h\cdot\boldsymbol{n}_e\}_e,[p_h^{n-1}]_e\big)_e = (q^n,\theta_h)_{\Omega_1}.
\end{aligned}$$

With the choice $\theta_h=p_h^{n,1}-p_h^{n-1}$, this becomes

$$\begin{aligned}
&\Big(\frac{1}{M}+\frac{\alpha^2}{K_b}\Big)\frac{1}{\Delta t}\|p_h^{n,1}-p_h^{n-1}\|^2_{L^2(\Omega_1)} + \frac{1}{\mu_f}\|p_h^{n,1}-p_h^{n-1}\|_h^2\\
&-\ \frac{2}{\mu_f}\sum_{e\in\mathcal{E}_h^1}\big(\{\boldsymbol{\kappa}\nabla(p_h^{n,1}-p_h^{n-1})\cdot\boldsymbol{n}_e\}_e,[p_h^{n,1}-p_h^{n-1}]_e\big)_e\\
&=-\frac{1}{\mu_f}(\!(p_h^{n-1}-m(P_h(p)),p_h^{n,1}-p_h^{n-1})\!)_h + \frac{1}{\mu_f}\sum_{e\in\mathcal{E}_h^1}\big(\{\boldsymbol{\kappa}\nabla(p_h^{n-1}-m(P_h(p)))\cdot\boldsymbol{n}_e\}_e,[p_h^{n,1}-p_h^{n-1}]_e\big)_e\\
&+\ \frac{1}{\mu_f}\sum_{e\in\mathcal{E}_h^1}\big(\{\boldsymbol{\kappa}\nabla(p_h^{n,1}-p_h^{n-1})\cdot\boldsymbol{n}_e\}_e,[p_h^{n-1}]_e\big)_e - \frac{1}{\mu_f}\sum_{E\in\mathcal{T}_h^1}\big(\boldsymbol{\kappa}(\nabla m(P_h(p))-\rho g\nabla\eta),\nabla(p_h^{n,1}-p_h^{n-1})\big)_E\\
&+\ \frac{1}{\mu_f}\sum_{e\in\mathcal{E}_h^1}\big(\{\boldsymbol{\kappa}(\nabla m(P_h(p))-\rho g\nabla\eta)\cdot\boldsymbol{n}_e\}_e,[p_h^{n,1}-p_h^{n-1}]_e\big)_e\\
&+\ (q^n-m(q),p_h^{n,1}-p_h^{n-1})_{\Omega_1} + (m(q),p_h^{n,1}-p_h^{n-1})_{\Omega_1}.
\end{aligned}$$

Let us examine the terms containing $\nabla m(P_h(p))-\rho g\nabla\eta$. Since the gradient of $P_h(p)$ does not jump at interfaces and $\boldsymbol{\kappa}$ is supposed to be sufficiently smooth, by Greens' formula applied in each E, we can write for any $\theta_h\in M_h$,

$$\begin{aligned}
&-\sum_{E\in\mathcal{T}_h^1}\big(\nabla\cdot(\boldsymbol{\kappa}(\nabla m(P_h(p))-\rho g\nabla\eta)),\theta_h\big)_E = \sum_{E\in\mathcal{T}_h^1}\big(\boldsymbol{\kappa}(\nabla m(P_h(p))-\rho g\nabla\eta),\nabla\theta_h\big)_E\\
&-\sum_{e\in\mathcal{E}_h^1}\big(\{\boldsymbol{\kappa}(\nabla m(P_h(p))-\rho g\nabla\eta)\cdot\boldsymbol{n}_e\}_e,[\theta_h]_e\big)_e - \int_{\Gamma_{12}}\boldsymbol{\kappa}(\nabla m(P_h(p))-\rho g\nabla\eta)\cdot\boldsymbol{n}_{12}\,\theta_h.
\end{aligned}$$

Hence

$$
\begin{aligned}
&-\frac{1}{\mu_f}\sum_{E\in\mathcal{T}_h^1}\big(\boldsymbol{\kappa}(\nabla m(P_h(p))-\rho g\nabla\eta),\nabla\theta_h\big)_E+\frac{1}{\mu_f}\sum_{e\in\mathcal{E}_h^1}\big(\{\boldsymbol{\kappa}(\nabla m(P_h(p))-\rho g\nabla\eta)\cdot\boldsymbol{n}_e\}_e,[\theta_h]_e\big)_e\\
&=\frac{1}{\mu_f}\sum_{E\in\mathcal{T}_h^1}\big(\nabla\cdot(\boldsymbol{\kappa}(\nabla m(P_h(p))-\rho g\nabla\eta)),\theta_h\big)_E-\frac{1}{\mu_f}\int_{\Gamma_{12}}\boldsymbol{\kappa}(\nabla m(P_h(p))-\rho g\nabla\eta)\cdot\boldsymbol{n}_{12}\,\theta_h\\
&=\frac{1}{\mu_f}\sum_{E\in\mathcal{T}_h^1}\big(\nabla\cdot(\boldsymbol{\kappa}\,\nabla m(P_h(p)-p)),\theta_h\big)_E-\frac{1}{\mu_f}\int_{\Gamma_{12}}\boldsymbol{\kappa}\,\nabla m(P_h(p)-p)\cdot\boldsymbol{n}_{12}\,\theta_h\\
&+\frac{1}{\mu_f}\int_{\Omega_1}\nabla\cdot(\boldsymbol{\kappa}(\nabla m(p)-\rho g\nabla\eta))\,\theta_h,
\end{aligned}
$$

where the no flux interface condition in (2.3) is used in the next to last term. Finally, let us integrate in time the flow equation in (2.3) from t_{n-1} and t_n, divided by Δt. Considering that $\boldsymbol{\kappa}$ and $\rho g\nabla\eta$ are independent of time, this gives for any $\theta_h\in M_h$

$$
(m(q),\theta_h)_{\Omega_1}+\frac{1}{\mu_f}\big(\nabla\cdot(\boldsymbol{\kappa}(\nabla m(p)-\rho g\nabla\eta)),\theta_h\big)_{\Omega_1}=\frac{1}{\Delta t}\int_{t_{n-1}}^{t_n}\big(\partial_t\big(\frac{1}{M}p+\alpha\nabla\cdot\boldsymbol{u}\big),\theta_h\big)_{\Omega_1}. \tag{7.5}
$$

By collecting these equalities, we obtain,

$$
\begin{aligned}
&\big(\frac{1}{M}+\frac{\alpha^2}{K_b}\big)\frac{1}{\Delta t}\|p_h^{n,1}-p_h^{n-1}\|^2_{L^2(\Omega_1)}+\frac{1}{\mu_f}\|p_h^{n,1}-p_h^{n-1}\|_h^2\\
&-\frac{2}{\mu_f}\sum_{e\in\mathcal{E}_h^1}\big(\{\boldsymbol{\kappa}\nabla(p_h^{n,1}-p_h^{n-1})\cdot\boldsymbol{n}_e\}_e,[p_h^{n,1}-p_h^{n-1}]_e\big)_e\\
&=-\frac{1}{\mu_f}(\!(p_h^{n-1}-m(P_h(p)),p_h^{n,1}-p_h^{n-1})\!)_h+\frac{1}{\mu_f}\sum_{e\in\mathcal{E}_h^1}\big(\{\boldsymbol{\kappa}\nabla(p_h^{n-1}-m(P_h(p)))\cdot\boldsymbol{n}_e\}_e,[p_h^{n,1}-p_h^{n-1}]_e\big)_e\\
&+\frac{1}{\mu_f}\sum_{e\in\mathcal{E}_h^1}\big(\{\boldsymbol{\kappa}\nabla(p_h^{n,1}-p_h^{n-1})\cdot\boldsymbol{n}_e\}_e,[p_h^{n-1}-m(p)]_e\big)_e+\frac{1}{\mu_f}\sum_{E\in\mathcal{T}_h^1}\big(\nabla\cdot(\boldsymbol{\kappa}\,\nabla m(P_h(p)-p)),p_h^{n,1}-p_h^{n-1}\big)_E\\
&-\frac{1}{\mu_f}\int_{\Gamma_{12}}\boldsymbol{\kappa}\,\nabla m(P_h(p)-p)\cdot\boldsymbol{n}_{12}\,(p_h^{n,1}-p_h^{n-1})+\big(q^n-m(q),p_h^{n,1}-p_h^{n-1}\big)_{\Omega_1}\\
&+\frac{1}{\Delta t}\int_{t_{n-1}}^{t_n}\big(\partial_t\big(\frac{1}{M}p+\alpha\nabla\cdot\boldsymbol{u}\big),p_h^{n,1}-p_h^{n-1}\big)_{\Omega_1}.
\end{aligned}
\tag{7.6}
$$

The assumption (A.12) on the penalty parameters γ_e implies that

$$
\frac{1}{\mu_f}\|p_h^{n,1}-p_h^{n-1}\|_h^2-\frac{2}{\mu_f}\sum_{e\in\mathcal{E}_h^1}\big(\{\boldsymbol{\kappa}\nabla(p_h^{n,1}-p_h^{n-1})\cdot\boldsymbol{n}_e\}_e,[p_h^{n,1}-p_h^{n-1}]_e\big)_e\geq\frac{1}{2\mu_f}\|p_h^{n,1}-p_h^{n-1}\|_h^2.
$$

With this, (7.4) is deduced from (7.6) by a straightforward variant of (A.9), suitable applications of Young's inequality, and the consequence (A.24) of the trace inequality on Γ_{12}. □

By substituting (7.4) into (7.3), by using (7.1), and recalling the definition (5.3) of the algorithmic error, and the notation (A.15), we obtain the following bound for $\eta_{\rm fs}^{n,\ell}$

$$\begin{aligned}\big(\eta_{\rm fs}^{n,\ell}\big)^2 \leq & \frac{1}{(\beta\, K_b)^{2\ell-2}} \Big[\big(1+\frac{K_b^2}{\lambda^2}\big)\frac{4\hat{C}}{\beta} \Big(|p_h^{n-1}-m(P_h(p))|_h^2 + J_h(p_h^{n-1}-m(p),\, p_h^{n-1}-m(p)) \\ & + \sum_{E\in\mathcal{T}_h^1} \|\nabla\cdot(\boldsymbol{\kappa}\,\nabla(P_h(p)-p))\|^2_{L^2(E\times]t_{n-1},t_n[)} \\ & + \big(\frac{h}{\Delta t}+1+\frac{h^{\frac12}}{\Delta t}+\frac{1}{(\Delta t)^{\frac12}}\big)\|\boldsymbol{\kappa}\,\nabla(P_h(p)-p)\cdot\boldsymbol{n}_{12}\|^2_{L^2(\Gamma_{12}\times]t_{n-1},t_n[)} \\ & + \|q^n-q\|^2_{L^2(\Omega_1\times]t_{n-1},t_n[)} + \|\partial_t\big(\frac{1}{M}p+\alpha\nabla\cdot\boldsymbol{u}\big)\|^2_{L^2(\Omega_1\times]t_{n-1},t_n[)} \Big) \\ & + \frac{K_b^2}{G\lambda}\frac{1}{\Delta t}\Big(\mathcal{P}^2\mathcal{K}^2\|\boldsymbol{f}^n-\boldsymbol{f}^{n-1}\|^2_{L^2(\Omega)} + C_1^2C_N^2\|\boldsymbol{t}_N^n-\boldsymbol{t}_N^{n-1}\|^2_{H^{-\frac12}(\Gamma_N)}\Big)\Big]. \end{aligned} \tag{7.7}$$

From the a posteriori point of view, this bound is not satisfactory because the three last terms cannot be interpreted as errors, but just involve the solution and data; this is strikingly true of the first of these terms that has no reason to be small. This reflects the inconsistency of the algorithm's starting value at each time step, and this effect can only be mitigated by iterating sufficiently, i.e., taking ℓ_n sufficiently large to guarantee a suitable estimate of the error

$$\sum_{n=1}^{m}\sqrt{\Delta t}\,\eta_{\rm fs}^n,$$

in (5.50). To this end, we prescribe the condition for all n

$$\frac{1}{(\beta K_b)^{\ell_n}} \leq C\Delta t, \tag{7.8}$$

with a constant C independent of n, h, Δt (to simplify, we do not explicit this constant). The next theorem summarizes this result.

Theorem 2. *Assume that (7.8) holds at each time step and that (A.12) is satisfied. If the data and solution are sufficiently smooth, we have*

$$\begin{aligned}\eta_{\rm fs}^{n,\ell_n} \leq & \hat{C}\Big[\,\Delta t\,|p_h^{n-1}-m(P_h(p))|_h + \Delta t\, J_h(p_h^{n-1}-m(p),\, p_h^{n-1}-m(p))^{\frac12} \\ & + \Delta t\,\Big(\sum_{E\in\mathcal{T}_h^1}\|\nabla\cdot(\boldsymbol{\kappa}\,\nabla(P_h(p)-p))\|^2_{L^2(E\times]t_{n-1},t_n[)}\Big)^{\frac12} \\ & + (\Delta t)^{\frac12}\big(h^{\frac12}+(\Delta t)^{\frac12}+h^{\frac14}+(\Delta t)^{\frac14}\big)\|\boldsymbol{\kappa}\,\nabla(P_h(p)-p)\cdot\boldsymbol{n}_{12}\|_{L^2(\Gamma_{12}\times]t_{n-1},t_n[)} \\ & + \Delta t\|q^n-q\|_{L^2(\Omega_1\times]t_{n-1},t_n[)} + \Delta t\|\partial_t\big(\frac{1}{M}p+\alpha\nabla\cdot\boldsymbol{u}\big)\|_{L^2(\Omega_1\times]t_{n-1},t_n[)} \\ & + (\Delta t)^{\frac32}\Big(\|\partial_t\boldsymbol{f}\|_{L^\infty(t_{n-1},t_n;L^2(\Omega))} + \|\partial_t\boldsymbol{t}_N\|_{L^\infty(t_{n-1},t_n;H^{-\frac12}(\Gamma_N))}\Big)\Big]. \end{aligned} \tag{7.9}$$

Remark 2. Observe that, if in addition to the assumptions of Theorem 2, the mesh size and time step are of the same order, i.e.,

$$h \leq \hat{C}\,\Delta t, \tag{7.10}$$

then (when ℓ_n achieves convergence)

$$\begin{aligned}\sum_{n=1}^{N}(\Delta t)^{\frac{1}{2}}\eta_{\rm fs}^{n} \le \hat{C}\,\Big[\ &(\Delta t)^{\frac{1}{2}}\Big(\sum_{n=1}^{N}\Delta t(|p_h^{n-1}-m(P_h(p))|_h^2+J_h(p_h^{n-1}-p,p_h^{n-1}-p))\Big)^{\frac{1}{2}}\\ &+\ \Delta t\Big(\sum_{E\in\mathcal{T}_h^1}\|\nabla\cdot(\boldsymbol{\kappa}\,\nabla(P_h(p)-p))\|^2_{L^2(E\times]0,T[)}\Big)^{\frac{1}{2}}\\ &+\ (\Delta t)^{\frac{3}{4}}\|\boldsymbol{\kappa}\,\nabla(P_h(p)-p)\cdot\boldsymbol{n}_{12}\|_{L^2(\Gamma_{12}\times]0,T[)}+\Delta t\|q^n-q\|_{L^2(\Omega_1\times]0,T[)}\\ &+\ \Delta t\Big(\|\partial_t\big(\frac{1}{M}p+\alpha\nabla\cdot\boldsymbol{u}\big)\|_{L^2(\Omega_1\times]0,T[)}+\|\partial_t\boldsymbol{f}\|_{L^\infty(0,T;L^2(\Omega))}+\|\partial_t\boldsymbol{t}_N\|_{L^\infty(0,T;H^{-\frac{1}{2}}(\Gamma_N))}\Big)\ \Big].\end{aligned}\tag{7.11}$$

Under the same assumption, the other term in $\eta_{\rm alg}^m$ is much more favorable because it is bounded as follows

$$\begin{aligned}\Big(\sum_{n=1}^{N}h^2\big(\eta_{\rm fs}^{n}\big)^2\Big)^{\frac{1}{2}} \le \hat{C}\,\Big[\ &(\Delta t)^{\frac{3}{2}}\Big(\sum_{n=1}^{N}\Delta t(|p_h^{n-1}-m(P_h(p))|_h^2+J_h(p_h^{n-1}-p,p_h^{n-1}-p))\Big)^{\frac{1}{2}}\\ &+\ (\Delta t)^2\Big(\sum_{E\in\mathcal{T}_h^1}\|\nabla\cdot(\boldsymbol{\kappa}\,\nabla(P_h(p)-p))\|^2_{L^2(E\times]0,T[)}\Big)^{\frac{1}{2}}\\ &+\ (\Delta t)^{\frac{7}{4}}\|\boldsymbol{\kappa}\,\nabla(P_h(p)-p)\cdot\boldsymbol{n}_{12}\|_{L^2(\Gamma_{12}\times]0,T[)}+(\Delta t)^2\|q^n-q\|_{L^2(\Omega_1\times]0,T[)}\\ &+\ (\Delta t)^2\Big(\|\partial_t\big(\frac{1}{M}p+\alpha\nabla\cdot\boldsymbol{u}\big)\|_{L^2(\Omega_1\times]0,T[)}+\|\partial_t\boldsymbol{f}\|_{L^\infty(0,T;L^2(\Omega))}+\|\partial_t\boldsymbol{t}_N\|_{L^\infty(0,T;H^{-\frac{1}{2}}(\Gamma_N))}\Big)\ \Big].\end{aligned}\tag{7.12}$$

7.2. The time errors indicator

A bound for the time errors indicators $\eta_{t,p}$ and $\eta_{t,J}$, defined in (5.9) and (5.10),

$$\eta_{t,p}^{n,\ell_n}=\Big(\frac{\Delta t}{3}\Big)^{\frac{1}{2}}\big|p_h^{n,\ell_n}-p_h^{n-1}\big|_h,\quad \eta_{t,J}^{n,\ell_n}=\Big(\frac{\Delta t}{3}\Big)^{\frac{1}{2}}\Big(\frac{\gamma_e}{h_e}\Big)^{\frac{1}{2}}\|[p_h^{n,\ell_n}-p_h^{n-1}]_e\|_{L^2(e)},$$

is derived by much the same argument as in estimating $\mathcal{E}_f^{n,\ell_n}$.

Proposition 13. *Under the assumptions of Theorem 2, we have*

$$\big(\eta_{t,p}^{n,\ell_n}\big)^2+\sum_{e\in\mathcal{E}_h^1}\big(\eta_{t,J}^{n,\ell_n}\big)^2\le 12\mu_f^2\Big[\big(\mathcal{E}_f^{n,\ell_n}\big)^2+\big(\frac{\hat{C}}{\mu_f}\big)^2\int_{t_{n-1}}^{t_n}\big(\|p_{h\tau}^{n,\ell_n}-p\|_h^2+\mathcal{A}_1(p)^2\big)\Big],\tag{7.13}$$

where the interpolation error $\mathcal{A}_1(p)$ is defined in (6.6).

Proof. Proceeding as in the proof of Proposition 10, we define X by (6.8) and write

$$\begin{aligned}&\frac{1}{\mu_f}\Big[(\!(p_h^n-p_{h\tau}^n,\theta_h)\!)_h-\sum_{e\in\mathcal{E}_h^1}\big(\{\boldsymbol{\kappa}\nabla(p_h^n-p_{h\tau}^n)\cdot\boldsymbol{n}_e\}_e,[\theta_h]_e\big)_e-\sum_{e\in\mathcal{E}_h^1}\big(\{\boldsymbol{\kappa}\nabla\,\theta_h\cdot\boldsymbol{n}_e\}_e,[p_h^n-p_{h\tau}^n]_e\big)_e\Big]\\ &=\big(X,\theta_h\big)_{\Omega_1}+\frac{1}{\mu_f}\ \Big[\ (\!(p-p_{h\tau}^n,\theta_h)\!)_h+\sum_{e\in\mathcal{E}_h^1}\big(\{\boldsymbol{\kappa}\nabla(p_{h\tau}^n-P_h(p))\cdot\boldsymbol{n}_e\}_e,[\theta_h]_e\big)_e\\ &\quad+\sum_{e\in\mathcal{E}_h^1}\big(\{\boldsymbol{\kappa}\nabla\,\theta_h\cdot\boldsymbol{n}_e\}_e,[p_{h\tau}^n-p]_e\big)_e\\ &\quad+\sum_{E\in\mathcal{T}_h^1}\big(\nabla\cdot(\boldsymbol{\kappa}\nabla(P_h(p)-p)),\theta_h-\theta\big)_E+\big(P_h(p)-p,\theta_h-\theta\big)_h-\int_{\Gamma_{12}}\boldsymbol{\kappa}\nabla(P_h(p)-p)\cdot\boldsymbol{n}_{12}(\theta_h-\theta)\ \Big].\end{aligned}$$

With the choice $\theta_h = p_h^n - p_{h\tau}^n$, we recognize in the above left-hand side $a_h(\theta_h, \theta_h)$ defined in (A.10). Assuming (A.12), $a_h(\theta_h, \theta_h)$ is bounded below by (A.13). Thus, by applying to the last three terms the estimates of Proposition 16, we derive

$$\frac{1}{2\mu_f}\|p_h^n - p_{h\tau}^n\|_h \le \sup_{\theta_h \in M_h/\mathbb{R}} \frac{(X, \theta_h)_{\Omega_1}}{\|\theta_h\|_h} + \frac{1}{\mu_f}\Big[\, \|p_{h\tau}^n - p\|_h + \hat{C}\big(\frac{\lambda_{\max}}{\min \gamma_e}\big)^{\frac{1}{2}}\big(\|p_{h\tau}^n - P_h(p)\|_h + |P_h(p) - p|_h\big) + \frac{\hat{C}}{\min \gamma_e^{\frac{1}{2}}}\big(\mathcal{A}_1(p) - |P_h(p) - p|_h\big)\Big].$$

Note that

$$p_{h\tau}^n - P_h(p) = (p_{h\tau}^n - p) + (p - P_h(p));$$

therefore, the argument in the third term can be replaced by $p_{h\tau}^n - p$ and the contribution of $p - P_h(p)$ can be incorporated into $\mathcal{A}_1(p)$. Then the proposition follows from

$$\frac{1}{4\mu_f^2}\int_{t_{n-1}}^{t_n} \|p_h^n - p_{h\tau}^n\|_h^2 \le 3\Big[\big(\mathcal{E}_f^n\big)^2 + \big(\frac{\hat{C}}{\mu_f}\big)^2 \int_{t_{n-1}}^{t_n} \big(\|p_{h\tau}^n - p\|_h^2 + \mathcal{A}_1(p)^2\big)\Big]. \quad \square$$

7.3. The local interior flow error indicator

Recall formula (5.5) for $\eta_{E,p}$,

$$\eta_{E,p}^{n,\ell_n} = h_E\big(\Delta t\big)^{\frac{1}{2}}\Big\|q_h^n + \frac{1}{\mu_f}\nabla\cdot\big(\boldsymbol{\kappa}(\nabla p_h^{n,\ell_n} - \rho g \nabla \eta)\big) - \partial_t\big(\frac{1}{M}p_{h\tau}^{n,\ell_n} + \alpha\nabla\cdot\boldsymbol{u}_{h\tau}^{n,\ell_n}\big)\Big\|_{L^2(E)}.$$

The bound for $\eta_{E,p}^n$ proceeds via a standard local argument in each element $E \subset \overline{\Omega}_1$. To simplify, we assume that restriction to each E of the density ρ and the components of the permeability tensor $\boldsymbol{\kappa}$ are polynomials. The pressure error equation (4.9) is tested with $\theta_h = 0$ and

$$\theta|_E = b_E\Big(q_h^n + \frac{1}{\mu_f}\nabla\cdot\big(\boldsymbol{\kappa}(\nabla\, p_h^n - \rho g\nabla\,\eta)\big) - \partial_t\big(\frac{1}{M}p_{h\tau}^n + \alpha\nabla\cdot\boldsymbol{u}_{h\tau}^n\big)\Big)|_E,$$

extended by zero outside E, where b_E is the lowest degree unit bubble function in E. Thus $\theta \in H_0^1(E)$ is a polynomial function and

$$\|\theta\|_{L^2(E)} \le \|q_h^n + \frac{1}{\mu_f}\nabla\cdot\big(\boldsymbol{\kappa}(\nabla\, p_h^n - \rho g\nabla\,\eta)\big) - \partial_t\big(\frac{1}{M}p_{h\tau}^n + \alpha\nabla\cdot\boldsymbol{u}_{h\tau}^n\big)\|_{L^2(E)}.$$

Let

$$A = \Big(q_h^n + \frac{1}{\mu_f}\nabla\cdot\big(\boldsymbol{\kappa}(\nabla\, p_h^n - \rho g\nabla\,\eta)\big) - \partial_t\big(\frac{1}{M}p_{h\tau}^n + \alpha\nabla\cdot\boldsymbol{u}_{h\tau}^n\big), \theta\Big)_E.$$

On the one hand, as θ is a polynomial function, a familiar scaling argument leads to

$$A \ge \hat{C}\Big\|q_h^n + \frac{1}{\mu_f}\nabla\cdot\big(\boldsymbol{\kappa}(\nabla p_h^n - \rho g\nabla\,\eta)\big) - \partial_t\big(\frac{1}{M}p_{h\tau}^n + \alpha\nabla\cdot\boldsymbol{u}_{h\tau}^n\big)\Big\|_{L^2(E)}^2.$$

On the other hand, (4.9) reduces to

$$A = (q_h^n - q + \partial_t\big(\frac{1}{M}(p - p_{h\tau}^n) + \alpha\nabla\cdot(\boldsymbol{u} - \boldsymbol{u}_{h\tau}^n)\big), \theta)_E + \frac{1}{\mu_f}\Big((p - p_{h\tau}^n, \theta)_{h,E} + (p_{h\tau}^n - p_h^n, \theta)_{h,E}\Big).$$

By collecting the above inequalities and applying (A.6), we derive

$$h_E\Big\|q_h^n + \frac{1}{\mu_f}\nabla\cdot\big(\boldsymbol{\kappa}(\nabla p_h^n - \rho g\nabla\,\eta)\big) - \partial_t\big(\frac{1}{M}p_{h\tau}^n + \alpha\nabla\cdot\boldsymbol{u}_{h\tau}^n\big)\Big\|_{L^2(E)}$$
$$\le \hat{C}\Big(\frac{1}{\mu_f}\lambda_{\max}^{\frac{1}{2}}\big(|p - p_{h\tau}^n|_{h,E} + |p_{h\tau}^n - p_h^n|_{h,E}\big) + \|q_h^n - q + \partial_t\big(\frac{1}{M}(p - p_{h\tau}^n) + \alpha\nabla\cdot(\boldsymbol{u} - \boldsymbol{u}_{h\tau}^n)\big)\|_{H^{-1}(E)}\Big).$$

By squaring both sides, integrating in time over $]t_{n-1}, t_n[$, and recalling the notation $\mathcal{E}_E^{n,\ell_n}$, we deduce an upper bound for $\eta_{E,p}^{n,\ell_n}$,

$$\big(\eta_{E,p}^{n,\ell_n}\big)^2 \le 3\hat{C}^2\Big[\big(\mathcal{E}_E^{n,\ell_n}\big)^2 + \frac{1}{\mu_f^2}\lambda_{\max}\Big(\int_{t_{n-1}}^{t_n} |p - p_{h\tau}^{n,\ell_n}|_{h,E}^2 + \big(\eta_{t,p,E}^{n,\ell_n}\big)^2\Big)\Big]. \tag{7.14}$$

7.4. The local jump flow error indicator

Recall the local jumps $\eta_{\rm pen}$ defined in (5.1),

$$\eta_{\rm pen}^{n,\ell_n} = \big(\Delta t\big)^{\frac{1}{2}}\Big(\frac{\gamma_e}{h_e}\Big)^{\frac{1}{2}}\|[p_h^{n,\ell_n}]_e\|_{L^2(e)}.$$

By inserting $p_{h\tau}^{n,\ell_n}$, $\eta_{\rm pen}^{n,\ell_n}$ has the bound

$$\begin{aligned}\big(\eta_{\rm pen}^{n,\ell_n}\big)^2 \le& 2\int_{t_{n-1}}^{t_n}\frac{\gamma_e}{h_e}\|[p_h^{n,\ell_n} - p_{h\tau}^{n,\ell_n}]_e\|_{L^2(e)}^2 + 2\Delta t\, J_h(p - p_{h\tau}^{n,\ell_n}, p - p_{h\tau}^{n,\ell_n})\\ =& 2\big(\eta_{t,J}^{n,\ell_n}\big)^2 + 2\int_{t_{n-1}}^{t_n} J_h(p - p_{h\tau}^{n,\ell_n}, p - p_{h\tau}^{n,\ell_n}).\end{aligned} \tag{7.15}$$

This is an acceptable bound, since the first term is an indicator and the second one an error term.

7.5. The local jump flux error indicator

The local flux jump $\eta_{{\rm flux},e}$ defined by (5.7) reads

$$\eta_{{\rm flux},e}^{n,\ell_n} = \big(h_e\Delta t\big)^{\frac{1}{2}}\big\|[\boldsymbol{\kappa}(\nabla\, p_h^{n,\ell_n} - \rho g\nabla\,\eta)\cdot\boldsymbol{n}_e]_e\big\|_{L^2(e)}.$$

The bound for $\eta_{{\rm flux},e}^n$ is derived by a classical argument on each face $e \in \mathcal{E}_h^1$. To simplify, we restrict the discussion to internal faces, the case of boundary faces (i.e., on Γ_{12}) being simpler, since jumps on Γ_{12} are just traces. Thus, let e be an internal face and let b_e be a unit bubble polynomial function of the lowest degree that vanishes on ∂e. Let $\hat{e}$ be a reference unit face and $\hat{\omega}_{\hat{e}}$ the union of two reference unit elements that share $\hat{e}$. By working first on $\hat{\omega}_{\hat{e}}$ and then switching to ω_e by a suitable transformation, we can construct an extension operator $\mathcal{G}$, linear from $H_{00}^{\frac{1}{2}}(e)$ into $H_0^1(\omega_e)$ and uniformly continuous with respect to e and h, i.e.,

$$\forall f \in H_{00}^{\frac{1}{2}}(e), \quad |\mathcal{G}(f)|_{H^1(\omega_e)} \le \hat{C}|f|_{H_{00}^{\frac{1}{2}}(e)}, \tag{7.16}$$

with $\hat{C}$ independent of h, e, and ω_e. The pressure error Eq. (4.9) is tested with $\theta_h = 0$ and

$$\theta|_{\omega_e} = \mathcal{G}\Big(\big[\boldsymbol{\kappa}(\nabla\, p_h^n - \rho g\nabla\,\eta)\cdot\boldsymbol{n}_e\big]_e b_e\Big).$$

Thus $\theta \in H_0^1(\omega_e)$, hence has no jump through e, and $\theta|_e \in H_{00}^{\frac{1}{2}}(e)$,

$$\|\theta\|_{L^2(e)} \le \big\|\big[\boldsymbol{\kappa}(\nabla\, p_h^n - \rho g\nabla\,\eta)\cdot\boldsymbol{n}_e\big]_e\big\|_{L^2(e)}.$$

Moreover, by the construction of $\mathcal{G}$ and the fact that the restriction of θ to e belongs to a finite dimensional space, we have on the one hand,

$$\big([\boldsymbol{\kappa}(\nabla\, p_h^n - \rho g\nabla\,\eta)\cdot\boldsymbol{n}_e]_e, \theta\big)_e \ge \hat{C}\big\|[\boldsymbol{\kappa}(\nabla\, p_h^n - \rho g\nabla\,\eta)\cdot\boldsymbol{n}_e]_e\big\|_{L^2(e)}^2.$$

On the other hand, (4.9) reduces to

$$\begin{aligned}\frac{1}{\mu_f}\big(\,[\boldsymbol{\kappa}(\nabla p_h^n - \rho g\nabla\eta)\cdot\boldsymbol{n}_e]_e, \theta\,\big)_e =& -\Big(\partial_t\big(\frac{1}{M}(p - p_{h\tau}^n) + \alpha\nabla\cdot(\boldsymbol{u} - \boldsymbol{u}_{h\tau}^n)\big) - (q - q_h^n), \theta\Big)_{\omega_e}\\ &+ \sum_{E\subset\omega_e}\big(q_h^n - \partial_t(\frac{1}{M}p_{h\tau}^n + \alpha\nabla\cdot\boldsymbol{u}_{h\tau}^n) + \frac{1}{\mu_f}\nabla\cdot\big(\boldsymbol{\kappa}(\nabla p_h^n - \rho g\nabla\,\eta)\big), \theta\big)_E\\ &- \frac{1}{\mu_f}\Big(\big(p - p_{h^\tau}^n, \theta\big)_{h,\omega_e} + \big(p_{h^\tau}^n - p_h^n, \theta\big)_{h,\omega_e}\Big).\end{aligned}$$

Therefore,

$$\frac{1}{\mu_f}\left\|[\boldsymbol{\kappa}(\nabla p_h^n-\rho g\nabla\eta)\cdot\boldsymbol{n}_e]_e\right\|^2_{L^2(e)}\le\hat{C}\Big[\ \|\partial_t\big(\frac{1}{M}(p-p_{h\tau}^n)+\alpha\nabla\cdot(\boldsymbol{u}-\boldsymbol{u}_{h\tau}^n)\big)-(q-q_h^n)\|_{H^{-1}(\omega_e)}|\theta|_{H^1(\omega_e)}$$
$$+\sum_{E\subset\omega_e}\|q_h^n-\partial_t(\frac{1}{M}p_{h\tau}^n+\alpha\nabla\cdot\boldsymbol{u}_{h\tau}^n)+\frac{1}{\mu_f}\nabla\cdot\boldsymbol{\kappa}(\nabla p_h^n-\rho g\nabla\eta)\|_{L^2(E)}\|\theta\|_{L^2(E)}$$
$$+\frac{1}{\mu_f}\Big(|p-p_{h\tau}^n|_{h,\omega_e}+|p_{h\tau}^n-p_h^n|_{h,\omega_e}\Big)|\theta|_{h,\omega_e}\ \Big].$$

Then, by applying (7.16), (A.1), and (A.8), we derive

$$\left\|[\boldsymbol{\kappa}(\nabla p_h^n-\rho g\nabla\eta)\cdot\boldsymbol{n}_e]_e\right\|_{L^2(e)}\le\hat{C}\Big[\ \mu_f\Big(\frac{1}{h_e^{\frac{1}{2}}}\|\partial_t\big(\frac{1}{M}(p-p_{h\tau}^n)+\alpha\nabla\cdot(\boldsymbol{u}-\boldsymbol{u}_{h\tau}^n)\big)-(q-q_h^n)\|_{H^{-1}(\omega_e)}$$
$$+h_e^{\frac{1}{2}}\Big(\sum_{E\subset\omega_e}\|q_h^n-\partial_t(\frac{1}{M}p_{h\tau}^n+\alpha\nabla\cdot\boldsymbol{u}_{h\tau}^n)+\frac{1}{\mu_f}\nabla\cdot\boldsymbol{\kappa}(\nabla p_h^n-\rho g\nabla\eta)\|^2_{L^2(E)}\Big)^{\frac{1}{2}}\Big)$$
$$+\big(\frac{\lambda_{\max}}{h_e}\big)^{\frac{1}{2}}\Big(|p-p_{h\tau}^n|_{h,\omega_e}+|p_{h\tau}^n-p_h^n|_{h,\omega_e}\Big)\ \Big].$$

By squaring both sides, multiplying by h_e, and integrating with respect to time, we obtain

$$\big(\eta_{\text{flux},e}^{n,\ell_n}\big)^2\le 3\hat{C}\Big[\mu_f^2\Big(\big(\mathcal{E}_{\omega_e}^{n,\ell_n}\big)^2+\sum_{E\subset\omega_e}\big(\eta_{E,p}^{n,\ell_n}\big)^2\Big)+2\lambda_{\max}\Big(\big(\eta_{t,p,\omega_e}^{n,\ell_n}\big)^2+\int_{t_{n-1}}^{t_n}|p-p_{h\tau}^{n,\ell_n}|^2_{h,\omega_e}\Big)\Big].\tag{7.17}$$

7.6. The time derivative pressure's jump indicator

Recall formula (5.17) for $\eta_{\partial p,J}$,

$$\eta_{\partial p,J}^{n,\ell_n}=h_e\Delta t\Big(\frac{\gamma_e}{h_e}\Big)^{\frac{1}{2}}\|\frac{1}{\Delta t}[p_h^{n,\ell_n}-p_h^{n-1}]_e\|_{L^2(e)}.$$

By comparing with $\eta_{t,J}^{n,\ell_n}$ defined in (5.10), we see that

$$\eta_{\partial p,J}^{n,\ell_n}=h_e\big(\frac{3}{\Delta t}\big)^{\frac{1}{2}}\eta_{t,J}^{n,\ell_n}.\tag{7.18}$$

This is an acceptable upper bound if we assume that

$$h_e^2\le\hat{C}\,\Delta t,\tag{7.19}$$

a condition less restrictive than (7.10).

7.7. The time derivative of displacement balance indicators

Take $i=1$ and consider the time derivative of the displacement equilibrium $\eta_{E,1,\partial\boldsymbol{u}}$ given by (5.19),

$$\eta_{E,1,\partial\boldsymbol{u}}^{n,\ell_n}=h_E\Delta t\|\partial_t\boldsymbol{f}_{h\tau}^n+\nabla\cdot\boldsymbol{\sigma}(\partial_t\boldsymbol{u}_{h\tau}^{n,\ell_n})-\alpha\nabla\,\partial_t p_{h\tau}^{n,\ell_n}\|_{L^2(E)}.$$

When Eq. (4.14) is tested with $\boldsymbol{v}_h=\boldsymbol{0}$ and

$$\boldsymbol{v}|_E=b_E\partial_t\big(\boldsymbol{f}_{h\tau}^n+\nabla\cdot\boldsymbol{\sigma}(\boldsymbol{u}_{h\tau}^n)-\alpha\nabla\,p_{h\tau}^n\big),$$

extended by zero outside E, it reduces to

$$\big(\partial_t\boldsymbol{f}_{h\tau}^n+\nabla\cdot\boldsymbol{\sigma}(\partial_t\boldsymbol{u}_{h\tau}^n)-\alpha\nabla\,\partial_t p_{h\tau}^n,\boldsymbol{v}\big)_E=\big(\boldsymbol{\sigma}(\partial_t(\boldsymbol{u}-\boldsymbol{u}_{h\tau}^n)),\boldsymbol{\varepsilon}(\boldsymbol{v})\big)_E-\alpha\big(\partial_t(p-p_{h\tau}^n),\nabla\cdot\boldsymbol{v}\big)_E$$
$$-\big(\partial_t(\boldsymbol{f}-\boldsymbol{f}_{h\tau}^n),\boldsymbol{v}\big)_E$$

Thus, by proceeding as in Section 7.3, we deduce that

$$\begin{aligned}
&\hat{C}\,\|\partial_t \boldsymbol{f}^n_{h\tau} + \nabla\cdot\boldsymbol{\sigma}(\partial_t \boldsymbol{u}^n_{h\tau}) - \alpha\nabla\,\partial_t p^n_{h\tau}\|^2_{L^2(E)}\\
&\le \Big(\frac{1}{|\boldsymbol{v}|_{H^1(E)}}\big|\big(\boldsymbol{\sigma}(\partial_t(\boldsymbol{u}-\boldsymbol{u}^n_{h\tau})),\boldsymbol{\varepsilon}(\boldsymbol{v})\big)_E - \alpha\big(\partial_t(p-p^n_{h\tau}),\nabla\cdot\boldsymbol{v}\big)_E - \big(\partial_t(\boldsymbol{f}-\boldsymbol{f}^n_{h\tau}),\boldsymbol{v}\big)_E\big|\Big)|\boldsymbol{v}|_{H^1(E)}\\
&\le \frac{\hat{C}}{h_E}\Big(\frac{1}{|\boldsymbol{v}|_{H^1(E)}}\big|\big(\boldsymbol{\sigma}(\partial_t(\boldsymbol{u}-\boldsymbol{u}^n_{h\tau})),\boldsymbol{\varepsilon}(\boldsymbol{v})\big)_E - \alpha\big(\partial_t(p-p^n_{h\tau}),\nabla\cdot\boldsymbol{v}\big)_E - \big(\partial_t(\boldsymbol{f}-\boldsymbol{f}^n_{h\tau}),\boldsymbol{v}\big)_E\big|\Big)\|\boldsymbol{v}\|_{L^2(E)},
\end{aligned}$$

where we have used (A.6). Therefore, by multiplying both sides with h_E and integrating in time, this leads to

$$\eta^{n,\ell_n}_{E,1,\partial\boldsymbol{u}} \le \hat{C}\,\mathcal{E}^{n,\ell_n}_{E,1,\partial\boldsymbol{\sigma}}. \tag{7.20}$$

When $i=2$, the treatment of $\eta_{E,2,\partial\boldsymbol{u}}$ defined by (5.20) is the same and leads to the bound

$$\eta^{n,\ell_n}_{E,2,\partial\boldsymbol{u}} \le \hat{C}\,\mathcal{E}^{n,\ell_n}_{E,2,\partial\boldsymbol{\sigma}}. \tag{7.21}$$

7.8. The time derivative of stress tensor's jump indicators

To bound the time derivative of the stress tensor's jump on $e\in\mathcal{E}^1_h\cup\mathcal{E}^{12}_h$ given by (5.21),

$$\eta^{n,\ell_n}_{e,1,\partial\boldsymbol{\sigma}} = h_e^{\frac12}\,\Delta t\,\|[(\boldsymbol{\sigma}(\partial_t\boldsymbol{u}^{n,\ell_n}_{h\tau}) - \alpha\,\partial_t p^{n,\ell_n}_{h\tau}\boldsymbol{I})\boldsymbol{n}_e]_e\|_{L^2(e)},$$

we proceed as for $\eta_{\rm flux}$ and use the same notation. Consider a face e in $\mathcal{E}^1_h$ and test (4.14) with $\boldsymbol{v}_h=\boldsymbol{0}$ and

$$\boldsymbol{v}|_{\omega_e} = \mathcal{G}\Big(\big[\big(\boldsymbol{\sigma}(\partial_t\boldsymbol{u}^n_{h\tau}) - \alpha\,\partial_t p^n_{h\tau}\boldsymbol{I}\big)\boldsymbol{n}_e\big]_e b_e\Big).$$

The equality (4.14) becomes

$$\begin{aligned}
\int_e b_e\big|\,\big[\big(\,\boldsymbol{\sigma}(\partial_t\boldsymbol{u}^n_{h\tau}) - \alpha\,\partial_t p^n_{h\tau}\boldsymbol{I}\,\big)\,\boldsymbol{n}_e\,\big]_e\big|^2 &= \sum_{E\subset\omega_e}\Big(\partial_t\boldsymbol{f}^n_{h\tau} + \nabla\cdot\boldsymbol{\sigma}(\partial_t\boldsymbol{u}^n_{h\tau}) - \alpha\nabla\,\partial_t p^n_{h\tau},\boldsymbol{v}\Big)_E\\
&\quad - \big(\boldsymbol{\sigma}(\partial_t(\boldsymbol{u}-\boldsymbol{u}^n_{h\tau})),\boldsymbol{\varepsilon}(\boldsymbol{v})\big)_{\omega_e} + \alpha\big(\partial_t(p-p^n_{h\tau}),\nabla\cdot\boldsymbol{v}\big)_{\omega_e} + \big(\partial_t(\boldsymbol{f}-\boldsymbol{f}^n_{h\tau}),\boldsymbol{v}\big)_{\omega_e}.
\end{aligned}$$

Thus

$$\begin{aligned}
&\hat{C}\,\big\|\big[\big(\boldsymbol{\sigma}(\partial_t\boldsymbol{u}^n_{h\tau}) - \alpha\,\partial_t p^n_{h\tau}\boldsymbol{I}\big)\boldsymbol{n}_e\big]_e\big\|^2_{L^2(e)}\\
&\le \Big(\frac{1}{|\boldsymbol{v}|_{H^1(\omega_e)}}\big| - \big(\boldsymbol{\sigma}(\partial_t(\boldsymbol{u}-\boldsymbol{u}^n_{h\tau})),\boldsymbol{\varepsilon}(\boldsymbol{v})\big)_{\omega_e} + \alpha\big(\partial_t(p-p^n_{h\tau}),\nabla\cdot\boldsymbol{v}\big)_{\omega_e} + \big(\partial_t(\boldsymbol{f}-\boldsymbol{f}^n_{h\tau}),\boldsymbol{v}\big)_{\omega_e}\big|\Big)|\boldsymbol{v}|_{H^1(\omega_e)}\\
&+ \sum_{E\subset\omega_e}\|\partial_t\boldsymbol{f}^n_{h\tau} + \nabla\cdot\boldsymbol{\sigma}(\partial_t\boldsymbol{u}^n_{h\tau}) - \alpha\nabla\,\partial_t p^n_{h\tau}\|_{L^2(E)}\|\boldsymbol{v}\|_{L^2(E)}\\
&\le \hat{C}\,\Big(\,\frac{1}{h_e^{\frac12}}\frac{1}{|\boldsymbol{v}|_{H^1(\omega_e)}}\big| - \big(\boldsymbol{\sigma}(\partial_t(\boldsymbol{u}-\boldsymbol{u}^n_{h\tau})),\boldsymbol{\varepsilon}(\boldsymbol{v})\big)_{\omega_e} + \alpha\big(\partial_t(p-p^n_{h\tau}),\nabla\cdot\boldsymbol{v}\big)_{\omega_e} + \big(\partial_t(\boldsymbol{f}-\boldsymbol{f}^n_{h\tau}),\boldsymbol{v}\big)_{\omega_e}\big|\\
&\qquad + h_e^{\frac12}\Big(\sum_{E\subset\omega_e}\|\partial_t\boldsymbol{f}^n_{h\tau} + \nabla\cdot\boldsymbol{\sigma}(\partial_t\boldsymbol{u}^n_{h\tau}) - \alpha\nabla\,\partial_t p^n_{h\tau}\|^2_{L^2(E)}\Big)^{\frac12}\,\Big)\,\|\boldsymbol{v}\|_{L^2(e)},
\end{aligned}$$

where we have used (7.16), (A.2), and (A.8). By multiplying both sides with $h_e^{\frac12}$ and integrating in time we infer

$$\eta^{n,\ell_n}_{e,1,\partial\boldsymbol{\sigma}} \le \hat{C}\Big(\mathcal{E}^{n,\ell_n}_{\omega_e,\partial\boldsymbol{\sigma}} + \Big(\sum_{E\subset\omega_e}(\eta^{n,\ell_n}_{E,1,\partial\boldsymbol{u}})^2\Big)^{\frac12}\Big). \tag{7.22}$$

When e lies on Γ_{12}, (7.22) is replaced by

$$\eta^{n,\ell_n}_{e,1,\partial\boldsymbol{\sigma}} \le \hat{C}\Big(\mathcal{E}^{n,\ell_n}_{\omega_e,\partial\boldsymbol{\sigma}} + \big((\eta^{n,\ell_n}_{E_1,1,\partial\boldsymbol{u}})^2 + (\eta^{n,\ell_n}_{E_2,2,\partial\boldsymbol{u}})^2\big)^{\frac12}\Big), \tag{7.23}$$

where $E_1\subset\Omega_1$ and $E_2\subset\Omega_2$ are the two elements adjacent to e. The case of $\eta_{e,2,\partial\boldsymbol{\sigma}}$ defined by (5.22) is the same; we obtain

$$\eta^{n,\ell_n}_{e,2,\partial\boldsymbol{\sigma}} \le \hat{C}\Big(\mathcal{E}^{n,\ell_n}_{\omega_e,\partial\boldsymbol{\sigma}} + \Big(\sum_{E\subset\omega_e}(\eta^{n,\ell_n}_{E,2,\partial\boldsymbol{u}})^2\Big)^{\frac12}\Big). \tag{7.24}$$

Finally, we consider $\eta_{e,N,\partial\boldsymbol{\sigma}}$ defined by (5.23),

$$\eta_{e,N,\partial\boldsymbol{\sigma}}^{n,\ell_n} = h_e^{\frac{1}{2}} \Delta t \|\boldsymbol{\sigma}(\partial_t \boldsymbol{u}_{h\tau}^{n,\ell_n})\boldsymbol{n}_\Omega - \partial_t \boldsymbol{t}_{N,h\tau}^n\|_{L^2(e)}.$$

As e lies on Γ_N, the jump reduces to the trace, ω_e is the element adjacent to e, and the lifting function $\boldsymbol{v}$ defined above vanishes on $\partial E \setminus e$, i.e. belongs to $H_e^1(E)$. Therefore, we readily obtain

$$\eta_{e,N,\partial\boldsymbol{\sigma}}^{n,\ell_n} \le \hat{C}\Big(\mathcal{E}_{e,N,\partial\boldsymbol{\sigma}}^{n,\ell_n} + \eta_{E,2,\partial\boldsymbol{u}}^{n,\ell_n}\Big), \tag{7.25}$$

where the auxiliary error $\mathcal{E}_{e,N,\partial\boldsymbol{\sigma}}^{n,\ell_n}$ is defined by (6.5).

7.9. Indicator of the pressure jump at time t_n

To bound $\eta_{p,J}$ defined by (5.29),

$$\eta_{p,J}^{n,\ell_n} = h_e\Big(\frac{\gamma_e}{h_e}\Big)^{\frac{1}{2}} \|[p_h^{n,\ell_n}]_e\|_{L^2(e)},$$

we compare it with η_{pen} defined by (5.1) and observe that

$$\eta_{p,J} = \frac{h_e}{(\Delta t)^{\frac{1}{2}}}\eta_{\text{pen}}.$$

Therefore, under the assumption (7.19), we have

$$\eta_{p,J}^{n,\ell_n} \le \hat{C}\eta_{\text{pen}}^{n,\ell_n}. \tag{7.26}$$

7.10. Indicator of the displacement equilibrium errors at time t_n

Recall the indicator of displacement equilibrium $\eta_{E,i,\boldsymbol{u}}$ in $\mathcal{T}_h^i$, see (5.30), with $p_h = 0$ in Ω_2,

$$\eta_{E,i,\boldsymbol{u}}^{n,\ell_n} = h_E\|\boldsymbol{f}_h^n + \nabla\cdot\boldsymbol{\sigma}(\boldsymbol{u}_h^{n,\ell_n}) - \alpha\nabla\, p_h^{n,\ell_n}\|_{L^2(E)}.$$

For $E \in \mathcal{T}_h^1$, by testing the displacement error equation (4.13), at time t_n, with $\boldsymbol{v}_h = \boldsymbol{0}$ and

$$\boldsymbol{v} = b_E\big(\boldsymbol{f}_h^n + \nabla\cdot\boldsymbol{\sigma}(\boldsymbol{u}_h^n) - \alpha\nabla\, p_h^n\big),$$

we obtain

$$\begin{aligned}\big(\boldsymbol{f}_h^n + \nabla\cdot\boldsymbol{\sigma}(\boldsymbol{u}_h^n) - \alpha\nabla\, p_h^n, \boldsymbol{v}\,\big)_E &= -(\boldsymbol{f} - \boldsymbol{f}_h^n, \boldsymbol{v})_E \\ &\quad + 2G(\boldsymbol{\varepsilon}(\boldsymbol{u} - \boldsymbol{u}_h^n), \boldsymbol{\varepsilon}(\boldsymbol{v}))_E + \lambda(\nabla\cdot(\boldsymbol{u} - \boldsymbol{u}_h^n), \nabla\cdot\boldsymbol{v})_E - \alpha(p - p_h^n, \nabla\cdot\boldsymbol{v})_E.\end{aligned}$$

Hence (A.6) implies

$$\begin{aligned}&\hat{C}\|\boldsymbol{f}_h^n + \nabla\cdot\boldsymbol{\sigma}(\boldsymbol{u}_h^n) - \alpha\nabla\, p_h^n\|_{L^2(E)}^2 \le \|\boldsymbol{f} - \boldsymbol{f}_h^n\|_{H^{-1}(E)}|\boldsymbol{v}|_{H^1(E)} \\ &+ \hat{C}\Big(2G\|\boldsymbol{\varepsilon}(\boldsymbol{u} - \boldsymbol{u}_h^n)\|_{L^2(E)} + \lambda\|\nabla\cdot(\boldsymbol{u} - \boldsymbol{u}_h^n)\|_{L^2(E)} + \alpha\|p - p_h^n\|_{L^2(E)}\Big)|\boldsymbol{v}|_{H^1(E)} \\ &\le \frac{\hat{C}}{h_E}\Big(\|\boldsymbol{f} - \boldsymbol{f}_h^n\|_{H^{-1}(E)} + 2G\|\boldsymbol{\varepsilon}(\boldsymbol{u} - \boldsymbol{u}_h^n)\|_{L^2(E)} + \lambda\|\nabla\cdot(\boldsymbol{u} - \boldsymbol{u}_h^n)\|_{L^2(E)} + \alpha\|p - p_h^n\|_{L^2(E)}\Big)\|\boldsymbol{v}\|_{L^2(E)}.\end{aligned}$$

The formula is similar when $E \subset \mathcal{T}_h^2$, and we have for $i = 1, 2$, with $p = p_h = 0$ when $i = 2$,

$$\eta_{E,i,\boldsymbol{u}}^{n,\ell_n} \le \hat{C}\Big(\|\boldsymbol{f} - \boldsymbol{f}_h^n\|_{H^{-1}(E)} + 2G\|\boldsymbol{\varepsilon}(\boldsymbol{u} - \boldsymbol{u}_h^{n,\ell_n})\|_{L^2(E)} + \lambda\|\nabla\cdot(\boldsymbol{u} - \boldsymbol{u}_h^{n,\ell_n})\|_{L^2(E)} + \alpha\|p - p_h^{n,\ell_n}\|_{L^2(E)}\Big). \tag{7.27}$$

7.11. Indicators of the stress tensor's jumps at time t_n

Here we consider the stress tensor's jump on $e \in \mathcal{E}_h^1 \cup \mathcal{E}_h^{12}$ defined by (5.31)

$$\eta_{e,1,\boldsymbol{\sigma}}^{n,\ell_n} = h_e^{\frac{1}{2}}\|[\big(\boldsymbol{\sigma}(\boldsymbol{u}_h^{n,\ell_n}) - \alpha p_h^{n,\ell_n}\boldsymbol{I}\big)\boldsymbol{n}_e]_e\|_{L^2(e)},$$

the one on $e \in \mathcal{E}_h^2$ defined by (5.32)

$$\eta_{e,2,\boldsymbol{\sigma}}^{n,\ell_n} = h_e^{\frac{1}{2}} \|[(\boldsymbol{\sigma}(\boldsymbol{u}_h^{n,\ell_n}))\boldsymbol{n}_e]_e\|_{L^2(e)},$$

and the one on $e \subset \Gamma_N$ defined by (5.33),

$$\eta_{e,N,\boldsymbol{\sigma}}^{n,\ell_n} = h_e^{\frac{1}{2}} \|\boldsymbol{\sigma}(\boldsymbol{u}_h^{n,\ell_n})\boldsymbol{n}_\Omega - \boldsymbol{t}_{N,h}^n\|_{L^2(e)}.$$

Let us consider the first one; the treatment of the others being much the same. Let e be an interior face of $\mathcal{E}_h^1$, ω_e the union of the two elements sharing e, and test (4.13) at time t_n with $\boldsymbol{v}_h = \boldsymbol{0}$ and

$$\boldsymbol{v} = \mathcal{G}\big(b_e[\big(\boldsymbol{\sigma}(\boldsymbol{u}_h^n) - \alpha p_h^n \boldsymbol{I}\big)\boldsymbol{n}_e]_e\big).$$

This yields

$$\begin{aligned}
&\int_e b_e \big|[\big(\boldsymbol{\sigma}(\boldsymbol{u}_h^n) - \alpha p_h^n \boldsymbol{I}\big)\boldsymbol{n}_e]_e\big|^2 \le \sum_{E\subset\omega_e} \|\boldsymbol{f}_h^n + \nabla\cdot\boldsymbol{\sigma}(\boldsymbol{u}_h^n) - \alpha\nabla\, p_h^n\|_{L^2(E)}\|\boldsymbol{v}\|_{L^2(E)}\\
&+ \hat{C}\Big(2G\|\boldsymbol{\varepsilon}(\boldsymbol{u}-\boldsymbol{u}_h^n)\|_{L^2(\omega_e)} + \lambda\|\nabla\cdot(\boldsymbol{u}-\boldsymbol{u}_h^n)\|_{L^2(\omega_e)} + \alpha\|p-p_h^n\|_{L^2(\omega_e)} + \|\boldsymbol{f}-\boldsymbol{f}_h^n\|_{H^{-1}(\omega_e)}\Big)|\boldsymbol{v}|_{H^1(\omega_e)}\\
&\le \hat{C}\ \Big(h_e^{\frac{1}{2}} \sum_{E\subset\omega_e} \|\boldsymbol{f}_h^n + \nabla\cdot\boldsymbol{\sigma}(\boldsymbol{u}_h^n) - \alpha\nabla\, p_h^n\|_{L^2(E)}\\
&+ \frac{1}{h_e^{\frac{1}{2}}}\big(2G\|\boldsymbol{\varepsilon}(\boldsymbol{u}-\boldsymbol{u}_h^n)\|_{L^2(\omega_e)} + \lambda\|\nabla\cdot(\boldsymbol{u}-\boldsymbol{u}_h^n)\|_{L^2(\omega_e)} + \alpha\|p-p_h^n\|_{L^2(\omega_e)} + \|\boldsymbol{f}-\boldsymbol{f}_h^n\|_{H^{-1}(\omega_e)}\big)\Big)\ \|\boldsymbol{v}\|_{L^2(e)}.
\end{aligned}$$

Then, after multiplying by $h_e^{\frac{1}{2}}$, we deduce

$$\begin{aligned}
\eta_{e,1,\boldsymbol{\sigma}}^{n,\ell_n} \le \hat{C}\ \Big(&2G\|\boldsymbol{\varepsilon}(\boldsymbol{u}-\boldsymbol{u}_h^{n,\ell_n})\|_{L^2(\omega_e)} + \lambda\|\nabla\cdot(\boldsymbol{u}-\boldsymbol{u}_h^{n,\ell_n})\|_{L^2(\omega_e)} + \alpha\|p-p_h^{n,\ell_n}\|_{L^2(\omega_e)} + \|\boldsymbol{f}-\boldsymbol{f}_h^n\|_{H^{-1}(\omega_e)}\\
&+ \Big(\sum_{E\subset\omega_e} (\eta_{E,1,\boldsymbol{u}}^{n,\ell_n})^2\Big)^{\frac{1}{2}}\Big).
\end{aligned} \tag{7.28}$$

When $e \subset \Gamma_{12}$, (7.28) becomes

$$\begin{aligned}
\eta_{e,1,\boldsymbol{\sigma}}^{n,\ell_n} \le \hat{C}\ \Big(&2G\|\boldsymbol{\varepsilon}(\boldsymbol{u}-\boldsymbol{u}_h^{n,\ell_n})\|_{L^2(\omega_e)} + \lambda\|\nabla\cdot(\boldsymbol{u}-\boldsymbol{u}_h^{n,\ell_n})\|_{L^2(\omega_e)} + \alpha\|p-p_h^{n,\ell_n}\|_{L^2(E_1)} + \|\boldsymbol{f}-\boldsymbol{f}_h^n\|_{H^{-1}(\omega_e)}\\
&+ \big((\eta_{E_1,1,\boldsymbol{u}}^{n,\ell_n})^2 + (\eta_{E_2,2,\boldsymbol{u}}^{n,\ell_n})^2\big)^{\frac{1}{2}}\Big),
\end{aligned} \tag{7.29}$$

where $E_1 \subset \Omega_1$ and $E_2 \subset \Omega_2$ are adjacent to e. When e is interior to Ω_2, (7.28) is replaced by

$$\eta_{e,2,\boldsymbol{\sigma}}^{n,\ell_n} \le \hat{C}\Big(2G\|\boldsymbol{\varepsilon}(\boldsymbol{u}-\boldsymbol{u}_h^{n,\ell_n})\|_{L^2(\omega_e)} + \lambda\|\nabla\cdot(\boldsymbol{u}-\boldsymbol{u}_h^{n,\ell_n})\|_{L^2(\omega_e)} + \|\boldsymbol{f}-\boldsymbol{f}_h^n\|_{H^{-1}(\omega_e)} + \Big(\sum_{E\subset\omega_e} (\eta_{E,2,\boldsymbol{u}}^{n,\ell_n})^2\Big)^{\frac{1}{2}}\Big). \tag{7.30}$$

Finally, when $e \subset \Gamma_N$, there is only one element E adjacent to e and we have

$$\begin{aligned}
\eta_{e,N,\boldsymbol{\sigma}}^{n,\ell_n} \le \hat{C}\ \Big(&2G\|\boldsymbol{\varepsilon}(\boldsymbol{u}-\boldsymbol{u}_h^{n,\ell_n})\|_{L^2(\omega_e)} + \lambda\|\nabla\cdot(\boldsymbol{u}-\boldsymbol{u}_h^{n,\ell_n})\|_{L^2(\omega_e)} + \|\boldsymbol{f}-\boldsymbol{f}_h^n\|_{H^{-1}(\omega_e)}\\
&+ \|\boldsymbol{t}_N - \boldsymbol{t}_{N,h}^n\|_{H^{-\frac{1}{2}}(e)} + \eta_{E,2,\boldsymbol{u}}^{n,\ell_n}\Big).
\end{aligned} \tag{7.31}$$

8. Numerical results

In this section, we present numerical results that validate the theoretical analysis and the algorithmic improvements built upon the a posteriori error indicators. All examples are computed with the open-source finite element package deal.II [43].

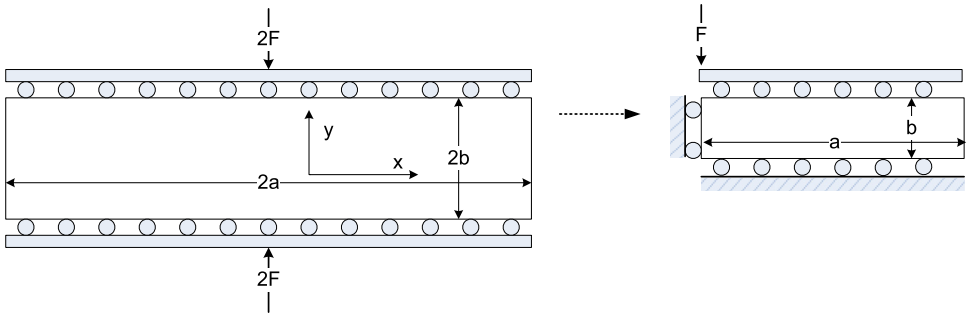

Fig. 2. The physical domain (left) and computational domain (right) of the Mandel's problem [18].

8.1. The Mandel problem

In this section, we solve the Mandel's problem to validate our solution algorithm and test the effectivity of the a posteriori error indicators. The Mandel's benchmark problem considers a $2a \times 2b$ rectangular poroelastic medium sandwiched between two impervious frictionless plates. At $t = 0$, the medium is loaded instantaneously by a constant force $2F$. Because of the bi-axial symmetry of the physical problem, the computational domain is taken as a quarter of the physical domain, see Fig. 2. The governing equations are those of Biot's system with no gravity:

$$\begin{aligned} -\nabla \cdot (\lambda(\nabla \cdot \boldsymbol{u})\boldsymbol{I} + 2G\boldsymbol{\varepsilon}(\boldsymbol{u}) - \alpha p \boldsymbol{I}) &= \boldsymbol{0} \quad \text{in } \Omega \times]0, T[, \\ \partial_t \left(\frac{1}{M} p + \alpha \nabla \cdot \boldsymbol{u} \right) - \frac{1}{\mu_f} \nabla \cdot (\boldsymbol{\kappa} \nabla p) &= 0 \quad \text{in } \Omega \times]0, T[, \end{aligned} \tag{8.1}$$

where $\Omega =]0, a[\times]0, b[$ is the computational domain. Following the approaches in [4], the boundary and initial conditions supplementing the governing equations are cast as

$$\begin{aligned} -\frac{1}{\mu_f} \boldsymbol{\kappa} \nabla p \cdot \boldsymbol{n} = 0, \quad \boldsymbol{u}_x = 0, \quad \sigma_{xy} = 0 \quad &\text{on } x = 0, \\ p = 0, \quad \boldsymbol{\sigma} \boldsymbol{n} = \boldsymbol{0} \quad &\text{on } x = a, \\ -\frac{1}{\mu_f} \boldsymbol{\kappa} \nabla p \cdot \boldsymbol{n} = 0, \quad \boldsymbol{u}_y = 0, \quad \sigma_{xy} = 0 \quad &\text{on } y = 0, \\ -\frac{1}{\mu_f} \boldsymbol{\kappa} \nabla p \cdot \boldsymbol{n} = 0, \quad \boldsymbol{u}_y = U_y(b, t), \quad \sigma_{xy} = 0 \quad &\text{on } y = b, \\ p|_{t=t_0} = P_{t_0}(x, y). \end{aligned} \tag{8.2}$$

Here $U_y(b, t)$ is the analytical solution of the y-displacement at $y = b$ and $P_{t_0}(x, y)$ is the analytical pressure solution at $t = t_0 > 0$. Analytical pressure, displacement, and stress solutions are provided as infinite series, see, e.g. [44].

The physical parameters used for the tests are listed in Table 1. We notice that the parameter α multiplying the pressure in the first line of (8.1) is much larger than $\frac{1}{M}$ in the second line, hence the serious imbalance between the two equations. Denote the energy norm of the displacement by

$$\|\boldsymbol{u} - \boldsymbol{u}_h\|_e := \left(2G \|\boldsymbol{\varepsilon}(\boldsymbol{u} - \boldsymbol{u}_h)\|^2_{L^2(\Omega)} + \lambda \|\nabla \cdot (\boldsymbol{u} - \boldsymbol{u}_h)\|^2_{L^2(\Omega)} \right)^{\frac{1}{2}}. \tag{8.3}$$

Numerical convergence of the pressure solution measured in the L^2 norm and the displacement solution measured in the energy norm are performed under spatial refinement. Since the pressure solution lacks regularity at early time [44], the simulations are run on the time interval $[0.01, 0.0101]$ s. In order to mitigate the errors caused by the time discretization and the fixed-stress split, a small time step Δt= 1e−6 s and a small fixed-stress threshold ε =1e−6 are used. The EG scheme is IIPG with a global penalty parameter of 1e5. The numerical errors are measured at final time $T = 0.0101$ s and summarized in Table 2. These spacial refinement tests show that the rate

Table 1
Parameters for Mandel's problem.

Parameter	Quantity	Value
a	x dimension	1 m
b	y dimension	1 m
k	permeability	1e−2 m^2
μ_f	fluid viscosity	1.0 Pa·s
F	point load intensity	2.0×10^3 N/m
E	Young's modulus	1.0×10^4 Pa
ν	Poisson's ratio	0.2
α	Biot's coefficient	1
M	Biot's modulus	10^4 Pa

Table 2
Convergence of pressure and displacement solutions under spatial refinement.

$\mathcal{T}_h$	$\|\frac{1}{\sqrt{M}}(p^N - p_h^N)\|_{L^2(\Omega)}$	Rate	$\|\boldsymbol{u}^N - \boldsymbol{u}_h^N\|_e$	Rate
32 × 32	4.0447e−04	–	2.5745e−02	–
64 × 64	1.0507e−04	1.945	1.2872e−02	1.0001
128 × 128	3.4714e−05	1.7712	6.4361e−03	1.0000
256 × 256	1.5875e−05	1.5554	3.2180e−03	0.9967

of convergence of the pressure in L^2 is between first- and second-order, and that of the displacement in the energy norm is close to first-order, as predicted by theoretical estimates for the displacement and better for the pressure.

The a posteriori error indicators in (5.41)–(5.48) are adapted, without change of notation, to (8.1)–(8.2), namely, the local error indicators on the interface of the pay-zone and the nonpay-zone $\mathcal{E}_h^{12}$, the faces in the nonpay-zone $\mathcal{E}_h^2$, and the elements in the nonpay-zone $\mathcal{T}_h^2$, are omitted. Regarding effectivity, considering the strong imbalance between the displacement and the flow equations, we collect the indicators into two sums,

$$\eta_{\text{FLOW}} \coloneqq \eta_{\text{alg}} + \eta_{\text{time}} + \eta_{\text{flow}} + \eta_{\text{jump}}, \tag{8.4}$$

$$\eta_{\text{MECH}} \coloneqq \eta_{\mathcal{E}_{\partial\sigma}} + \eta_{\mathcal{E}_\sigma} + \eta_{\mathcal{T}_{\partial\boldsymbol{u}}} + \eta_{\mathcal{T}_{\boldsymbol{u}}}, \tag{8.5}$$

and we associate respectively to η_{FLOW} and η_{MECH} the error norms,

$$|||(p,\boldsymbol{u}) - (p_h,\boldsymbol{u}_h)|||_1 \coloneqq \left(\frac{1}{4M}\|p - p_h\|_{L^2(\Omega)}^2 + \frac{1}{4}\|\boldsymbol{u} - \boldsymbol{u}_h\|_e^2 + \frac{\Delta t}{2\mu_f}\sum_{n=1}^{N}\|p - p_h\|_h^2\right)^{\frac{1}{2}}, \tag{8.6}$$

$$|||(p,\boldsymbol{u}) - (p_h,\boldsymbol{u}_h)|||_2 \coloneqq 2G\|\boldsymbol{\varepsilon}(\boldsymbol{u} - \boldsymbol{u}_h)\|_{L^2(\Omega)} + \lambda\|\nabla\cdot(\boldsymbol{u} - \boldsymbol{u}_h)\|_{L^2(\Omega)} + \alpha\|p - p_h\|_{L^2(\Omega)}. \tag{8.7}$$

Then we define the effectivity indices

$$\mathcal{I}_{\text{eff, FLOW}} = \frac{\sqrt{\eta_{\text{FLOW}}}}{|||(p,\boldsymbol{u}) - (p_h,\boldsymbol{u}_h)|||_1}, \quad \mathcal{I}_{\text{eff, MECH}} = \frac{\sqrt{\eta_{\text{MECH}}}}{|||(p,\boldsymbol{u}) - (p_h,\boldsymbol{u}_h)|||_2}. \tag{8.8}$$

Given the assumption that the mesh size and time step are of the same order, see (7.10), we test the effectivity of the a posteriori indicators under simultaneously spatial and temporal refinements. We performed two groups of convergence tests to examine the effectivity indices. The first group of simulations are run from 0.01 s to 0.02 s with a fixed-stress convergence tolerance ε =1e−6. The convergence of the individual error indicators in (5.41) to (5.48) and the effectivity indices are summarized in Tables 3 and 4, respectively. All the individual error indicators except η_{alg} and η_{jump} exhibit near second order convergence. $\sqrt{\eta_{\text{FLOW}}}$, $|||(p_h^N,\boldsymbol{u}_h^N) - (p^N,\boldsymbol{u}^N)|||_1$, $\sqrt{\eta_{\text{MECH}}}$, and $|||(p_h^N,\boldsymbol{u}_h^N) - (p^N,\boldsymbol{u}^N)|||_2$ all exhibit asymptotically first-order convergences, which gives converging $\mathcal{I}_{\text{eff, FLOW}}$ and $\mathcal{I}_{\text{eff, MECH}}$. In this group of tests, $\mathcal{I}_{\text{eff, FLOW}}$ is around 2.3 and $\mathcal{I}_{\text{eff, MECH}}$ around 1.8.

Another group of tests are performed with simulations from 0.001 s to 0.002 s using smaller time steps. The convergence of the individual error indicators and the effectivity indices are summarized in Tables 5 and 6 respectively. We observe similar convergence behavior as demonstrated by the first group of tests with $\mathcal{I}_{\text{eff, FLOW}}$

Table 3
Convergence of individual a posteriori error indicators under simultaneous spatial and temporal refinement with simulations from 0.01 s to 0.02 s.

$\Delta t, \mathcal{T}_h$	η_{alg}	η_{time}	Rate	η_{flow}	Rate	η_{jump}	Rate
1e−3, 32 × 32		1.3215e−02	–	1.7039e−04	–	2.6802e−05	–
5e−4, 64 × 64	1.7100e−10	3.4323e−03	1.9449	4.4629e−05	1.9327	9.7493e−06	1.4589
2.5e−4, 128 × 128	4.8416e−10	8.7498e−04	1.9583	1.1422e−05	1.9494	4.3753e−06	1.3074
1.25e−4, 256 × 256	2.3276e−09	2.2091e−04	1.9679	2.8891e−06	1.9612	2.1219e−06	1.2132

$\Delta t, \mathcal{T}_h$	$\eta_{\mathcal{E}_{\partial\sigma}}$	Rate	$\eta_{\mathcal{E}_\sigma}$	Rate	$\eta_{\mathcal{T}_{\partial u}}$	Rate	$\eta_{\mathcal{T}_u}$	Rate
1e−3, 32 × 32	6.9317e+01	–	5.2784e+01	–	7.1801e+01	–	5.4670e+01	–
5e−4, 64 × 64	1.8223e+01	1.9274	1.2049e+01	2.1311	1.8542e+01	1.9532	1.2259e+01	2.1569
2.5e−4, 128 × 128	4.6724e+00	1.9454	2.8727e+00	2.0998	4.7128e+00	1.9646	2.8975e+00	2.1189
1.25e−4, 256 × 256	1.1830e+00	1.9581	7.0101e−01	2.0771	1.1881e+00	1.9727	7.0402e−01	2.0917

Table 4
Effectivity indices under simultaneously spatial and temporal refinement with simulations from 0.01 s to 0.02 s.

$\Delta t, \mathcal{T}_h$	$\sqrt{\eta_{\text{FLOW}}}$	Rate	$\|\|\|(p_h^N, \boldsymbol{u}_h^N) - (p^N, \boldsymbol{u}^N)\|\|\|_1$	Rate	$\mathcal{I}_{\text{eff, FLOW}}$
1e−3, 32 × 32	1.1581e−01	–	5.0968e−02	–	2.2722
5e−4, 64 × 64	5.9048e−02	0.9717	2.5947e−02	0.9740	2.2757
2.5e−4, 128 × 128	2.9845e−02	0.9780	1.3115e−02	0.9791	2.2757
1.25e−4, 256 × 256	1.5031e−02	0.9821	6.6144e−03	0.9822	2.2724

$\Delta t, \mathcal{T}_h$	$\sqrt{\eta_{\text{MECH}}}$	Rate	$\|\|\|(p_h^N, \boldsymbol{u}_h^N) - (p^N, \boldsymbol{u}^N)\|\|\|_2$	Rate	$\mathcal{I}_{\text{eff, MECH}}$
1e−3, 32 × 32	1.5766e+01	–	8.2160e+00	–	1.9190
5e−4, 64 × 64	7.8149e+00	1.0125	4.2061e+00	0.9659	1.8580
2.5e−4, 128 × 128	3.8929e+00	1.0089	2.1283e+00	0.9743	1.8291
1.25e−4, 256 × 256	1.9432e+00	1.0066	1.0706e+00	0.9802	1.8150

Table 5
Convergence of individual a posteriori error indicators under simultaneous spatial and temporal refinement with simulations from 0.001 s to 0.002 s.

$\Delta t, \mathcal{T}_h$	η_{alg}	η_{time}	Rate	η_{flow}	Rate	η_{jump}	Rate
1e−4, 32 × 32	3.2536e−11	1.3955e−03	–	4.0207e−04	–	1.6878e−04	–
5e−4, 64 × 64	1.1379e−10	3.5982e−04	1.9554	1.0239e−04	1.9733	3.4890e−05	2.2742
2.5e−5, 128 × 128	1.6658e−10	9.1408e−05	1.9661	2.5828e−05	1.9802	1.1203e−05	1.9565
1.25e−5 256 × 256	1.0063e−09	2.3039e−05	1.9738	6.4856e−06	1.9849	4.8081e−06	1.7039

$\Delta t, \mathcal{T}_h$	$\eta_{\mathcal{E}_{\partial\sigma}}$	Rate	$\eta_{\mathcal{E}_\sigma}$	Rate	$\eta_{\mathcal{T}_{\partial u}}$	Rate	$\eta_{\mathcal{T}_u}$	Rate
1e−4, 32 × 32	7.0473e+01	–	1.9244e+03	–	7.5991e+01	–	2.0115e+03	–
5e−5, 64 × 64	1.8809e+01	1.9056	4.8834e+02	1.9784	1.9495e+01	1.9627	4.9899e+02	2.0111
2.5e−5, 128 × 128	4.8541e+00	1.9298	1.2294e+02	1.9841	4.9394e+00	1.9717	1.2426e+02	2.0084
1.25e−5, 256 × 256	1.2327e+00	1.9465	3.0840e+01	1.9880	1.2433e+00	1.9781	3.1004e+01	2.0064

around 1.01 and $\mathcal{I}_{\text{eff, MECH}}$ around 8.4. These results suggest that the effectivity indices may depend on the initial condition, final condition, and the relationships between h and Δt, as far as the Mandel problem is concerned.

8.2. Dynamic mesh adaptivity guided by the a posteriori error indicators

We demonstrate the potential of using the a posteriori error indicators to guide dynamic mesh adaptivity in unconventional reservoirs with the following prototype unconventional model (Fig. 3). The domain size is $[0, 1] \times [0, 1]$ m^2, the fracture width is $1/64$ m. The permeability is 10e−16 m^{-1} in the matrix and 10e−11 m^{-1} in the fractures. The fluid density is 1 kg/m^3 and its viscosity is 10e-6 Pa·s. The Young modulus is 5e6 Pa for the matrix and 10e4 Pa for the fractures. Two wells are located at the center of each horizontal fracture, producing at a

Table 6
Effectivity indices under simultaneously space and time refinement with simulations from 0.001 s to 0.002 s.

$\Delta t, \mathcal{T}_h$	$\sqrt{\eta_{\text{FLOW}}}$	Rate	$\|\|\|(p_h^N, \boldsymbol{u}_h^N) - (p^N, \boldsymbol{u}^N)\|\|\|_1$	Rate	$\mathcal{I}_{\text{eff, FLOW}}$
1e−4, 32 × 32	4.4344e−02	–	4.3794e−02	–	1.0126
5e−5, 64 × 64	2.2296e−02	0.9919	2.2165e−02	0.9824	1.0059
2.5e−5, 128 × 128	1.1333e−02	0.9841	1.1205e−02	0.9832	1.0114
1.25e−5, 256 × 256	5.8595e−03	0.9735	5.6862e−03	0.9819	1.0305
$\Delta t, \mathcal{T}_h$	$\sqrt{\eta_{\text{MECH}}}$	Rate	$\|\|\|(p_h^N, \boldsymbol{u}_h^N) - (p^N, \boldsymbol{u}^N)\|\|\|_2$	Rate	$\mathcal{I}_{\text{eff, MECH}}$
1e−4, 32 × 32	6.3893e+01	–	7.5442e+00	–	8.4691
5e−5, 64 × 64	3.2026e+01	0.9964	3.8195e+00	0.9819	8.3847
2.5e−5, 128 × 128	1.6031e+01	0.9973	1.9220e+00	0.9863	8.3409
1.25e−5, 256 × 256	8.0199e+00	0.9980	9.6411e−01	0.9895	8.3185

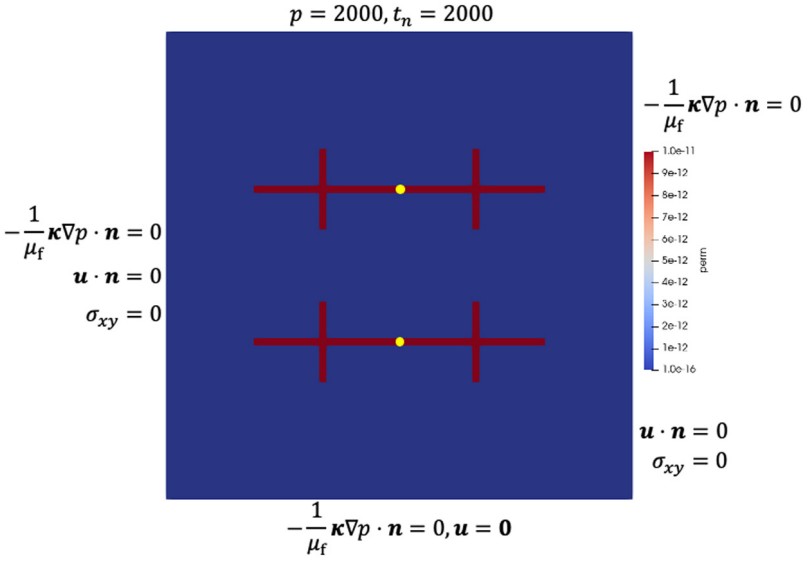

Fig. 3. Permeability field and model boundary conditions of the prototype unconventional reservoir model.

rate of 10 m^3/s. IIPG with a global penalty parameter of 100 is employed in the EG scheme. The time of simulation is $[0, 500]$ s with a uniform time step size $\Delta t = 20$ s.

The following dynamic mesh adaptation strategy is applied, starting with a uniform 64 × 64 rectangular mesh. The local discretization error indicators in $L^2(E \times]t_{n-1}, t_n[)$ is computed on each element $E \in \mathcal{T}_h$ at time step t_n and summed into two indicators, one associated with the flow equation and one associated with the mechanics equation. Namely, let

$$\eta_{E,\text{flow}} := \underbrace{(\eta^n_{t,p,E})^2 + \sum_{e\subset\partial E}(\eta^n_{t,J})^2}_{\text{local time errors}} + \underbrace{(\eta^n_{E,p})^2 + \sum_{e\subset\partial E}(\eta^n_{\text{flux},e})^2}_{\text{local flow errors}} + \underbrace{\sum_{e\subset\partial E}\left((\eta^n_{\text{pen}})^2 + (\eta^n_{\partial p,J})^2 + (\eta^n_{p,J})^2\right)}_{\text{local penalty jumps}}, \tag{8.9}$$

and

$$\begin{aligned}\eta_{E,\text{mechanics}} := &\underbrace{\sum_{e\subset\partial E}(\eta^n_{e,1,\partial\boldsymbol{\sigma}})^2}_{\text{local errors on the stress tensor's time derivative}} + \underbrace{\sum_{e\subset\partial E}(\eta^n_{e,1,\boldsymbol{\sigma}})^2}_{\text{local errors on the stress tensor}} \\ &+ \underbrace{(\eta^n_{E,1,\partial\boldsymbol{u}})^2}_{\text{local errors on the displacement's time derivative}} + \underbrace{(\eta^n_{E,1,\boldsymbol{u}})^2}_{\text{local errors on the displacement}},\end{aligned} \tag{8.10}$$

Table 7
Comparison of DoFs between the adaptive mesh and the uniform mesh.

Domain	Uniform mesh 128 × 128	Adaptive mesh $t = 100$ s (%)	Adaptive mesh $t = 500$ s (%)
Flow	131585	18815 (14.3%)	29018 (22.1%)
Mechanics	132098	20060 (15.2%)	30932 (23.4%)

then each of the two indicators are normalized by the maximum value and added up to obtain a refinement indicator:

$$\eta_{E,\text{refine}} := \frac{\eta_{E,\text{flow}}}{\|\eta_{E,\text{flow}}\|_{l^\infty(\mathcal{T}_h)}} + \frac{\eta_{E,\text{mechanics}}}{\|\eta_{E,\text{mechanics}}\|_{l^\infty(\mathcal{T}_h)}}. \tag{8.11}$$

The top 10% elements with the largest refinement indicator $\eta_{E,\text{refine}}$ values are refined isotropically, unless the element width is smaller than or equal to $1/512$ m; the bottom 20% elements with the smallest refinement indicator values are coarsened unless the element width is greater than or equal to $1/8$ m. The dynamic mesh adaptivity and solutions are presented in Fig. 4. Clearly, the mesh is adaptively refined near the well, across the fractures, at fracture joints, and around fracture tips. As the fluid is being depleted inside the fractures, more refinements are put inside and across the fractures.

We compare the number of degree of freedoms (DoFs) of the adaptive mesh at $t = 100$ s and $t = 500$ s to the DoFs of a static uniform 128 × 128 mesh in Table 7. As time progresses, the DoFs of the adaptive mesh increase, but overall the adaptive mesh utilizes less than 24% of the DoFs of the 128 × 128 uniform mesh for both the flow and the mechanics domains. The accuracy of the adaptive solutions is demonstrated by comparing the pressure and volumetric strain solution profiles along the center of the top horizontal fracture to those obtained on the 128 × 128 static mesh, presented in Fig. 5. Results show that the adaptive solutions achieve excellent accuracy, especially at later time $t = 500$ s. Moreover, a close examination of the top right plot of Fig. 5 shows that the adaptive mesh refinement near the fracture boundaries helps to eliminate the nonphysical pressure oscillations at fracture tips, where the permeability and Young's modulus change orders of magnitude across the matrix/fracture interface.

8.3. Novel stopping criterion for the fixed-stress iterations

A hyperparameter arises from the fixed-stress iterative coupling algorithm (3.9)–(3.17), namely, the convergence threshold ε in

criterion 1

$$\left\| \bar{\sigma}_h^{n,\ell} - \bar{\sigma}_h^{n,\ell-1} \right\|_{L^\infty(\Omega)} \leq \varepsilon. \tag{8.12}$$

For large-scale engineering applications, the relative change in mean stress is also a widely used stopping criterion for the fixed-stress iterations: [4,5,9,12,18,45]:

criterion 2

$$\left\| \frac{\bar{\sigma}_h^{n,\ell} - \bar{\sigma}_h^{n,\ell-1}}{\bar{\sigma}_h^{n,\ell}} \right\|_{L^\infty(\Omega)} \leq \varepsilon. \tag{8.13}$$

The choice of a "sufficienty small" convergence threshold ε in either (8.12) or (8.13) is usually based on the user's experience, or tuned for each simulation scenario. We propose a new stopping criterion for the fixed-stress iterations that utilizes the a posteriori error estimators to balance the fixed-stress split error with the discretization errors without tuning the hyperparameter :

Marching forward to the next time step $n + 1$ when

new criterion

$$\eta_{\text{alg}}^{n,\ell} \leq \delta(\eta_{\text{time}}^{n,\ell} + \eta_{\text{jump}}^{n,\ell} + \eta_{\text{flow}}^{n,\ell} + \eta_{\mathcal{E}_{\partial\boldsymbol{\sigma}}}^{n,\ell} + \eta_{\mathcal{T}_{\partial\boldsymbol{u}}}^{n,\ell} + \eta_{\mathcal{E}_{\boldsymbol{\sigma}}}^{n,\ell} + \eta_{\mathcal{T}_{\boldsymbol{u}}}^{n,\ell}). \tag{8.14}$$

We argue that $\delta = 0.1$ is sufficient for most simulation scenarios without the need of further tuning. Namely, (8.14) with $\delta = 0.1$ indicates that the error caused by the fixed-stress split is an order of magnitude less that the errors caused by the spatial and temporal discretizations, hence the fixed-stress loop is sufficiently iterated and one can march forward to the next time step. We demonstrate its performance in the following subsections.

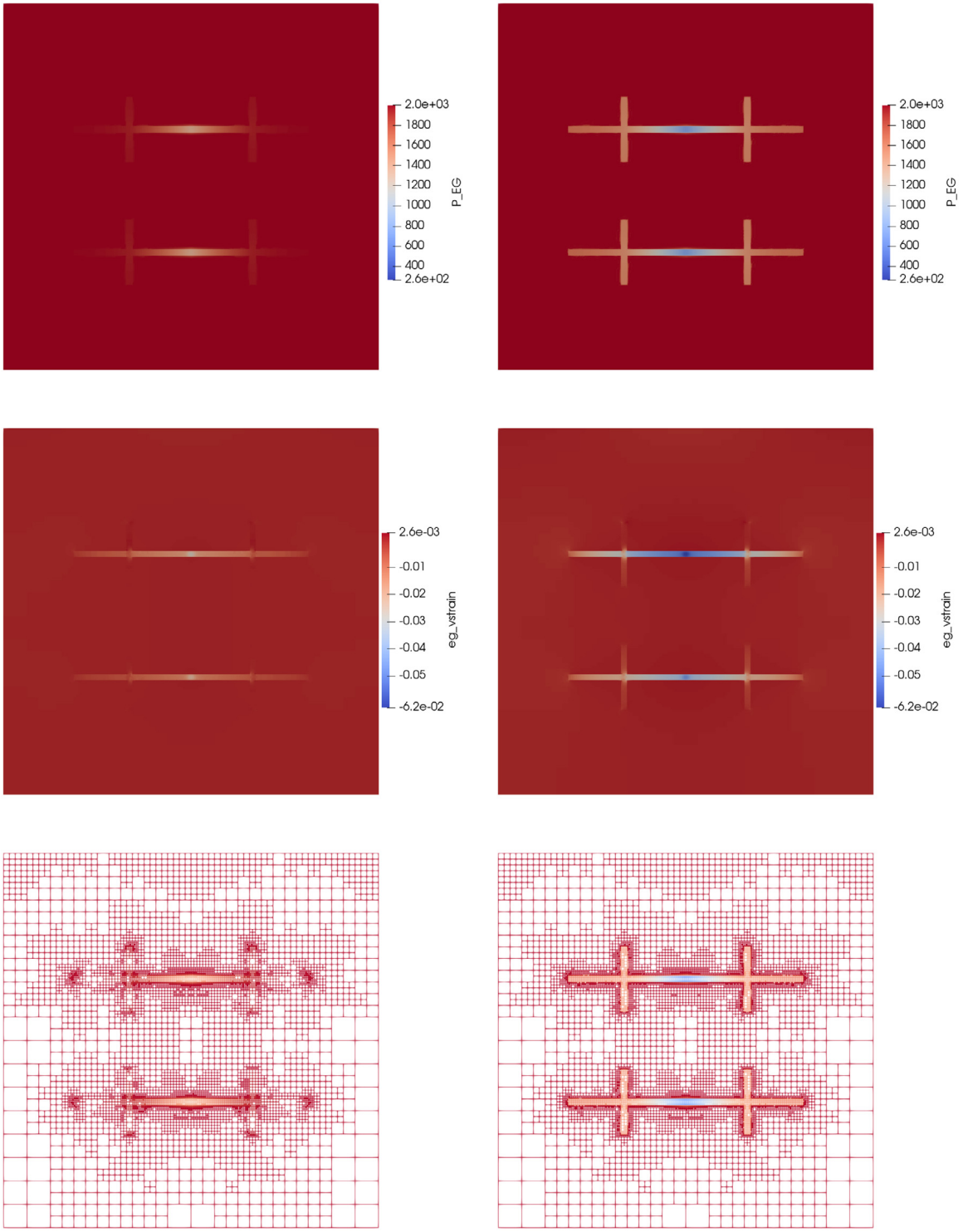

Fig. 4. Dymanic mesh adaptivity guided by the a posteriori error indicators: top: pressure, middle: volumetric strain, bottom: adaptive mesh; left: $t = 100$ s, right: $t = 500$ s.

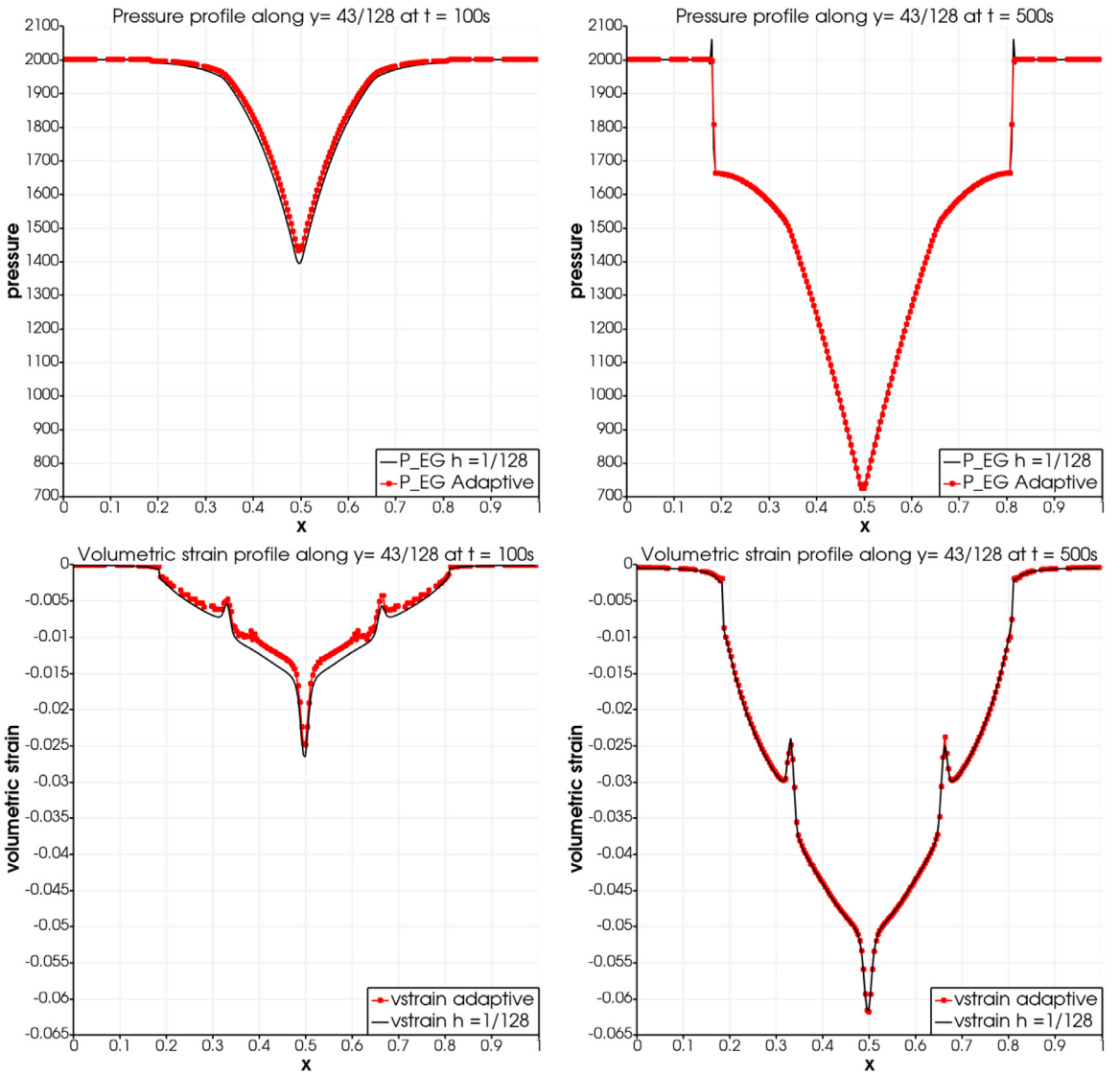

Fig. 5. Comparison of the solutions on the dynamic adaptive mesh and on a uniform fine mesh 128 × 128 along $y = 43/128$: top: pressure, bottom: volumetric strain; left: $t = 100$ s, right: $t = 500$ s.

8.3.1. New stopping criterion tested with the Mandel problem

We first test the new stopping criterion (8.14) for the Mandel problem. The model parameters shown in Table 1 are used for these tests. The simulations are run from 0 s to 1 s, with a time step $\Delta t = 0.1$ s and mesh 64 × 64. The performance of the new stopping criterion (8.14) with $\delta = 0.1$ is compared to criterion 1 (with $\varepsilon = 1e-6$) and 2 (with $\varepsilon = 1e-4$) in Figs. 6 and 7. Fig. 6 shows the number of fixed-stress iterations required to meet the stopping criterion for each time step. The new criterion (8.14) requires significantly less number of iterations compared to criterion 1 and 2, especially at initial time steps. On average, the new criterion requires 1.4 fixed-stress iterations per time step; in contrast, criterion 1 requires 4.4 iterations and criterion 2 requires 2.0 iterations. Fig. 7 compares the solution errors obtained using different stopping criteria. The accuracy of the new criterion is very close to that of criteria 1 and 2 for all the time steps, especially at initial time steps where the errors are relatively large.

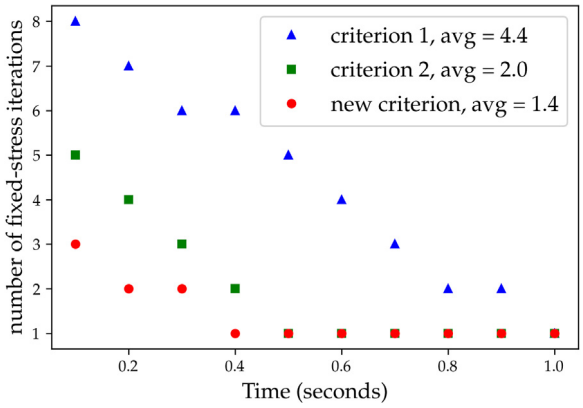

Fig. 6. Comparison of the number of fixed-stress iterations for each time step using difference stopping criteria for the Mandel problem.

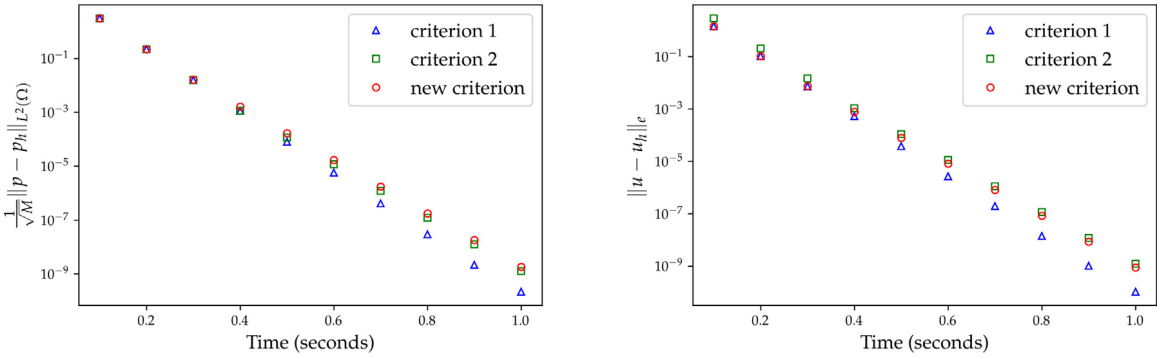

(a) Pressure solution errors comparison

(b) Displacement solution errors comparison

Fig. 7. Comparison of pressure and displacement solution errors using different stopping criteria for the Mandel problem.

Table 8
Comparison of average number of fixed-stress iterations per time step using different stopping criteria for the unconventional reservoir model.

criterion	Avg # of fixed-stress iterations
criterion 1 (ε = 1e−3)	3
criterion 2 (ε = 1e−3)	2
new criterion ($\delta = 0.1$)	1

8.3.2. New stopping criterion tested with the unconventional reservoir model

The second group of tests for the new stopping criterion is performed using the unconventional reservoir model presented in Section 8.2. The simulations are run with a uniform mesh 128 × 128 and a uniform time step $\Delta t = 20$ s from 0 s to 500 s. The average number of fixed-stress iterations for different stopping criteria is summarized in Table 8. In this case the new criterion also requires less fixed-stress iterations per time step than criterion 1 and 2. An examination of the solutions along the center of the top fracture shown in Fig. 8 reveals that the new stopping criterion achieves the same accuracy in pressure and volumetric strain as criteria 1 and 2.

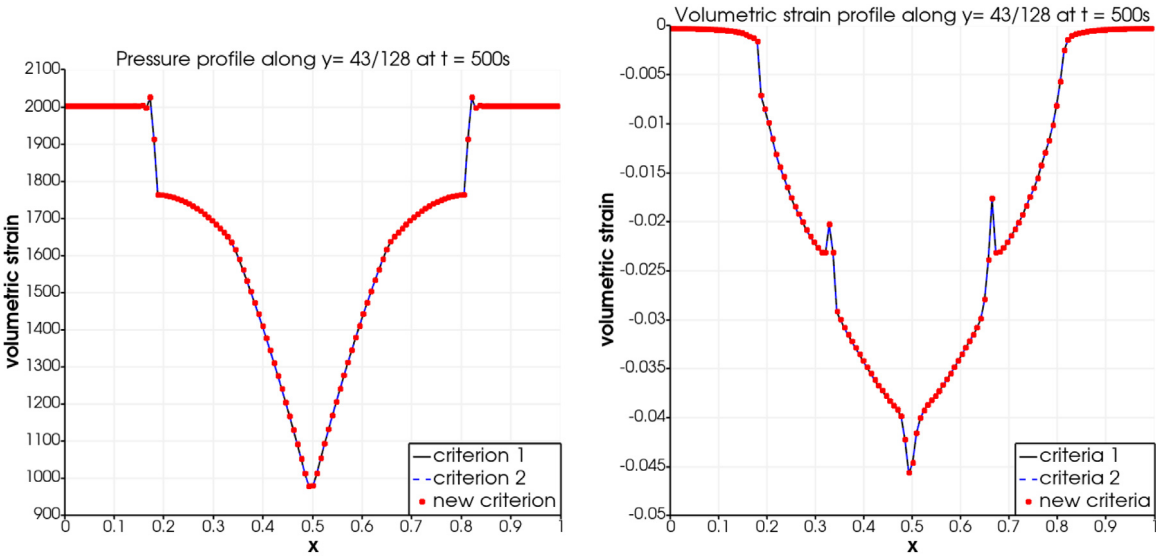

(a) Pressure solutions

(b) Volumetric strain solutions

Fig. 8. Comparison of pressure and solutions at $t = 500$ s using different stopping criteria for the unconventional reservoir model.

We conclude that stopping criteria (8.12) and (8.13) may easily lead to over-iteration (or under-iteration), unless the convergence threshold is carefully tuned. Without the need of tuning any hyperparameter, the new stopping criterion is efficient and accurate since the fixed-stress loops are sufficiently iterated to balance the fixed-stress split error with the discretization errors, achieving the same accuracy compared to the stopping criteria (8.12) and (8.13) with less number of fixed-stress iterations.

9. Conclusions and discussions

We have established residual-based a posteriori error estimators for the Biot system solved with the fixed-stress iterative split, EG for the flow equation, and CG for the mechanics equation. The residual-based error estimators do not require solving auxiliary local problems and are therefore computationally efficient. Both upper and lower bounds of the errors are obtained, although some lower bounds require weak error terms that unfortunately are not easily included in the formulas of the effectivity index. These theoretical results are validated by numerical experiments of the Mandel's problem. We demonstrated the effectiveness of the a posteriori error estimators when guiding dynamic mesh adaptation in a prototype unconventional reservoir model containing a fracture network. Our numerical investigation suggests that the error estimators are effective by achieving dynamic mesh refinement near the wells, across the fractures, at the fracture joints and around the fracture tips; and dynamic mesh coarsening elsewhere. The numerical solutions on the dynamic mesh have the same accuracy as the solutions on a static fine mesh, while using less than 24% of the DoFs of the fine mesh. We further proposed a novel stopping criterion relying on the a posteriori error indicators. The new stopping criterion balances the fixed-stress split error with the discretization errors and does not require tuning of the convergence threshold hyperparameter. Numerical experiments using the Mandel's benchmark problem and the synthetic unconventional reservoir model have demonstrated the efficiency and accuracy of the new stopping criterion. Namely, the new stopping criterion achieves the same accuracy compared to other commonly used stopping criteria (8.12) and (8.13), while avoiding over-iteration that the stopping criteria (8.12) and (8.13) may easily encounter.

Declaration of competing interest

The authors declare that they have no known competing financial interests or personal relationships that could have appeared to influence the work reported in this paper.

Acknowledgments

The authors would like to acknowledge that contributions from V. Girault were supported by the Oden Institute for Computational Engineering and Sciences JTOden Fellowship, USA and the Center for Subsurface Modeling Industrial Affiliates program, USA. X. Lu and M.F. Wheeler were supported by the NSF, USA grant 1911320 and the Center for Subsurface Modeling Industrial Affiliates program, USA.

Appendix

For the reader's convenience, we recall here some useful bounds, either with or without proofs when they are well-known. As usual, the family of meshes is regular, see (3.1). Let us start with a number of local inequalities, with constants $\hat{C}$ independent of h, E, e, etc. First a local Poincaré inequality,

$$\forall \theta \in H_0^1(E), \quad \|\theta\|_{L^2(E)} \leq \hat{C} h_E |\theta|_{H^1(E)}. \tag{A.1}$$

With a different constant $\hat{C}$, (A.1) also applies to functions that vanish on a part of the boundary of E with positive measure. It carries over to the union ω_e of elements adjacent to e, again with a different constant,

$$\forall \theta \in H_0^1(\omega_e), \quad \|\theta\|_{L^2(\omega_e)} \leq \hat{C} h_{\omega_e} |\theta|_{H^1(\omega_e)}, \tag{A.2}$$

where h_{ω_e} is the maximum diameter of the elements sharing e. We also recall a local Poincaré–Wirtinger inequality for functions with zero mean value

$$\forall \theta \in H^1(E) \cap L_0^2(E), \quad \|\theta\|_{L^2(E)} \leq \hat{C} h_E |\theta|_{H^1(E)}. \tag{A.3}$$

Thus the mean value operator m_E has the following approximation error:

Proposition 14. *There exists a constant $\hat{C}$, independent of h, such that for any $e \in \mathcal{E}_h$ and E adjacent to e, the mean value operator m_E defined by (4.18) satisfies*

$$\forall v \in H^1(E), \quad \|v - m_E(v)\|_{L^2(e)} \leq \hat{C} h_E^{\frac{1}{2}} |v|_{H^1(E)}. \tag{A.4}$$

Next, a trace inequality and a scaling argument gives for any E adjacent to e,

$$\forall \theta \in H_0^1(\omega_e), \quad \|\theta\|_{L^2(e)} \leq \hat{C} h_e^{\frac{1}{2}} |\theta|_{H^1(E)}. \tag{A.5}$$

On the other hand, we shall need local inverse inequalities valid for functions θ in finite dimensional spaces, the dimension being independent of h, e, E. First,

$$|\theta|_{H^1(E)} \leq \frac{\hat{C}}{h_E} \|\theta\|_{L^2(E)}. \tag{A.6}$$

Next, we have the inverse trace inequality

$$\|\theta\|_{L^2(e)} \leq \frac{\hat{C}}{\sqrt{h_e}} \|\theta\|_{L^2(E)}. \tag{A.7}$$

If, in addition, θ belongs to $H_{00}^{\frac{1}{2}}(e)$,

$$\|\theta\|_{H_{00}^{\frac{1}{2}}(e)} \leq \frac{\hat{C}}{\sqrt{h_e}} \|\theta\|_{L^2(e)}. \tag{A.8}$$

The above constants depend only on the dimension of the local spaces.

Next, let us recall the bounds of some interface jump terms.

Proposition 15. *There exists a constant $\hat{C}$, independent of h, such that for all $p_h \in M_h$ and all constants $\delta > 0$*

$$\Big| \sum_{e \in \mathcal{E}_h^1} \big(\{\boldsymbol{\kappa} \nabla p_h \cdot \boldsymbol{n}_e\}_e, [p_h]_e \big)_e \Big| \leq \frac{\delta}{2} J_h(p_h, p_h) + \frac{1}{4\delta} (d+1) \hat{C}^2 \frac{\lambda_{\max}}{\min \gamma_e} |p_h|_h^2. \tag{A.9}$$

Proof. All constants $\hat{C}$ below are independent of h. Let $e \in \mathcal{E}_h^1$ and let E be one of the two elements of $\mathcal{T}_h^1$ sharing e. By (A.7), there exists a constant $\hat{C}$ such that

$$\begin{aligned}\Big|\big(\boldsymbol{\kappa}\nabla p_h|_E\cdot\boldsymbol{n}_e,[p_h]_e\big)_e\Big| &\le \lambda_{\max}^{\frac12}\hat{C}\big(\frac{|e|}{|E|}\big)^{\frac12}\|\boldsymbol{\kappa}^{\frac12}\nabla p_h\|_{L^2(E)}\|[p_h]_e\|_{L^2(e)}\\ &\le \hat{C}\big(\frac{\gamma_e}{h_e}\big)^{\frac12}\|[p_h]_e\|_{L^2(e)}\big(\frac{\lambda_{\max}}{\gamma_e}\big)^{\frac12}\|\boldsymbol{\kappa}^{\frac12}\nabla p_h\|_{L^2(E)}\\ &\le \frac12\Big[\delta\frac{\gamma_e}{h_e}\|[p_h]_e\|^2_{L^2(e)}+\frac{1}{\delta}\hat{C}^2\frac{\lambda_{\max}}{\gamma_e}\|\boldsymbol{\kappa}^{\frac12}\nabla p_h\|^2_{L^2(E)}\Big],\end{aligned}$$

and the constant $\hat{C}$ is independent of δ. Therefore

$$\Big|\big(\{\boldsymbol{\kappa}\nabla p_h\cdot\boldsymbol{n}_e\}_e,[p_h]_e\big)_e\Big| \le \frac{\delta}{2}\frac{\gamma_e}{h_e}\|[p_h]_e\|^2_{L^2(e)}+\hat{C}^2\frac{1}{4\delta}\frac{\lambda_{\max}}{\gamma_e}\|\boldsymbol{\kappa}^{\frac12}\nabla p_h\|^2_{L^2(E_1\cup E_2)},$$

where E_1 and E_2 are the two elements of $\mathcal{T}_h^1$ sharing e. Then (A.9) follows from the fact that, when summing this inequality over each e in $\mathcal{E}_h^1$, each element E appears at most $d+1$ times. □

Let $a_h(p_h,\theta_h)$ be the bilinear form with $\tau_p = 1$, i.e., we consider SIPG,

$$a_h(p_h,\theta_h) = \frac{1}{\mu_f}(\!(p_h,\theta_h)\!)_h - \frac{1}{\mu_f}\sum_{e\in\mathcal{E}_h^1}\Big(\big(\{\boldsymbol{\kappa}\nabla p_h\cdot\boldsymbol{n}_e\}_e,[\theta_h]_e\big)_e+\big(\{\boldsymbol{\kappa}\nabla\theta_h\cdot\boldsymbol{n}_e\}_e,[p_h]_e\big)_e\Big). \tag{A.10}$$

Then (A.9) implies for any $\delta>0$,

$$a_h(\theta_h,\theta_h) \ge \frac{1}{\mu_f}\Big(\|\theta_h\|_h^2-\delta J_h(\theta_h,\theta_h)-\frac{1}{2\delta}(d+1)\hat{C}^2\frac{\lambda_{\max}}{\min\gamma_e}|\theta_h|_h^2\Big).$$

Hence the choice $\delta=\frac12$ gives

$$a_h(\theta_h,\theta_h) \ge \frac{1}{\mu_f}\Big(\frac12 J_h(\theta_h,\theta_h)+\big(1-(d+1)\hat{C}^2\frac{\lambda_{\max}}{\min\gamma_e}\big)|\theta_h|_h^2\Big), \tag{A.11}$$

and the ellipticity of a_h follows from a suitable choice of γ_e. Thus, we have the following lemma.

Lemma 2. *If*

$$\min_{e\in\mathcal{E}_h^1}\gamma_e \ge 2(d+1)\hat{C}^2\lambda_{\max}, \tag{A.12}$$

with $\hat{C}$ the constant of (A.9), then

$$\forall\theta_h\in M_h,\quad a_h(\theta_h,\theta_h)\ge\frac{1}{2\mu_f}\|\theta_h\|_h^2. \tag{A.13}$$

The contraction property of the fixed stress algorithm (3.12)–(3.17) holds under the same sufficient condition (A.12). More precisely, (A.12) implies in particular

$$\forall\ell\ge2,\quad \|\bar\sigma_h^{n,\ell}-\bar\sigma_h^{n,\ell-1}\|_{L^2(\Omega_1)}\le\frac{1}{\beta K_b}\|\bar\sigma_h^{n,\ell-1}-\bar\sigma_h^{n,\ell-2}\|_{L^2(\Omega_1)}, \tag{A.14}$$

where

$$\beta=\frac{1}{\alpha^2 M}+\frac{1}{K_b}. \tag{A.15}$$

As $\beta K_b>1$, (A.14) means that the sequence $\bar\sigma_h^{n,\ell}$ is contracting in $L^2(\Omega_1)$.

Now, we recall some properties of the approximation operators. We start with θ_h defined by (4.18). It follows from Proposition 14 that for any e in $\mathcal{E}_h$,

$$\begin{aligned}\forall v\in H^1(\Omega),\quad \|[v-\theta_h]_e\|_{L^2(e)} &\le \hat{C}\big(h_{E_1}+h_{E_2}\big)^{\frac12}\big(|v|^2_{H^1(E_1)}+|v|^2_{H^1(E_2)}\big)^{\frac12},\\ \|\{v-\theta_h\}_e\|_{L^2(e)} &\le \frac{\hat{C}}{2}\big(h_{E_1}+h_{E_2}\big)^{\frac12}\big(|v|^2_{H^1(E_1)}+|v|^2_{H^1(E_2)}\big)^{\frac12}.\end{aligned} \tag{A.16}$$

Next we turn to the operator S_h defined by (4.22). Let v be a function that is constant in each element; recall that

$$S_h(v) = \sum_{\boldsymbol{a}} v(E_{\boldsymbol{a}})\phi_{\boldsymbol{a}}(\boldsymbol{x}).$$

Let $E \in \mathcal{T}_h^1$ with vertices $\boldsymbol{a}_i$, $1 \le i \le d+1$. Since $\boldsymbol{a}_i$ is one of the vertices of $E_{\boldsymbol{a}_i}$, there is a sequence of adjacent elements of $\mathcal{T}_h^1$, $E = E_1, E_2 \ldots, E_{k_i} = E_{\boldsymbol{a}_i}$, with E_ℓ adjacent to $E_{\ell+1}$. Since the mesh is regular, the number k_i is bounded by a fixed integer K independent of $\boldsymbol{a}_i$ and h.

Now, as in E,

$$\sum_{i=1}^{d+1} \phi_{\boldsymbol{a}_i}(\boldsymbol{x}) = 1,$$

we can write $v(E) = v(E)\sum_{i=1}^{d+1} \phi_{\boldsymbol{a}_i}(\boldsymbol{x})$. Thus,

$$\forall \boldsymbol{x} \in E, \quad S_h(v)(\boldsymbol{x}) - v(\boldsymbol{x}) = \sum_{i=1}^{d+1} \big(v(E_{\boldsymbol{a}_i}) - v(E)\big)\phi_{\boldsymbol{a}_i}(\boldsymbol{x}).$$

By considering the above sequence of elements E_j, this implies that

$$\forall \boldsymbol{x} \in E, \quad S_h(v)(\boldsymbol{x}) - v(\boldsymbol{x}) = \sum_{i=1}^{d+1} \Big(\sum_{j=1}^{k_i-1} [v]_{e_j} \Big) \phi_{a_i}(\boldsymbol{x}), \tag{A.17}$$

where e_j is the interface between E_j and E_{j+1}. Hence

$$\forall \boldsymbol{x} \in E, \quad \big|S_h(v)(\boldsymbol{x}) - v(\boldsymbol{x})\big| \le \sum_{i=1}^{d+1} \Big(\sum_{j=1}^{k_i-1} |e_j|^{-\frac{1}{2}} \|[v]_{e_j}\|_{L^2(e_j)} \Big) \phi_{\boldsymbol{a}_i}(\boldsymbol{x}). \tag{A.18}$$

From here, we deduce the following proposition:

Proposition 16. *There exists a constant $\hat{C}$, related to the regularity of the mesh but independent of h, such that for all functions v that are constant in each element E of $\mathcal{T}_h^1$,*

$$\|S_h(v) - v\|_{L^2(\Omega_1)}^2 \le \hat{C}(K-1)^2 \sum_{e \in \mathcal{E}_h^1} h_e \|[v]_e\|_{L^2(e)}^2, \tag{A.19}$$

$$\sum_{E \in \mathcal{T}_h^1} \|\nabla(S_h(v) - v)\|_{L^2(E)}^2 \le \hat{C}\Big(\frac{d+1}{d}\Big)^2 (K-1)^2 \sum_{e \in \mathcal{E}_h^1} \frac{1}{h_e} \|[v]_e\|_{L^2(e)}^2, \tag{A.20}$$

and

$$\|S_h(v) - v\|_{L^2(\Gamma_{12})}^2 \le \hat{C}(K-1)^2 \sum_{e \in \mathcal{E}_h^1} \|[v]_e\|_{L^2(e)}^2. \tag{A.21}$$

Proof. By recalling that the set of functions $\phi_{\boldsymbol{a}_i}$, $1 \le i \le d+1$, form a convex combination in E, we infer from (A.18) that

$$\forall \boldsymbol{x} \in E, \quad \big|S_h(v)(\boldsymbol{x}) - v(\boldsymbol{x})\big|^2 \le \sum_{i=1}^{d+1} \Big(\sum_{j=1}^{k_i-1} |e_j|^{-\frac{1}{2}} \|[v]_{e_j}\|_{L^2(e_j)} \Big)^2 \phi_{\boldsymbol{a}_i}(\boldsymbol{x}).$$

Then, considering that $k_i \le K$, we have

$$\forall \boldsymbol{x} \in E, \quad \big|S_h(v)(\boldsymbol{x}) - v(\boldsymbol{x})\big|^2 \le (K-1) \sum_{i=1}^{d+1} \Big(\sum_{j=1}^{k_i-1} |e_j|^{-1} \|[v]_{e_j}\|_{L^2(e_j)}^2 \Big) \phi_{\boldsymbol{a}_i}(\boldsymbol{x}).$$

But, as $\phi_{\boldsymbol{a}_i}$ is a polynomial of degree one, that takes the value $\frac{1}{d+1}$ at the center of E, the Gauss quadrature formula gives

$$\int_E \phi_{\boldsymbol{a}_i} = \frac{|E|}{d+1}.$$

Hence

$$\|S_h(v) - v\|^2_{L^2(E)} \le \frac{|E|}{d+1}(K-1)\sum_{i=1}^{d+1}\sum_{j=1}^{k_i-1}\frac{1}{|e_j|}\|[v]_{e_j}\|^2_{L^2(e_j)}.$$

When summing this inequality over all E in $\mathcal{T}_h^1$, each jump is repeated at most $(K-1)(d+1)$ times. Therefore

$$\|S_h(v) - v\|^2_{L^2(\Omega_1)} \le (K-1)^2\sum_{e\in\mathcal{E}_h^1}\bar{h}_e\|[v]_e\|^2_{L^2(e)},$$

where $\bar{h}_e = \frac{\max|E|}{\min|e'|}$ for all e' in a neighborhood of E. The regularity of the mesh implies that $\bar{h}_e \le \hat{C}h_e$. This yields (A.19).

Regarding the gradient of the error, note that

$$|\nabla\phi_{\boldsymbol{a}_i}| = \frac{1}{d}\frac{|\tilde{e}_i|}{|E|},$$

where $\tilde{e}_i$ is the face opposite $\boldsymbol{a}_i$. Therefore, (A.17) implies that in E

$$|\nabla(S_h(v)(\boldsymbol{x}) - v(\boldsymbol{x}))|^2 \le \frac{d+1}{d^2}(K-1)\sum_{i=1}^{d+1}\Big(\frac{|\tilde{e}_i|}{|E|}\Big)^2\Big(\sum_{j=1}^{k_i-1}|e_j|^{-1}\|[v]_{e_j}\|^2_{L^2(e_j)}\Big).$$

Hence

$$\|\nabla(S_h(v) - v)\|^2_{L^2(E)} \le \frac{d+1}{d^2}(K-1)\sum_{i=1}^{d+1}\frac{|\tilde{e}_i|^2}{|E|}\Big(\sum_{j=1}^{k_i-1}|e_j|^{-1}\|[v]_{e_j}\|^2_{L^2(e_j)}\Big),$$

and the same argument as above yields (A.20).

Finally, the proof of the trace inequality (A.21) is similar to that of (A.19). Indeed, we have

$$\forall\boldsymbol{x}\in e,\quad \big|S_h(v)(\boldsymbol{x}) - v(\boldsymbol{x})\big|^2 \le (K-1)\sum_{i=1}^{d}\Big(\sum_{j=1}^{k_i-1}|e_j|^{-1}\|[v]_{e_j}\|^2_{L^2(e_j)}\Big)\phi_{\boldsymbol{a}_i}(\boldsymbol{x}),$$

and

$$\int_e \phi_{\boldsymbol{a}_i} = \frac{|e|}{d}.$$

Thus

$$\|S_h(v) - v\|^2_{L^2(e)} \le \frac{|e|}{d}(K-1)\sum_{i=1}^{d}\sum_{j=1}^{k_i-1}\frac{1}{|e_j|}\|[v]_{e_j}\|^2_{L^2(e_j)},$$

and (A.21) follows by summing over all face e of $\mathcal{E}_h^{12}$. □

An interesting by-product of Proposition 16 is the following trace inequality for the functions of M_h.

Corollary 1. *There exists a constant $\hat{C}$, related to the regularity of the mesh but independent of h, such that for all $\theta_h \in M_h$,*

$$\begin{aligned}\|\theta_h\|_{L^2(\Gamma_{12})} \le \hat{C}\Big[\ &\|\theta_h\|_{L^2(\Omega_1)} + \Big(\sum_{e\in\mathcal{E}_h^1}h_e\|[\theta_h]_e\|^2_{L^2(e)}\Big)^{\frac12}\\ &+\Big(\|\theta_h\|^{\frac12}_{L^2(\Omega_1)} + \Big(\sum_{e\in\mathcal{E}_h^1}h_e\|[\theta_h]_e\|^2_{L^2(e)}\Big)^{\frac14}\Big)\Big(\Big(\sum_{E\in\mathcal{T}_h^1}\|\nabla\theta_h\|^2_{L^2(E)}\Big)^{\frac14} + \Big(\sum_{e\in\mathcal{E}_h^1}\frac{1}{h_e}\|[\theta_h]_e\|^2_{L^2(e)}\Big)^{\frac14}\Big)\ \Big].\end{aligned} \tag{A.22}$$

Proof. Recall that $\theta_h = \theta_h^{\rm ct} + \theta_h^{\rm disc}$ with $\theta_h^{\rm ct} \in Q_h$ and $\theta_h^{\rm disc}$ constant in each cell. Then, we write

$$\|\theta_h\|_{L^2(\Gamma_{12})} = \|\big(\theta_h^{\rm ct} + S_h(\theta_h^{\rm disc})\big) + \big(\theta_h^{\rm disc} - S_h(\theta_h^{\rm disc})\big)\|_{L^2(\Gamma_{12})},$$

and in view of (A.21), it suffices to bound the sum in the first brackets. As this function is in $H^1(\Omega_1)$, the trace theorem in Ω_1, see [40], yields

$$\|\theta_h^{\rm ct} + S_h(\theta_h^{\rm disc})\|_{L^2(\Gamma_{12})} \le \hat{C}\Big[\|\theta_h^{\rm ct} + S_h(\theta_h^{\rm disc})\|_{L^2(\Omega_1)} + \|\theta_h^{\rm ct} + S_h(\theta_h^{\rm disc})\|^{\frac12}_{L^2(\Omega_1)}\|\nabla(\theta_h^{\rm ct} + S_h(\theta_h^{\rm disc}))\|^{\frac12}_{L^2(\Omega_1)}\Big].$$

Now, by (A.19),

$$\|\theta_h^{\rm ct} + S_h(\theta_h^{\rm disc})\|_{L^2(\Omega_1)} \le \|\theta_h\|_{L^2(\Omega_1)} + \|S_h(\theta_h^{\rm disc}) - \theta_h^{\rm disc}\|_{L^2(\Omega_1)} \le \|\theta_h\|_{L^2(\Omega_1)} + \hat{C}(K-1)\Big(\sum_{e\in\mathcal{E}_h^1} h_e\|[\theta_h]_e\|^2_{L^2(e)}\Big)^{\frac12}.$$

Similarly, by (A.20),

$$\begin{aligned}\Big(\sum_{E\in\mathcal{T}_h^1}\|\nabla(\theta_h^{\rm ct} + S_h(\theta_h^{\rm disc}))\|^2_{L^2(E)}\Big)^{\frac12} &\le \Big(\sum_{E\in\mathcal{T}_h^1}\|\nabla\,\theta_h\|^2_{L^2(E)}\Big)^{\frac12} + \Big(\sum_{E\in\mathcal{T}_h^1}\|\nabla(S_h(\theta_h^{\rm disc}) - \theta_h^{\rm disc})\|^2_{L^2(E)}\Big)^{\frac12}\\ &\le \Big(\sum_{E\in\mathcal{T}_h^1}\|\nabla\,\theta_h\|^2_{L^2(E)}\Big)^{\frac12} + \hat{C}\frac{d+1}{d}(K-1)\Big(\sum_{e\in\mathcal{E}_h^1}\frac{1}{h_e}\|[\theta_h]_e\|^2_{L^2(e)}\Big)^{\frac12}.\end{aligned}$$

Then (A.22) follows from (A.21) and these two inequalities. □

Note that (A.22) readily implies that

$$\|\theta_h\|_{L^2(\Gamma_{12})} \le \hat{C}\Big[\|\theta_h\|_{L^2(\Omega_1)} + h\,J_h(\theta_h,\theta_h)^{\frac12} + \Big(\|\theta_h\|^{\frac12}_{L^2(\Omega_1)} + h^{\frac12}J_h(\theta_h,\theta_h)^{\frac14}\Big)\|\theta_h\|_h^{\frac12}\Big]. \tag{A.23}$$

This inequality has the following application.

Corollary 2. *For all real numbers $\delta > 0$ and $\delta' > 0$ there exists a constant $C(\delta,\delta')$ independent of h and Δt such that for all functions $f \in L^2(\Gamma_{12})$ and $\theta_h \in M_h$,*

$$\Big|\int_{\Gamma_{12}} f\,\theta_h\Big| \le \frac12\Big[\frac{\delta}{\Delta t}\|\theta_h\|^2_{L^2(\Omega_1)} + \delta'\|\theta_h\|_h^2 + C(\delta,\delta')\big(\Delta t + h + (\Delta t)^{\frac12} + h^{\frac12}\big)\|f\|^2_{L^2(\Gamma_{12})}\Big]. \tag{A.24}$$

Proof. By applying to θ_h the trace inequality (A.23) in

$$\Big|\int_{\Gamma_{12}} f\,\theta_h\Big| \le \|f\|_{L^2(\Gamma_{12})}\|\theta_h\|_{L^2(\Gamma_{12})},$$

we infer

$$\begin{aligned}\Big|\int_{\Gamma_{12}} f\,\theta_h\Big| &\le \frac12\Big(\frac{\delta_1}{\Delta t}\|\theta_h\|^2_{L^2(\Omega_1)} + \frac{\Delta t}{\delta_1}\hat{C}\|f\|^2_{L^2(\Gamma_{12})} + \delta_2 J_h(\theta_h,\theta_h) + \frac{h^2}{\delta_2}\hat{C}\|f\|^2_{L^2(\Gamma_{12})}\Big)\\ &\quad + \frac12\Big(\frac{\delta_3}{(\Delta t)^{\frac12}}\|\theta_h\|_{L^2(\Omega_1)}\|\theta_h\|_h + \frac{(\Delta t)^{\frac12}}{\delta_3}\hat{C}\|f\|^2_{L^2(\Gamma_{12})} + \delta_4 J_h(\theta_h,\theta_h)^{\frac12}\|\theta_h\|_h + \frac{h}{\delta_4}\hat{C}\|f\|^2_{L^2(\Gamma_{12})}\Big).\end{aligned}$$

The factor of δ_3 can be further bounded by

$$\frac{\delta_3}{(\Delta t)^{\frac12}}\|\theta_h\|_{L^2(\Omega_1)}\|\theta_h\|_h \le \frac{\delta_3}{2}\Big(\frac{\delta_5}{\Delta t}\|\theta_h\|^2_{L^2(\Omega_1)} + \frac{1}{\delta_5}\|\theta_h\|_h^2\Big).$$

Therefore, by collecting all factors, we deduce

$$\Big|\int_{\Gamma_{12}} f\,\theta_h\Big| \le \frac12\Big[\Big(\delta_1 + \frac{\delta_3}{2}\delta_5\Big)\frac{1}{\Delta t}\|\theta_h\|^2_{L^2(\Omega_1)} + \Big(\delta_2 + \frac{\delta_3}{2\delta_5} + \delta_4\Big)\|\theta_h\|_h^2 + \Big(\frac{\Delta t}{\delta_1} + \frac{h^2}{\delta_2} + \frac{(\Delta t)^{\frac12}}{\delta_3} + \frac{h}{\delta_4}\Big)\hat{C}\|f\|^2_{L^2(\Gamma_{12})}\Big].$$

It is easy to check that numbers $\delta_i > 0$ can be picked, independent of h and Δt, so that both $\delta_1 + \frac{\delta_3}{2}\delta_3\delta_5$ and $\delta_2 + \frac{\delta_3}{2\delta_5} + \delta_4$ are arbitrary. This proves the corollary. □

References

[1] J. Kim, H. Tchelepi, R. Juanes, Stability and convergence of sequential methods for coupled flow and geomechanics: fixed-stress and fixed-strain splits, Comput. Methods Appl. Mech. Engrg. 200 (13–16) (2011) 1591–1606.

[2] A. Mikelić, M.F. Wheeler, On the interface law between a deformable porous medium containing a viscous fluid and an elastic body, Math. Models Methods Appl. Sci. 22 (11) (2012) 1250031.

[3] A. Mikelić, M.F. Wheeler, Convergence of iterative coupling for coupled flow and geomechanics, Comput. Geosci. 17 (3) (2013) 455–461.

[4] A. Mikelić, B. Wang, M.F. Wheeler, Numerical convergence study of iterative coupling for coupled flow and geomechanics, Comput. Geosci. 18 (3–4) (2014) 325–341.

[5] X. Gai, S. Sun, M.F. Wheeler, H. Klie, et al., A time-stepping scheme for coupled reservoir flow and geomechanics, in: SPE Annual Technical Conference and Exhibition, Society of Petroleum Engineers, 2005.

[6] X. Gai, A Coupled Geomechanics and Reservoir Flow Model on Parallel Computers (Ph.D. thesis), The University of Texas at Austin, Austin, Texas, 2004.

[7] N. Castelletto, J. White, H. Tchelepi, Accuracy and convergence properties of the fixed-stress iterative solution of two-way coupled poromechanics, Int. J. Numer. Anal. Methods Geomech. 39 (2015) 1593–1618.

[8] N. Castelletto, J.A. White, H.A. Tchelepi, A unified framework for fully-implicit and sequential-implicit schemes for coupled poroelasti, in: ECMOR XIV, 14th European Conference on the Mathematics of Oil Recovery, 2014.

[9] T. Almani, K. Kumar, A. Dogru, G. Singh, M.F. Wheeler, Convergence analysis of multirate fixed-stress split iterative schemes for coupling flow with geomechanics, Comput. Methods Appl. Mech. Engrg. 311 (2016) 180–207.

[10] K. Kumar, T. Almani, G. Singh, M.F. Wheeler, Multirate undrained splitting for coupled flow and geomechanics in porous media, in: Numerical Mathematics and Advanced Applications ENUMATH 2015, Springer, 2016, pp. 431–440.

[11] M. Borregales, F.A. Radu, K. Kumar, J.M. Nordbotten, Robust iterative schemes for non-linear poromechanics, Comput. Geosci. 22 (4) (2018) 1021–1038.

[12] S. Dana, B. Ganis, M.F. Wheeler, A multiscale fixed stress split iterative scheme for coupled flow and poromechanics in deep subsurface reservoirs, J. Comput. Phys. 352 (2018) 1–22.

[13] S. Dana, M.F. Wheeler, Convergence analysis of two-grid fixed stress split iterative scheme for coupled flow and deformation in heterogeneous poroelastic media, Comput. Methods Appl. Mech. Engrg. 341 (2018) 788–806.

[14] M. Bause, F.A. Radu, U. Köcher, Space–time finite element approximation of the Biot poroelasticity system with iterative coupling, Comput. Methods Appl. Mech. Engrg. 320 (2017) 745–768.

[15] M. Borregales, K. Kumar, F.A. Radu, C. Rodrigo, F.J. Gaspar, A parallel-in-time fixed-stress splitting method for Biot consolidation model, 2018, arXiv preprint arXiv:1802.00949.

[16] C. Rodrigo, F.J. Gaspar, X. Hu, L.T. Zikatanov, Stability and monotonicity for some discretizations of the Biot consolidation model, Comput. Methods Appl. Mech. Engrg. 298 (2016) 183–204.

[17] E. Storvik, J.W. Both, K. Kumar, J.M. Nordbotten, F.A. Radu, On the optimization of the fixed-stress splitting for Biot's equations, Internat. J. Numer. Methods Engrg. 120 (2) (2019) 179–194.

[18] X. Lu, M.F. Wheeler, Three-way coupling of multiphase flow and poromechanics in porous media, J. Comput. Phys. 401 (2020) 109053.

[19] V. Girault, M.F. Wheeler, T. Almani, S. Dana, A priori error estimates for a discretized poro-elastic-elastic system solved by a fixed-stress algorithm, Oil Gas Sci. Technol. Rev. IFP Energies Nouv. (2019).

[20] B. Wang, Parallel Simulation of Coupled Flow and Geomechanics in Porous Media (Ph.D. thesis), 2014.

[21] S. Lee, A. Mikelić, M.F. Wheeler, T. Wick, Phase-field modeling of proppant-filled fractures in a poroelastic medium, Comput. Methods Appl. Mech. Engrg. 312 (2016) 509–541.

[22] J. Choo, S. Lee, Enriched Galerkin finite elements for coupled poromechanics with local mass conservation, Comput. Methods Appl. Mech. Engrg. 341 (2018) 311–332.

[23] E. Ahmed, F.A. Radu, J.M. Nordbotten, Adaptive poromechanics computations based on a posteriori error estimates for fully mixed formulations of Biot's consolidation model, Comput. Methods Appl. Mech. Engrg. 347 (2019) 264–294.

[24] E. Ahmed, J.M. Nordbotten, F.A. Radu, Adaptive asynchronous time-stepping, stopping criteria, and a posteriori error estimates for fixed-stress iterative schemes for coupled poromechanics problems, J. Comput. Appl. Math. 364 (2020) 112312.

[25] Y. Li, L.T. Zikatanov, Residual-based a posteriori error estimates of mixed methods for three-field Biot's consolidation model, IMA J. Numer. Anal. (2020).

[26] A. Ern, S. Meunier, A posteriori error analysis of Euler-Galerkin approximations to coupled elliptic-parabolic problems, ESAIM Math. Model. Numer. Anal. 43 (2) (2008) 353–375.

[27] R.A. Adams, J.J. Fournier, Sobolev Spaces, vol. 140, Elsevier, 2003.

[28] J. Nečas, Les méthodes directes en théorie des équations elliptiques, Masson, Paris, 1967, p. 351.

[29] J.-L.L.E. Magenes, Non-Homogeneous Boundary Value Problems and Applications. Vol. I, Springer-Verlag, New York, 1972, p. xvi+357.

[30] P. Grisvard, Elliptic Problems in Nonsmooth Domains, in: Monographs and Studies in Mathematics, vol. 24, Pitman, Boston, MA, 1985, p. xiv+410.

[31] S. Dib, V. Girault, F. Hecht, T. Sayah, A posteriori error estimates for Darcy's problem coupled with the heat equation, ESAIM Math. Model. Numer. Anal. 53 (6) (2019) 2121–2159.

[32] V. Girault, G.V. Pencheva, M.F. Wheeler, T.M. Wildey, Domain decomposition for linear elasticity with DG jumps and mortars, Comput. Methods Appl. Mech. Engrg. 198 (21–26) (2009) 1751–1765.

[33] P.J. Phillips, M.F. Wheeler, A coupling of mixed and continuous Galerkin finite element methods for poroelasticity. I. The continuous in time case, Comput. Geosci. 11 (2) (2007) 131–144.
[34] P.G. Ciarlet, Basic error estimates for elliptic problems, in: Handbook of Numerical Analysis, Vol. II, North-Holland, Amsterdam, 1991, pp. 17–351.
[35] L.R. Scott, S. Zhang, Finite element interpolation of non-smooth functions satisfying boundary conditions, Math. Comp. 54 (1990) 483–493.
[36] S. Lee, Y.-J. Lee, M.F. Wheeler, A locally conservative enriched Galerkin approximation and efficient solver for elliptic and parabolic problems, SIAM J. Sci. Comput. 38 (3) (2016) A1404–A1429.
[37] P.J. Phillips, M.F. Wheeler, A coupling of mixed and continuous Galerkin finite element methods for poroelasticity II: The discrete-in-time case, Comput. Geosci. 11 (2) (2007) 145–158.
[38] O. Karakashian, F. Pascal, A posteriori error estimates for a discontinuous Galerkin approximation of second-order elliptic problems, SIAM J. Numer. Anal. 41 (2003) 2374–2399.
[39] V. Girault, J.-L. Lions, Two-grid finite-element scheme for the transient Navier–Stokes problem, Modél. Math. Anal. Numér. 35 (2001) 945–980.
[40] S.C. Brenner, L.R. Scott, The Mathematical Theory of Finite Element Methods, third ed., Springer-Verlag, 2008.
[41] S. Zhang, A family of 3D continuously differentiable finite elements on tetrahedral grids, Appl. Numer. Math. 59 (1) (2009) 219–233.
[42] V. Girault, P.A. Raviart, Finite Element Methods for Navier-Stokes Equations: Theory and Algorithms, in: Springer Series in Computational Mathematics, vol. 5, Springer-Verlag, Berlin, 1986, p. x+374.
[43] W. Bangerth, R. Hartmann, G. Kanschat, deal. II Differential Equations Analysis Library, Technical Reference, 2004, Available online at http://www.dealii.org.
[44] P.J. Phillips, Finite Element Methods in Linear Poroelasticity: Theoretical and Computational Results (Ph.D. thesis), 2005.
[45] R. Dean, X. Gai, C.M. Stone, S. Minkoff, A comparison of techniques for coupling porous flow and geomechanics, SPE J. 11 (01) (2006) 132–140.